

Bio-protocol Selections

# Stimulated Emission Depletion (STED) Microscopy Protocols for Super-Resolution

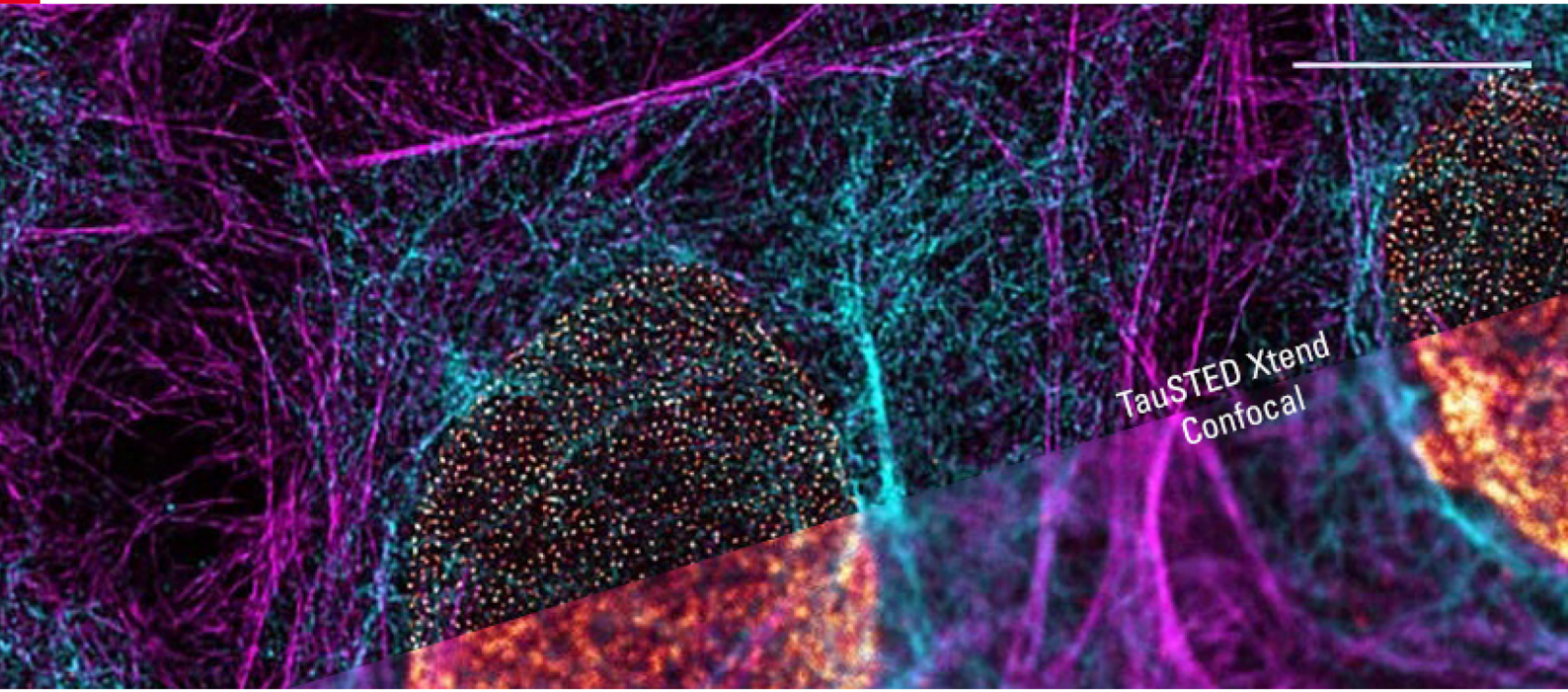
Applications of STED from Microbiology to Mammalian Systems

STED

Confocal

bio-protocol





## TauSTED Xtend: Sharp. Simple. Stunning.

TauSTED Xtend is the next step in the evolution of TauSTED imaging. It combines lifetime-based information with an additional spatial readout. This results in a significant gain in resolution, especially at lower STED depletion powers, allowing to extend multicolor live imaging capabilities at remarkable nanoscale.

### POWER

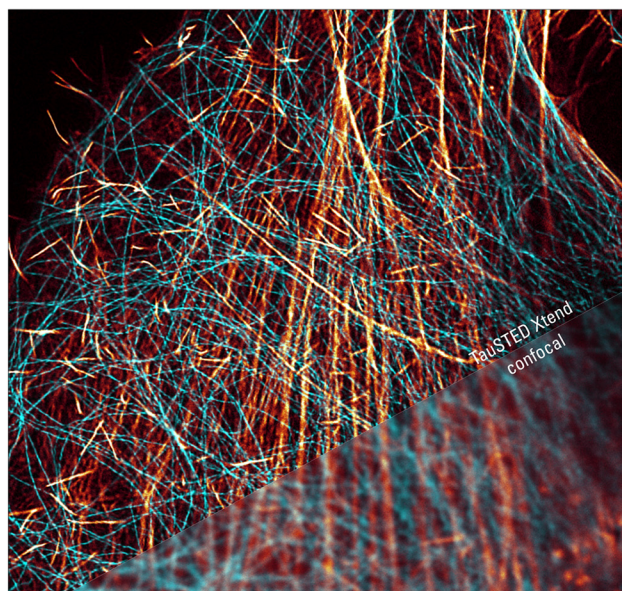
Resolve smaller details in context at nanoscale. Perform longer live imaging at cutting-edge resolution.

### POTENTIAL

Use standard fluorophores and follow your preferred protocols for STED. Perform expanded multicolor imaging, even with a single STED laser line.

### PRODUCTIVITY

Directly monitor fast processes with nanoscale resolution. Get instant feedback on the results while performing your experiments.



Learn more at <https://go.leica-ms.com/tausted-xtend-na>

## Foreword

We are pleased to release the reprint collection “*Stimulated Emission Depletion (STED) Microscopy Protocols for Super-Resolution*,” which showcases various applications of STED that span microbiology, developmental biology, neuroscience, immunology, and stem cell research.

STED microscopy, invented in 1994 by Stefan Hell, has been a revolutionary technique in fluorescence microscopy. By overcoming the diffraction limit of light microscopy, STED microscopy enables super-resolution imaging of biological structures, facilitating detailed and in-depth cellular and molecular studies. This breakthrough technology has opened new avenues for understanding subcellular processes and molecular relationships across life sciences research.

This year marks for Leica Microsystems the 20th anniversary of innovation in super-resolution. Throughout the last two decades Leica has worked closely with the scientific community to develop groundbreaking advancements in imaging that have enabled scientific discovery, with TauSTED Xtend as latest step in evolution of STED imaging.

A key feature of this collection is the emphasis on detailed, step-by-step protocols that are the focus of *Bio-protocol* journal and that significantly enhance experimental reproducibility and reliability. In our annual user surveys, approximately 90% of users who apply the protocols published in *Bio-protocol* report that they are able to successfully reproduce them.

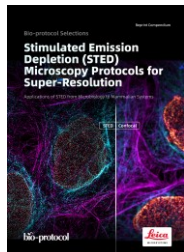
We are grateful to Leica Microsystems for their support in freely disseminating advanced microscopy technologies and furthering our mission to improve research reproducibility.

We hope this collection not only serves as a valuable resource but also inspires further research. You can explore our full protocol archive at [www.bio-protocol.org](http://www.bio-protocol.org). We hope you will consider contributing your own protocols to *Bio-protocol* in the future.

For more information, please contact:  
Fanglian He  
Publisher, *Bio-protocol*  
[fhe@bio-protocol.org](mailto:fhe@bio-protocol.org)  
June 2024

## Table of Contents

Preparation of Human Kidney Progenitor Cultures and Their Differentiation into Podocytes .....	1
Biophysical Analysis of Mechanical Signals in Immotile Cilia of Mouse Embryonic Nodes Using Advanced Microscopic Techniques .....	14
Tracking the Subcellular Localization of Surface Proteins in <i>Staphylococcus aureus</i> by Immunofluorescence Microscopy.....	27
Super-resolution Imaging of the T cell Central Supramolecular Signaling Cluster Using Stimulated Emission Depletion Microscopy .....	42
Optical Clearing and Index Matching of Tissue Samples for High-resolution Fluorescence Imaging Using SeeDB2.....	53
Multicolor Stimulated Emission Depletion (STED) Microscopy to Generate High-resolution Images of Respiratory Syncytial Virus Particles and Infected Cells .....	65
Staining of Membrane Receptors with Fluorescently-labeled DNA Aptamers for Super-resolution Imaging .....	75
Dissection and Staining of Mouse Brain Ventricular Wall for the Analysis of Ependymal Cell Cilia Organization.....	87



### On the Cover:

Multicolor TauSTED Xtend 775 for cell biology applications that require nanoscopy resolution for multiple cellular components. Cells showing vimentin fibrils (AF 594), actin network (ATTO 647N), and nuclear pore basket (CF 680R). Sample courtesy of Brigitte Bergner, Mariano Gonzalez Pisfil, Steffen Dietzel, Core Facility Bioimaging, Biomedical Center, Ludwig-Maximilians-University, Munich, Germany.

# Preparation of Human Kidney Progenitor Cultures and Their Differentiation into Podocytes

Maria Elena Melica<sup>1, 2, \*</sup>, Maria Lucia Angelotti<sup>1, 2</sup>, Giulia Antonelli<sup>1, 2, 3</sup>, Anna J. Peired<sup>1, 2</sup>, Carolina Conte<sup>1, 2, 3</sup>, Letizia De Chiara<sup>1, 2</sup>, Benedetta Mazzinghi<sup>3</sup>, Elena Lazzeri<sup>1, 2</sup>, Laura Lasagni<sup>1, 2</sup>, and Paola Romagnani<sup>1, 2, 3, \*</sup>

<sup>1</sup>Excellence Centre for Research, Transfer and High Education for the development of DE NOVO Therapies (DENOTHE), University of Florence, Florence, Italy

<sup>2</sup>Department of Experimental and Clinical Biomedical Sciences “Mario Serio”, University of Florence, Florence, Italy

<sup>3</sup>Nephrology and Dialysis Unit, Meyer Children’s Hospital IRCCS, Florence, Italy

\*For correspondence: [paola.romagnani@unifi.it](mailto:paola.romagnani@unifi.it); [mariaelena.melica@unifi.it](mailto:mariaelena.melica@unifi.it)

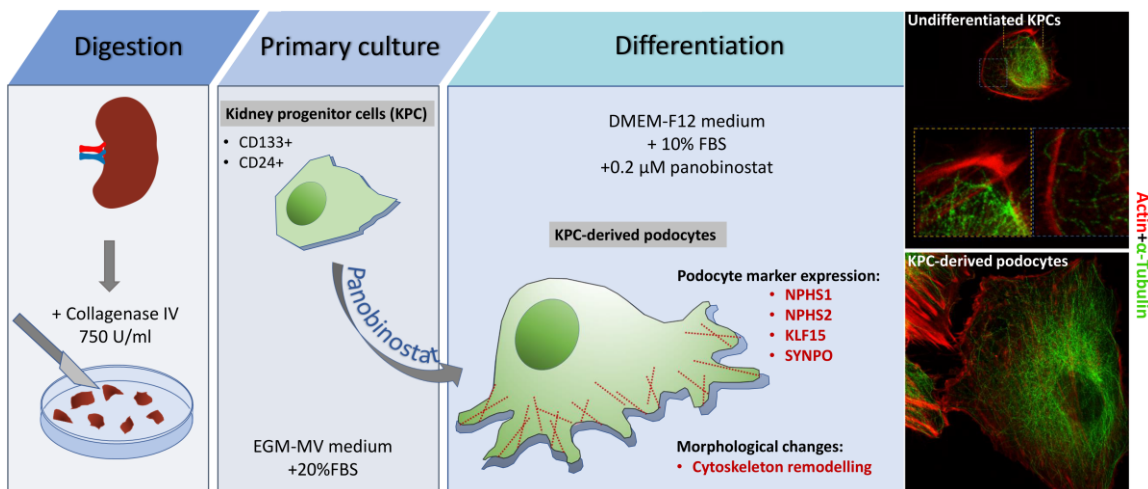
## Abstract

Kidney diseases are a global health concern. Modeling of kidney disease for translational research is often challenging because of species specificities or the postmitotic status of kidney epithelial cells that make primary cultures, for example podocytes. Here, we report a protocol for preparing primary cultures of podocytes based on the isolation and in vitro propagation of immature kidney progenitor cells subsequently differentiated into mature podocytes. This protocol can be useful for studying physiology and pathophysiology of human kidney progenitors and to obtain differentiated podocytes for modeling podocytopathies and other kidney disorders involving podocytes.

**Keywords:** Kidney progenitor cells, Kidney, Podocytes, Tubular cells, Organoids, Chronic kidney disease

**This protocol is used in:** Sci. Transl. Med. (2022), DOI: 10.1126/scitranslmed.abg3277

## Graphical overview



## Background

Kidney diseases, a global health issue, are the consequence of injury to the functional components of the kidney, the nephrons (Romagnani et al., 2017). Nephrons are constituted by a blood filtering unit, the glomerulus, and the respective tubule where the filtrate is modified by solute reabsorption and metabolite secretion up to when the final urine is excreted via the urinary tract (Romagnani et al., 2017). The nephrons respond to injury in two ways: a) differentiated epithelial cells undergo polyploidization and hypertrophy to rapidly support residual kidney function and b) immature epithelial cells, referred to as kidney progenitors (Lazzeri et al., 2019), proliferate to recover at least a part of the lost cells, i.e., kidney regeneration (Lazzeri et al., 2019). Kidney progenitors are localized along the inside of the Bowman capsule of the glomerulus and are scattered among tubular epithelial cells along the tubule, being identified by the expression of the surface markers CD133 and CD24, in humans (Sagrinati et al., 2006; Lazzeri et al., 2019). Kidney progenitors can be obtained from kidney tissue or urine and cultured long term (Angelotti et al., 2012) because they retain the capacity for self-renewal. Kidney progenitors have the capacity to differentiate into multiple types of kidney epithelial cells in vitro and in vivo (Sagrinati et al., 2006; Lazzeri et al., 2019). Hence, kidney progenitors can be expanded and differentiated into different types of tubular epithelial cells (Angelotti et al., 2012) and even cultured in 3D, generating tubuloids, a selective property among other kidney tubular cells (Xu et al., 2022). This property makes them ideal for modeling of genetic tubular disorders, e.g., upon isolation from the urine of patients with genetic tubular disorders or upon introduction of pathogenic genetic variants (e.g., using CRISPR-Cas system) (Xu et al., 2022). In addition, kidney progenitors can be differentiated in culture into podocytes, the main constituent of the glomerular filtration barrier. Podocytes are highly differentiated postmitotic cells unable to proliferate (Kopp et al., 2020). For this reason, they are impossible to expand in primary cultures, unless using artificial systems of immortalization (Shankland et al., 2007).

Here, we report detailed protocols on how to prepare human kidney progenitor cultures from human kidney tissue, maintain them, and differentiate them into podocytes. Differentiation of kidney progenitors using specific factors and compounds (Lasagni et al., 2015), as recently reported for the histone deacetylase inhibitor panobinostat, induces a change in their phenotype, promoting transcription of podocyte genes such as nephrin, podocin, and synaptopodin (Melica et al., 2022). We also report methods to assess their phenotype by qRT-PCR, FACS, and confocal and stimulated emission depletion (STED) microscopy. Applying the same culturing method described here to the isolation procedure reported by Lazzeri et al. (2015) permits the preparation of kidney progenitor cultures also from the urine of patients with kidney disorders, making them particularly suitable for studying genetic podocytopathies for diagnostic purposes. Given the importance of kidney progenitors and podocytes in the

pathogenesis of chronic kidney disease, the possibility to prepare and maintain these cultures has wide implications and possible uses.

## Materials and reagents

### Biological materials

Normal-appearing kidney fragments are obtained from the pole opposite to the tumor from patients that underwent nephrectomy for localized renal tumors.

**CAUTION:** All the experiments involving human specimens should be performed in accordance with the recommendations of the Institutional Ethical Committee for human experimentation. All procedures in this protocol were conducted under protocols approved by the Ethical Committee on human experimentation of the Careggi University Hospital.

### Reagents

1. Physiological saline solution, NaCl 0.9% (B. Braun Melsungen AG, A.I.C. n. 030902391)
2. HyClone defined fetal bovine serum (FBS), US origin (Cytiva, catalog number: SH30070.03)
3. Endothelial cell growth basal medium (EBM), 500 mL (LONZA, catalog number: CC-3121)
4. Microvascular endothelial growth medium (EGM-MV) SingleQuots kit (LONZA, catalog number: CC-4123) [contains growth factors, cytokines, and supplements: bovine brain extract w/o heparin (BBE); hydrocortisone (hEGF); gentamicin, amphotericin B (GA-1000); and FBS]
5. DMSO (Merck KGaA, catalog number: D8418)
6. Dulbecco's modified Eagle's medium/Ham's nutrient mixture F-12 (DMEM-F12-1L) (Merck KGaA, catalog number: D2906)
7. Collagenase type IV (Sigma, catalog number: C-5138)
8. Panobinostat, LBH589 (MedChem Express, catalog number: HY-10224)
9. Trypsin/EDTA solution 0.025% (LONZA, catalog number: CC-5012)
10. Sodium hydrogen carbonate ( $\text{NaHCO}_3$ ) (Merck KGaA, catalog number: S5761)
11. Bi-distilled water (dd $\text{H}_2\text{O}$ )
12. D-PBS, no calcium, no magnesium (Gibco, catalog number: 14190-094)
13. Ammonium chloride ( $\text{NH}_4\text{Cl}$ ) (Carlo Erba, catalog number: 419416, CAS number: 12125-02-9)
14. FcR blocking reagent human (Miltenyi Biotec, catalog number: 130-059-901)
15. Bovine serum albumin (BSA) (Merck KGaA, catalog number: A9747)
16. Sodium azide ( $\text{NaN}_3$ ) (Merck KGaA, catalog number: S2002, CAS number: 26628-22-8)
17. RNeasy Micro kit (Qiagen, catalog number: 74004)
18. TaqMan reverse transcription reagents (Invitrogen, catalog number: N8080234)
19. TaqMan Fast Universal PCR Master Mix (2 $\times$ ), no AmpErase<sup>TM</sup> UNG (Applied Biosystems, catalog number: 4352042)
20. Human GAPD (GAPDH) endogenous control (VIC<sup>TM</sup>/TAMRA<sup>TM</sup> probe, primer limited) (Applied Biosystems, catalog number: 4310884E)
21. TaqMan Gene Expression Assay Mix (20 $\times$ ) (Table 1)

**Table1. TaqMan assay list**

Gene symbol	Gene name	TaqMan assay ID
NPHS1	NPHS1, nephrin	Hs00190446_m1
NPHS2	NPHS2, podocin	Hs00387817_m1
SYNPO	Synaptopodin	Hs00200768_m1
KLF15	Kruppel like factor 15	Hs00362736_m1

22. Paraformaldehyde solution 4% in PBS (PFA) (Santa Cruz, catalog number: sc-281692)
23. Triton X-100 (Merck KGaA, catalog number: X100RS-SG)
24. 4',6-Diamidino-2-phenylindole (DAPI) (Merck KGaA, catalog number: D9542)
25. Goat serum (Vector Laboratories, catalog number: S-1000)
26. Donkey serum (Merck KGaA, catalog number: D9663)
27. Antibodies used for FACS assay and immunofluorescence (Table 2)

**Table 2. Antibodies list**

Antibody	Vendor	Catalog number	Final concentration
<b>Primary antibody</b>			
CD133/2	Miltenyi Biotec	130-090-851	10 µL/test
CD24 (clone SN3)	Santa Cruz	SC-19585	10 µg/mL
mouse IgG1	Miltenyi Biotec	130-106-545	10 µg/mL
mouse IgG2b	Miltenyi Biotec	130-106-547	10 µg/mL
α-Tubulin	Merck KGaA	T6074	2 µg/mL
Sir-Actin	Spirochrome	SC001	1 µM
Nephrin (NPHS1)	R&D system	AF4269	4 µg/mL
Podocin (NPHS2)	Abcam	ab50339	30 µg/mL
<b>Secondary antibody</b>			
Goat anti-mouse IgG1-Alexa Fluor 488	Molecular Probes	A-21121	6 µg/mL
Goat anti-mouse IgG2b-Alexa Fluor 647	Molecular Probes	A-21242	6 µg/mL
Goat anti-mouse IgG1-Alexa Fluor 594	Molecular Probes	A-21125	20 µg/mL
Donkey anti-sheep IgG(H+L)-Alexa Fluor 488	Molecular Probes	A-11015	2 µg/mL
Goat anti-rabbit IgG(H+L)-Alexa Fluor 546	Molecular Probes	A-11035	2 µg/mL

28. Kidney progenitor cell growth medium (see Recipes)
29. Kidney progenitor cell washing medium (see Recipes)
30. Red blood cell lysis buffer (NH<sub>4</sub>Cl 0.08%) (see Recipes)
31. Freezing medium (see Recipes)
32. DMEM-F12 + 10% HyClone defined FBS (see Recipes)
33. FACS buffer (PBS 1× 0.5% BSA - 0.02% NaN<sub>3</sub> buffer) (see Recipes)

## Equipment

1. Pipettes
2. Vacuum filtration system with 0.22 µm cellulose acetate (CA) membrane, 500 mL filters (Corning, catalog number: 430769).
3. Sharp forceps, straight (2-biol, catalog number: 91156-11)
4. Sterile plates 100 mm × 20 mm (Corning, catalog number: 430167)
5. Cell dissociation sieves (Merck KGaA, catalog number: S1145)
6. Screen for cell dissociation, size 80 mesh screens (Merck KGaA, catalog number: S3770)
7. Screen for cell dissociation, size 60 mesh screens (Merck KGaA, catalog number: S1020)
8. Glass pestle
9. Ice bucket
10. 6-well clear TC-treated multiple well plates (Corning, catalog number: 3516)
11. Cryogenic vial (Corning, catalog number: CC430659)
12. Freezing container (Thermo Scientific, catalog number: 5100-0001)
13. 75 cm<sup>2</sup> flask (Corning, catalog number: CC430641)
14. Polypropylene urine container, 120 mL (Biosigma, catalog number: BSC258)
15. Serological pipettes 2 mL (Corning, catalog number: CLS4486)

16. Serological pipettes 5 mL (Corning, catalog number: CLS4487)
17. Serological pipettes 10 mL (Corning, catalog number: CLS4488)
18. 15 mL tube (Corning, catalog number: 430791)
19. 50 mL tube (Corning, catalog number: 430829)
20. 1.5 mL microcentrifuge tubes (Axygen, catalog number: MCT-150-C-S)
21. 0.2 mL RNase-free PCR tubes (Invitrogen, catalog number: AM12225)
22. MicroAmp fast optical 96-well reaction plate with barcode (Applied Biosystems, catalog number: 4346906)
23. MicroAmp optical adhesive film (Applied Biosystems, catalog number: 4360954)
24. GeneExplorer thermal cycler 96 × 0.2 mL (Bioer, catalog number: GE-96G)
25. 7900HT Fast Real-Time PCR system (Applied Biosystems, catalog number: 4351405)
26. Centrifuge with plate holders
27. Inverted phase contrast microscope (Zeiss, Z-AXIO40C)
28. Heracell 150i CO<sub>2</sub> incubator
29. Bürker counting chamber (Merck KGaA, catalog number: BR719505-1EA)
30. Flow cytometer (Miltenyi Biotec, MacsQuant Analyzer)
31. 2-well chamber slide coverslip (Nunc Lab-Tek II, catalog number: 155379PK)
32. Confocal microscope (Leica Microsystems, LEICA SP8 STED 3X confocal microscope)
33. Biological safety cabinet (Angelantoni Life Science Srl, catalog number: CTH48C2)
34. 4 °C fridge, -20 °C freezer, and -80 °C freezer

## Software

1. Flow Cytometry Analysis software (Inivai, Flowlogic software)
2. Confocal microscope acquisition software Las X (Leica Microsystems)
3. Huygens Professional software version 18.04 (Scientific Volume Imaging B.V.)

## Procedure

### A. Human kidney progenitor cells (KPC): isolation, maintenance, and cryopreservation

In this section, we describe how to isolate primary kidney progenitor cells from human tissue. The method we describe exploits the ~50-fold higher proliferative capacity of KPC cells in comparison to other renal cell types in a specific growth medium (Peired et al., 2020). Based on our experience, this method allows to obtain a pure population of viable kidney progenitors more easily than the multi-step process based on separation using magnetic beads.

1. Isolation of KPC from human kidney tissue
  - a. Collect a fragment of kidney cortex (from 1 to 3 cm<sup>3</sup>) from the pole opposite to the tumor. Store the tissue in sterile physiological saline solution during transport to the laboratory. We recommend performing the kidney cell isolation within 1 h after surgical tissue collection.
  - b. Remove the kidney capsule and transfer the sample to a 100 mm sterile dish. Mince the cortex in pieces as small as possible using a scalpel. Add to the dish 5 mL of 750 U/mL collagenase type IV prepared in EBM medium. Incubate for 45 min at 37 °C in the incubator. Neutralize the enzymatic reaction by adding 10 mL of EBM containing 10 % FBS. **CAUTION:** During mincing, maintain the tissue fragments humidified by adding a drop of sterile physiological saline solution.
  - c. Transfer the suspension to graded mesh screens (60 and 80 mesh). Mechanically break down the tissue suspension using a glass pestle and pass it through the 60 and 80 mesh screens. Wash thoroughly with 20 mL of kidney progenitor cell washing medium and recover the flowthrough in a polypropylene urine container. Transfer this suspension to a 50 mL polypropylene tube and centrifuge at 400× g for 5 min at 4 °C.

- d. Aspirate the supernatant and wash the pellet with 5 mL of PBS. Centrifuge at  $400\times g$  for 5 min at 4 °C. Discard the supernatant and resuspend the pellet in 5 mL of red blood cell lysis buffer.
  - e. Incubate for 4 min at 37 °C and then stop the reaction by adding 10 mL of kidney progenitor cell washing medium.
  - f. Centrifuge at  $400\times g$  for 5 min at 4 °C.
  - g. Remove supernatant and resuspend the pellet in 10 mL of kidney progenitor cell growth medium.
  - h. Count cell suspension using a Bürker counting chamber.
  - i. Transfer the cells in  $75\text{ cm}^2$  flask (500,000 cells/flask) in 8 mL/flask kidney progenitor cell growth medium. Label as passage 0.
  - j. Place the cells in a 5% CO<sub>2</sub>, 37 °C incubator.
  - k. After three days, replace the medium with fresh kidney progenitor cell growth medium to remove unattached cells and continue with twice-a-week changes until cells reach 80% confluence. It usually takes 7–10 days.
2. Expansion and sub-culturing of KPC
    - a. Sub-culture when the cells are approximately 80% confluent.
    - b. Aspirate the medium and wash with 6 mL of PBS.
    - c. Aspirate PBS and add 2 mL of a 0.25 mg/mL trypsin/EDTA solution. Incubate in a 37 °C incubator for approximately 5 min. Check under the microscope if cells are detached.
    - d. Neutralize the enzymatic reaction by adding 4 mL of kidney progenitor cell washing medium and collect the cells in a 15 mL polystyrene tube. Centrifuge the cells at  $400\times g$  for 5 min at 4 °C.
    - e. Aspire supernatant without disturbing the cell pellet and resuspend the cells in 5 mL of kidney progenitor cell growth medium.
    - f. Count the number of cells using a Bürker counting chamber.
    - g. Replate the cells in  $75\text{ cm}^2$  flasks with a ratio of 1:3 in kidney progenitor cell growth medium.
    - h. Change medium twice a week during maintenance of cultures in a 5% CO<sub>2</sub>, 37 °C incubator.
  3. Cryopreservation of KPC
    - i. Kidney progenitors are cryo-stored in 1 mL of freezing medium at a density from  $5 \times 10^5$  up to  $1 \times 10^6$  cells/cryogenic vial.
    - a. Aspirate the medium from the  $75\text{ cm}^2$  flask and wash with 6 mL of PBS.
    - b. Aspirate the PBS and add 2 mL of a 0.25 mg/mL trypsin/EDTA solution. Incubate in a 37 °C incubator for approximately 5 min. Check under the microscope if cells are detached.
    - c. Neutralize the enzymatic reaction by adding 4 mL of kidney progenitor cell washing medium and collect the cells in a 15 mL polystyrene tube. Centrifuge the cells at  $400\times g$  for 5 min at 4 °C.
    - d. Aspire supernatant without disturbing the cell pellet and resuspend the cells in 5 mL of kidney progenitor cell growth medium.
    - e. Count the number of cells using a Bürker counting chamber.
    - f. Centrifuge the cells at  $400\times g$  for 5 min at 4 °C.
    - g. Resuspend the cell pellet in freezing medium at a density of  $1 \times 10^6$  cells/mL. Mix well.
    - h. Aliquot in 1 mL per cryovial.
    - i. Transfer the cryovials to a freezing container and put the freezing container into a -80 °C freezer.
    - j. The next day, transfer the cryovials to a liquid nitrogen tank for long-time storage. **CAUTION:** Minimize as much as possible the time cells remain in freezing medium at room temperature. Transfer immediately in the freezing container to -80 °C.
  4. Thawing of kidney progenitor cells
    - a. Thaw a vial of cells. To achieve rapid warming, place the frozen vial into a 37 °C water bath.
    - b. Transfer immediately the content of each vial to a 15 mL tube containing 4 mL of kidney progenitor cell washing medium.
    - c. Centrifuge at  $400\times g$  for 5 min at 4 °C.
    - d. Remove the supernatant and resuspend the cells into 2 mL of kidney progenitor cell growth medium.
    - e. Transfer the cell suspension to  $75\text{ cm}^2$  flasks at a density of approximately 500,000 cells/flask in 8 mL/flask of kidney progenitor cell growth medium. Place the cells in a 5% CO<sub>2</sub>, 37 °C incubator.

## B. Differentiation of KPC into podocytes

1. Detach the cells at 60%–80% confluence with trypsin as described above.
2. Count cells and plate in a 6-well plate at a density of 80,000 cell/well in 1.5 mL/well of kidney progenitor cell growth medium.
3. Place the cells in a 5% CO<sub>2</sub>, 37 °C incubator.
4. After 5–6 h (or when cells are attached to the plate), gently remove the medium and replace with 1.5 mL/well of EBM without any supplement and without serum. Place the cells in a 5% CO<sub>2</sub>, 37 °C incubator.
5. After 16 h, remove the EBM medium and stimulate the cells for 48 h with 1.5 mL/well of differentiation medium containing 0.2 µM panobinostat in DMEM-F12 + 10% HyClone Defined FBS.
6. At the end of differentiation, characterize the cells using qRT-PCR and immunofluorescence. **CAUTION:** To obtain better differentiation results, use cells at early passages (P1–P2).

## Data analysis

### A. Flow cytometry analysis for purity check

It is important to characterize each primary kidney progenitor cell culture, evaluating in the various passages (from passage P0 to at least passage P3) the expression of surface markers CD133 and CD24. To evaluate CD133 and CD24 expression, perform flow cytometry analysis as reported:

1. Detach the cells with trypsin as described above.
2. Count cells.
3. Prepare two 1.5 mL tubes: label one *Isotype control* and the other *Antibody* (CD133 and CD24).
4. Transfer 100,000 cells in each tube.
5. Centrifuge at 400× g for 5 min at 4 °C.
6. Aspirate supernatant without disturbing the cell pellet. Add 5 µL of FcR blocking reagent human on cell pellet.
7. Prepare the staining solutions as follows:
  - a. Isotype control mix I: Add 1 µL of mouse IgG2b (to obtain a final concentration of 10 µg/mL) and 1 µL of mouse IgG1 (to obtain a final concentration of 10 µg/mL) in 98 µL of FACS buffer.
  - b. Antibody mix I: Add 10 µL of CD133/2 (10 µL/test) antibody and 2 µL of CD24 (to obtain a final concentration of 10 µg/mL) antibody in 28 µL of FACS buffer.
8. Add 30 µL of the staining solutions to the corresponding tube containing cells and FcR blocking reagent human. Resuspend the pellet.
9. Incubate on ice for 15–30 min covered with a tin foil.
10. Add 500 µL of FACS buffer.
11. Centrifuge at 400× g for 5 min at 4 °C and aspirate the supernatant without disturbing the cell pellet.
12. Resuspend each pellet in 30 µL of the staining solution II, prepared as follows:  
Staining Solution II: add 1 µL of goat anti-mouse IgG2b-647 (to obtain a final concentration of 5 µg/mL) and 1 µL of goat anti-mouse IgG1-488 (to obtain a final concentration of 5 µg/mL) to 300 µL of FACS buffer.
13. Incubate on ice for 15–30 min covered with a tin foil.
14. Add 500 µL of FACS buffer.
15. Run FACS assay by using MacsQuant Analyzer.
16. Analyze the FACS data using Flowlogic software. A representative FACS assay for kidney progenitor cells is shown in Figure 1. **CAUTION:** Use primary cultures consisting of at least 95% of CD133 and CD24 double-positive cells. The percentage of double-positive cells tend to increase during the first two passages because the kidney progenitor cell growth medium allows the selective growth of undifferentiated kidney progenitors.

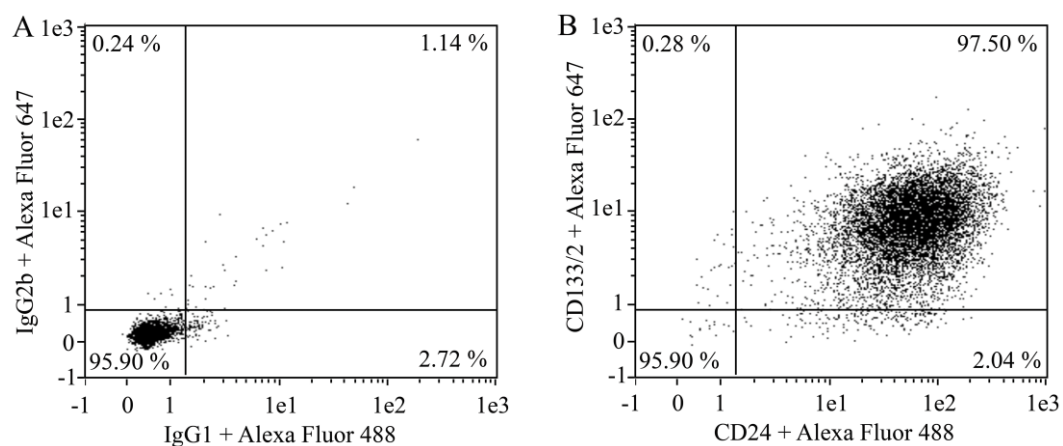


**Figure 1. Evaluation of CD133/2 and CD24 expression in kidney progenitor cells by flow cytometry.** Representative flow cytometry dot plot graphs showing the percentage of CD133 and CD24 positive cells in primary kidney progenitor cells at passage P1 (B). Staining of the same cells with isotype control antibodies is shown in (A).

## B. Evaluation of differentiation

After 48 h of stimuli with differentiation medium, it is possible to evaluate differentiation status of the cells by using qRT-PCR and immunofluorescence (Figure 2).

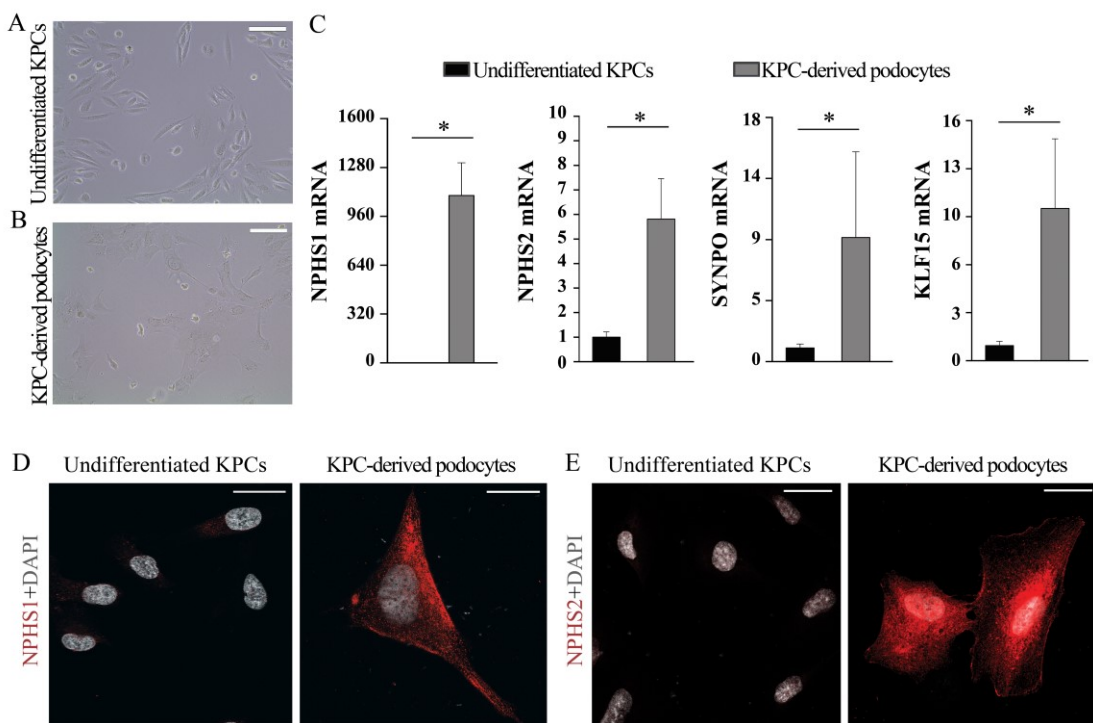


**Figure 2. Evaluation of podocytes derived from kidney progenitor cells.** Representative phase contrast images of (A) undifferentiated kidney progenitor cells and (B) podocytes derived from kidney progenitor cells after 48 h of differentiation. Scale bars, 100  $\mu$ m. (C) qRT-PCR assay of the podocyte markers NPHS1, NPHS2, KLF15, and SYNPO in undifferentiated kidney progenitor cells and in podocytes derived from kidney progenitor cells. mRNA expression of the podocytes markers was determined by qRT-PCR and reported as

mean  $\pm$  SEM of fold increase over undifferentiated cells. (D, E) Representative confocal microscopy images showing expression of the podocyte markers NPHS1 and NPHS2 (red) in undifferentiated kidney progenitor cells and in podocytes derived from kidney progenitor cells. DAPI (white) was used to counterstain nuclei. Scale bars, 25  $\mu$ m. KPC, kidney progenitor cell.

### C. qRT-PCR assay

One of the methods to check the differentiation status of the cells is to use real-time PCR assay to evaluate mRNA expression level of podocyte markers, such as NPHS1, NPHS2, KLF15, and SYNPO. We perform qRT-PCR for each marker on the RNA extracted from an equal number of undifferentiated and differentiated cells independently from the RNA concentration obtained. The qRT-PCR protocol is detailed below:

1. Collect pellets from 100,000 undifferentiated and differentiated cells and extract RNA using the RNeasy Micro kit, followed by the DNase digestion protocol in a final volume of 15  $\mu$ L per sample.
2. Proceed to the synthesis of the cDNA using the TaqMan reverse transcription reagents:
  - a. Prepare the following cDNA synthesis mix on ice in a 0.2 mL PCR tube. Mix thoroughly and centrifuge briefly.

Component	Volume for reaction
10× buffer	5 $\mu$ L
25 mM MgCl <sub>2</sub>	3.5 $\mu$ L
dNTPs	10 $\mu$ L
RNase inhibitor	2.5 $\mu$ L
Random hexamers	2.5 $\mu$ L
Multiscribe (MULV)	2.5 $\mu$ L
RNA	15 $\mu$ L
RNase-free water	To 50 $\mu$ L

3. Proceed with the following incubation protocol in a thermal cycler.

Step	Temperature	Run time
1	25 °C	10 min
2	48 °C	30 min
3	95 °C	5 min
4	4 °C	Hold

4. Collect cDNA synthesis product for qPCR or store in a -20 °C freezer.
5. Prepare the qPCR mix for each podocyte gene (NPHS1, NPHS2, KLF15, or SYNPO) on ice by adding the components below. Mix extra 10% for more reactions. Mix thoroughly and centrifuge briefly.

Component	Volume for one reaction
TaqMan Fast Universal PCR Master Mix (2×)	10 $\mu$ L
TaqMan Assay (NPHS1, NPHS2, KLF15, or SYNPO)	1 $\mu$ L
ddH <sub>2</sub> O	4 $\mu$ L
<b>Final volume</b>	<b>15 <math>\mu</math>L</b>

6. Prepare the qPCR mix for GAPDH housekeeping gene on ice by adding the components below. Mix extra 10% for more reactions. Mix thoroughly and centrifuge briefly.

Component	Volume for one reaction
TaqMan Fast Universal PCR Master Mix (2×)	10 $\mu$ L
GAPDH endogenous control	1 $\mu$ L
ddH <sub>2</sub> O	8 $\mu$ L
<b>Final volume</b>	<b>19 <math>\mu</math>L</b>

7. Dispense 15 µL of the mix for NPHS1, NPHS2, KLF15, or SYNPO into each well of a 96-well PCR plate. For GAPDH, dispense 19 µL of the mix.
8. Add 5 µL of cDNA samples to the well containing the mix for NPHS1, NPHS2, KLF15, or SYNPO and add 1 µL of cDNA samples to the well containing the mix for GAPDH.
9. Seal the plate and centrifuge briefly. Proceed to the incubation below by selecting fast mode:

Step	Temperature	Run time
1	95 °C	20 s
2	95 °C	1 s
3	60 °C	20 s + data collection
4	Repeat steps C2–C3	40 times

10. Perform data analysis: gene expression of each marker is normalized to that of the GAPDH. For each marker, results are reported as fold change of expression of the differentiated cells over undifferentiated cells (Figure 2).

## D. Immunofluorescence

A differentiative program induces morphology changes and leads to cell-specific protein expression that can be evaluated by immunofluorescence assay. The differentiation of kidney progenitor cells into podocytes is confirmed on the basis of the NPHS1 and NPHS2 podocyte marker expression (Figure 2), while the tubulin and actin expression assessed by super-resolution microscopy shows the drastic cytoskeleton changes associated with differentiation (Figure 3). The immunofluorescence procedure is detailed below:

1. Detach the cells with trypsin as described above.
2. Count cells.
3. Plate cells onto a 2-well chamber slide at a density of 20,000 cell/well in 1 mL/well of kidney progenitor cell growth medium.
4. Place the cells in a 5% CO<sub>2</sub>, 37 °C incubator.
5. After 5–6 h (or when cells are attached to the plate), gently remove the medium and replace with 1.5 mL/well of EBM without any supplement and without serum. Place the cells in the incubator with 5% CO<sub>2</sub> and 37 °C.
6. After 16 h, remove the EBM medium and stimulate cells for 48 h with 1 mL/well of 0.2 µM panobinostat in DMEM-F12 + 10% HyClone defined FBS.
7. At the end of the differentiation, remove chamber slides from the incubator.
8. Aspirate the medium and wash the cells with 500 µL/chamber of PBS.
9. Add 1 mL/chamber of 4% PFA and incubate for 20 min at room temperature.
10. Gently wash the slides three times with 1 mL of PBS.
11. Add permeabilizing solution (composed of 0.5% Triton X-100 in PBS) if required from the antibody user manual (antibody information is reported in Table 2 and Table 3) for 5 min at room temperature.

**Table 3. Immunofluorescence details**

Primary antibody		Secondary antibody		Final concentration	Permeabilization	Blocking serum required
Antibody	Final concentration	Antibody	Final concentration			
α-Tubulin	2 µg/mL	Goat anti-mouse IgG1-Alexa Fluor 594	20 µg/mL	Required	Goat	
Sir-Actin	1 µM	/	/	Required	/	
Nephrin (NPHS1)	4 µg/mL	Donkey anti-sheep IgG(H+L)-Alexa Fluor 488	2 µg/mL	Not required	Donkey	
Podocin (NPHS2)	30 µg/mL	Goat anti-rabbit IgG(H+L)-Alexa Fluor 546	2 µg/mL	Required	Goat	

12. Wash for 5 min with PBS.
13. Incubate with blocking solution containing 3% BSA and 0.3% serum (goat or donkey, as reported in Table 3) in PBS.
14. Remove blocking solution without washing.
15. Incubate with primary antibody (Table 3) for 15 min at 37 °C and subsequently for 1 h at 4 °C covered with a tin foil.
16. Wash for 5 min with PBS.
17. Incubate with the secondary antibodies listed in Table 3 and with 1 µg/mL DAPI in PBS 1× for 30 min at room temperature covered with a tin foil to block the light.
18. Acquire images using a LEICA SP8 STED 3X confocal microscope.
19. For STED analysis, frame sequential acquisition can be applied to avoid fluorescence overlap. A 775 nm pulsed-depletion laser was used and a gating between 0.3 and 6 ns was applied to avoid collection of reflection and autofluorescence. Images were acquired with Leica HC PL APO CS2 100×/1.40 oil STED white objective. De-convolve with Huygens Professional software (Romoli et al., 2018).

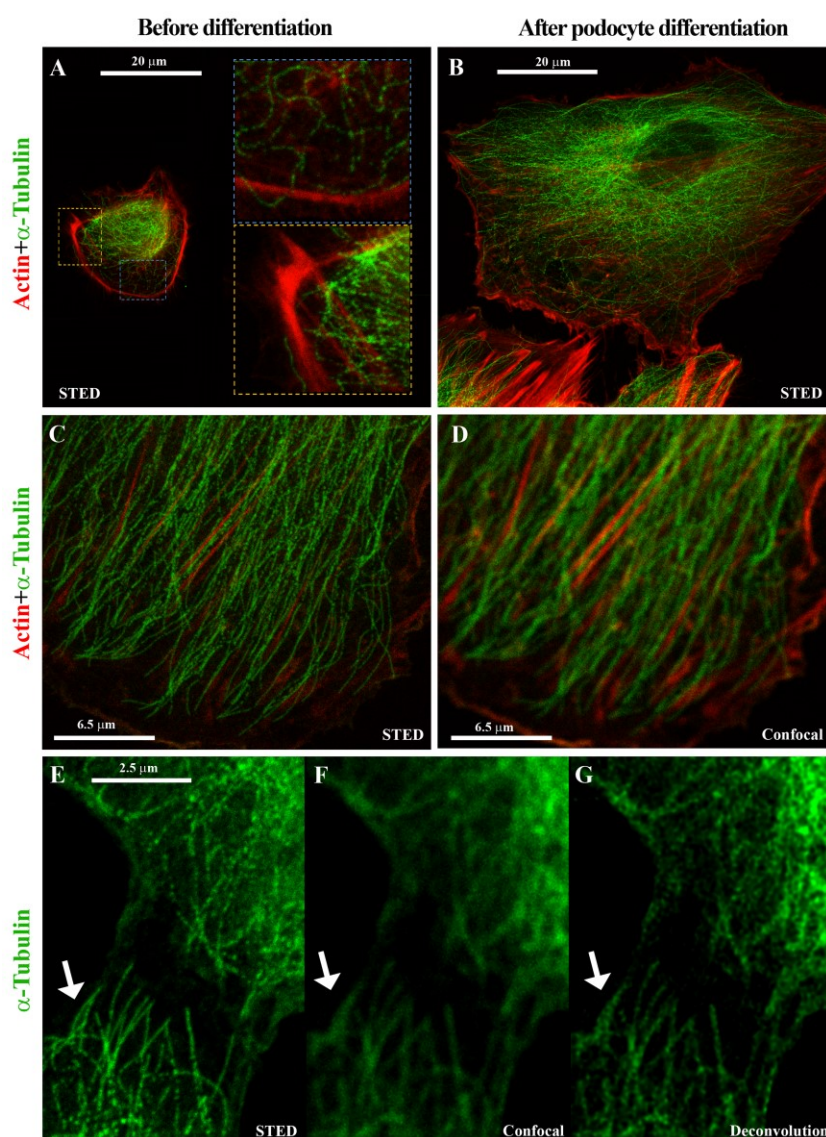


**Figure 3. Stimulated emission depletion (STED) super-resolution microscopy shows cytoskeleton changes associated with differentiation.** Representative STED images showing cytoskeleton changes associated with

differentiation into podocytes based on  $\alpha$ -Tubulin (green) and Actin (red) expression in primary human kidney progenitor cells before (A) and after 48 h differentiation (B–G). Compared to confocal microscopy (D, F), the use of STED microscopy and deconvolution software allows to identify the cytoskeleton organization with nanoscopic spatial resolution (C, E, and G).

## Recipes

### 1. Kidney progenitor cell growth medium (EGM-MV medium + 20% HyClone defined FBS)

The renal progenitor cells are grown in EGM-MV medium supplemented with 20% HyClone defined FBS, prepared as follows:

Supplement 400 mL of EBM medium with BBE and hEGF provided in the microvascular endothelial growth medium (EGM-MV) SingleQuots kit and with 100 mL of HyClone defined FBS. Filter using a vacuum filtration system with 0.22  $\mu$ m CA membrane and store at 4 °C.

### 2. Kidney progenitor cell washing medium (EBM medium + 10% FBS)

Supplement EBM medium with 10% FBS by using the serum provided with the SingleQuots kit (and not used for EGM-MV + 20% HyClone formulation). Other commercial FBS can be used. Filter the solution using a vacuum filtration system with 0.22  $\mu$ m CA membrane.

### 3. Red blood cell lysis buffer (NH<sub>4</sub>Cl 0.08%)

Dissolve 0.4 g of NH<sub>4</sub>Cl in 500 mL of bi-distilled water. Filter using a vacuum filtration system with 0.22  $\mu$ m CA membrane and store at 4 °C.

### 4. Kidney progenitor cell freezing medium

Immediately before freezing the cells, prepare a solution containing HyClone defined FBS supplemented with 10% DMSO.

### 5. DMEM-F12 + 10% HyClone defined FBS

Dissolve 15.6 g of powder DMEM-F12 (one vial of DMEM-F12) in 1 L of MilliQ water and supplement with 1.2 g/L NaHCO<sub>3</sub>. Filter using 0.22  $\mu$ m filters and store at 4 °C. Add FBS HyClone at a final concentration of 10% (w/v) only for the volume of medium necessary for the experiment.

### 6. FACS BUFFER (PBS 1× 0.5% BSA - 0.02% NaN<sub>3</sub> buffer)

Dissolve 2 g of NaN<sub>3</sub> in 10 mL of PBS to obtain a 20% (w/v) NaN<sub>3</sub> stock solution, which can be stored at room temperature for at least two years.

Dissolve 1.25 g of BSA in 250 mL of D-PBS, no calcium, no magnesium, and then add 250  $\mu$ L of 20% NaN<sub>3</sub> stock solution. Store at 4 °C.

## Acknowledgments

This protocol was derived from the original work of Melica et al. (2022).

This study was funded by the European Research Council (ERC) under the European Union's Horizon 2020 research and innovation program (grant agreement no. 101019891). M.E.M. was supported by a FIRC-AIRC fellowship for Italy.

## Competing interests

The authors have no competing financial interests.

## Ethics considerations

Normal-appearing kidney fragments were obtained from the pole opposite to the tumor of patients who underwent nephrectomy for renal tumors, in agreement with the Ethical Committee on human experimentation of the Careggi University Hospital.

## References

- Angelotti, M. L., Ronconi, E., Ballerini, L., Peired, A., Mazzinghi, B., Sagrinati, C., Parente, E., Gacci, M., Carini, M., Rotondi, M., et al. (2012). [Characterization of renal progenitors committed toward tubular lineage and their regenerative potential in renal tubular injury](#). *Stem Cells* 30(8): 1714-1725.
- Kopp, J. B., Anders, H. J., Susztak, K., Podesta, M. A., Remuzzi, G., Hildebrandt, F. and Romagnani, P. (2020). [Podocytopathies](#). *Nat Rev Dis Primers* 6(1): 68.
- Lasagni, L., Angelotti, M., Ronconi, E., Lombardi, D., Nardi, S., Peired, A., Becherucci, F., Mazzinghi, B., Sisti, A., Romoli, S., et al. (2015). [Podocyte Regeneration Driven by Renal Progenitors Determines Glomerular Disease Remission and Can Be Pharmacologically Enhanced](#). *Stem Cell Reports* 5(2): 248-263.
- Lazzeri, E., Angelotti, M. L., Conte, C., Anders, H. J. and Romagnani, P. (2019). [Surviving Acute Organ Failure: Cell Polyploidization and Progenitor Proliferation](#). *Trends Mol Med* 25(5): 366-381.
- Lazzeri, E., Ronconi, E., Angelotti, M. L., Peired, A., Mazzinghi, B., Becherucci, F., Conti, S., Sansavini, G., Sisti, A., Ravaglia, F., et al. (2015). [Human Urine-Derived Renal Progenitors for Personalized Modeling of Genetic Kidney Disorders](#). *J Am Soc Nephrol* 26(8): 1961-1974.
- Melica, M. E., Antonelli, G., Semeraro, R., Angelotti, M. L., Lugli, G., Landini, S., Ravaglia, F., Regina, G., Conte, C., De Chiara, L., et al. (2022). [Differentiation of crescent-forming kidney progenitor cells into podocytes attenuates severe glomerulonephritis in mice](#). *Sci Transl Med* 14(657): eabg3277.
- Peired, A. J., Antonelli, G., Angelotti, M., Allinovi, M., Guzzi, F., Sisti, A., Semeraro, R., Conte, C., Mazzinghi, B., Nardi, S., et al. (2020). [Acute kidney injury promotes development of papillary renal cell adenoma and carcinoma from renal progenitor cells](#). *Sci Transl Med* 12(536): eaaw6003.
- Romagnani, P., Remuzzi, G., Glasscock, R., Levin, A., Jager, K. J., Tonelli, M., Massy, Z., Wanner, C. and Anders, H. J. (2017). [Chronic kidney disease](#). *Nat Rev Dis Primers* 3: 17088.
- Romoli, S., Angelotti, M. L., Antonelli, G., Kumar Vr, S., Mulay, S. R., Desai, J., Anguiano Gomez, L., Thomasova, D., Eulberg, D., Klussmann, S., et al. (2018). [CXCL12 blockade preferentially regenerates lost podocytes in cortical nephrons by targeting an intrinsic podocyte-progenitor feedback mechanism](#). *Kidney Int* 94(6): 1111-1126.
- Sagrinati, C., Netti, G. S., Mazzinghi, B., Lazzeri, E., Liotta, F., Frosali, F., Ronconi, E., Meini, C., Gacci, M., Squecco, R., et al. (2006). [Isolation and characterization of multipotent progenitor cells from the Bowman's capsule of adult human kidneys](#). *J Am Soc Nephrol* 17(9): 2443-2456.
- Shankland, S. J., Pippin, J. W., Reiser, J. and Mundel, P. (2007). [Podocytes in culture: past, present, and future](#). *Kidney Int* 72(1): 26-36.
- Xu, Y., Kuppe, C., Perales-Patón, J., Hayat, S., Kranz, J., Abdallah, A. T., Nagai, J., Li, Z., Peisker, F., Saritas, T., et al. (2022). [Adult human kidney organoids originate from CD24<sup>+</sup> cells and represent an advanced model for adult polycystic kidney disease](#). *Nat Genet* 54(11): 1690-1701.

# Biophysical Analysis of Mechanical Signals in Immotile Cilia of Mouse Embryonic Nodes Using Advanced Microscopic Techniques

Takanobu A. Katoh<sup>1,\*</sup>, Toshihiro Omori<sup>2,\*</sup>, Takuji Ishikawa<sup>2</sup>, Yasushi Okada<sup>3,4</sup>, and Hiroshi Hamada<sup>1</sup>

<sup>1</sup>Laboratory for Organismal Patterning, RIKEN Center for Biosystems Dynamics Research, Kobe, Hyogo, Japan

<sup>2</sup>Graduate School of Biomedical Engineering, Tohoku University, Aoba Aramaki, Sendai, Miyagi, Japan

<sup>3</sup>Laboratory for Cell Polarity Regulation, RIKEN Center for Biosystems Dynamics Research, Suita, Osaka, Japan

<sup>4</sup>Department of Cell Biology and Physics, Universal Biology Institute and International Research Center for Neurointelligence, The University of Tokyo, Hongo, Tokyo, Japan

\*For correspondence: [takanobu.a.katoh@gmail.com](mailto:takanobu.a.katoh@gmail.com); [omori@tohoku.ac.jp](mailto:omori@tohoku.ac.jp)

## Abstract

Immotile cilia of crown cells at the node of mouse embryos are required for sensing leftward fluid flow that gives rise to the breaking of left-right (L-R) symmetry. The flow-sensing mechanism has long remained elusive, mainly because of difficulties inherent in manipulating and precisely analyzing the cilium. Recent progress in optical microscopy and biophysical analysis has allowed us to study the mechanical signals involving primary cilia. In this study, we used high-resolution imaging with mechanical modeling to assess the membrane tension in a single cilium. Optical tweezers, a technique used to trap sub-micron-sized particles with a highly focused laser beam, allowed us to manipulate individual cilia. Super-resolution microscopy allowed us to discern the precise localization of ciliary proteins. Using this protocol, we provide a method for applying these techniques to cilia in mouse embryonic nodes. This method is widely applicable to the determination of mechanical signals in other cilia.

**Keywords:** Left-right symmetry breaking, mRNA imaging, Super-resolution imaging, Optical tweezers, Mathematical modeling, Mechanical Simulation

**This protocol is used in:** Science (2023), DOI: 10.1126/science.abq8148

---

**Cite as:** Katoh, T. A. et al. (2023). Biophysical Analysis of Mechanical Signals in Immotile Cilia of Mouse Embryonic Nodes Using Advanced Microscopic Techniques. *Bio-protocol* 13(14): e4715. DOI: 10.21769/BioProtoc.4715.

Copyright: © 2023 The Authors; exclusive licensee Bio-protocol LLC.

This is an open access article under the CC BY-NC license (<https://creativecommons.org/licenses/by-nc/4.0/>).

## Background

Primary cilia—hair-like protrusions on the cell surface—function as *antennas*. Cilia sense extracellular stimuli, such as flow stimulation, and regulate/organize many signals; one of which governs left-right (L-R) determination (Shinohara and Hamada, 2017). Research concerning flow sensing in cilia began with two techniques: a micropipette (Praetorius and Spring, 2001) and a flow chamber (Nauli et al., 2003) approach. Using these techniques in combination with genetic engineering, we now understand the correlation between flow and chemical reactions, such as calcium responses, within the cilia (Su et al., 2013). However, the sensory capability of cilia with respect to flow, particularly whether cilia sense flow-mediated chemical or mechanical stimuli, is difficult to determine (Ferreira et al., 2019). In this protocol, we provide a method for dissecting the forces acting on cilia.

Recently, Katoh et al. reported the application of optical tweezers (Ashkin, 1970) to a single cilium, which enabled the application of only mechanical force to cilia (Katoh et al., 2018). We further updated this technique to apply to early mouse embryos and combined them with mRNA imaging (Minegishi et al., 2021). We now provide a method for observing the responses to mechanical stimuli by cilia, such as mRNA degradation in ciliated cells (Katoh et al., 2023).

Ascertaining how forces acting on cilia are affected by fluid flow and, in particular, how these forces affect the membrane tension of cilia, is a challenging issue. Owing to the size of cilia, which have a length of ~5 µm and a diameter of only ~200 nm, direct measurement of the tension on the ciliary membrane is difficult. Previously, membrane tension of the cilium was estimated only by flow simulation (Rydholm et al., 2010; Omori et al., 2018). By controlling the extracellular flow and concurrently measuring changes in the shape of cilia using high-resolution microscopy, we first reported the membrane strain of cilia driven by the actual extracellular flow (Katoh et al., 2023). Finally, we introduced a method for analyzing the precise location of membrane proteins in cilia using 3D stimulated emission depletion (STED) (Klar et al., 2000; Vicidomini et al., 2011), a super-resolution microscope whose lateral resolution is close to 30 nm, using a biophysical approach. In this study, we provide useful protocols for applying state-of-the-art microscopy to cilia in mouse embryos. These methods allow us to study mechanical signals in other cilia as well as in other small organelles.

## Materials and reagents

1. Coverslip (18 mm × 18 mm or 24 mm × 24 mm; No. 1S HT, Matsunami)
2. 400 µm silicone rubber spacer (discontinued product; alternatively, use AS ONE, catalog number: 6-9085-14)
3. 100 µm silicone rubber spacer (AS ONE, catalog number: 6-9085-12)
4. Rat serum (purchased from Charles River Laboratories Japan)
5. Fluorescent beads for Point Spread Function (PSF) measurement (Thermo Fisher, catalog number: F8811)
6. Polystyrene beads for optical tweezers (diameter 3.5 µm) (Thermo Fisher, catalog number: S37224)
7. Wide bore tip (Funakoshi, catalog number: T-205-WB-C)
8. FluoroBrite Dulbecco modified Eagle medium (DMEM) (Thermo Fisher, catalog number: A1896701)
9. Anti-acetylated tubulin antibody (Sigma, catalog number: T6793)
10. Anti-green fluorescent protein antibody (Abcam, catalog number: ab13970)
11. Secondary antibody: STAR RED, anti-mouse (Abberior, catalog number: STRED-1001-500UG)
12. Secondary antibody: STAR ORANGE, anti-chick (Abberior, catalog number: STORANGE-1005-500UG)
13. 2,2'-thiodiethanol (TDE) (Tokyo Chemical Industry, catalog number: T0202)
14. 1,4-diazabicyclo[2.2.2]octane (DABCO) (Sigma-Aldrich, catalog number: 290734-100 ML)
15. Triton X-100 (Nacalai Tesque, catalog number: 35501-15)
16. Medium for observation: FluoroBrite DMEM supplemented with 75% rat serum (see Recipes)
17. PBST (see Recipes)
18. TDE-DABCO (see Recipes)

## Equipment

### A. Microscopy for measurement of flow-dependent changes in ciliary shape (Figure 1A and 1B)

1. IX83 microscope (OLYMPUS; equipped with shutter (Sh1))
2. Spinning disk confocal unit (CSU) (Yokogawa, CSU-W1)
3. Objective lens (Obj.1): UPLAPO100XOHR 1.5 N.A. (Olympus)
4. UV laser, 375 nm, 70 mW (Kyocera SOC, JUNO 375)
5. z-Piezo (Physik Instrumente, model: P-721)
6. FL1: red-light band-pass filter (Asahi, model: LV0630)
7. Dichroic mirror (DM1) (Chroma, zt405/488/561rpc)
8. Beam expander (Ex1) (Thorlabs, GBE15-A)
9. Iris (Linos, G061653000)
10. Shutter (Sh2) (SURUGA SEIKI, model: F116)
11. Lens (L1) (Thorlabs, AC254-300-A))
12. EM-CCD camera (Andor, iXon Ultra 888), water cooled (ASONE, LTB-125A)
13. Stage top incubator (Tokai Hit, STXF-IX83WX and GM3000)
14. Optical table (Nippon Boushin Industry, AS-1809)

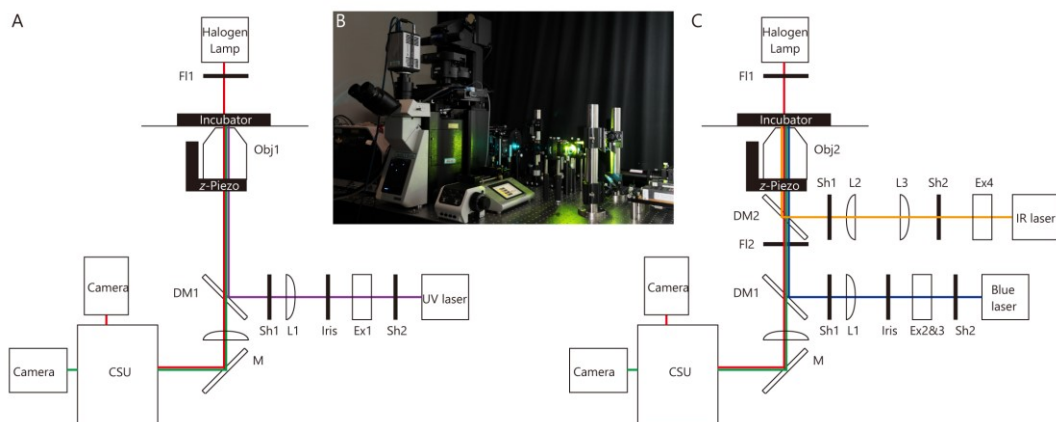


**Figure 1. Microscope and optical pathway.** (A) Microscope for measurement of flow-dependent changes in ciliary shape. (B) Image of the microscope shown in A and C. Optical pathways are constructed on the optical table. (C) Microscope for optical tweezers and whole-cell fluorescence recovery after photobleaching (FRAP). For abbreviations, see Equipment section in the main text.

### B. Microscope for optical tweezers and whole-cell fluorescence recovery after photobleaching (FRAP) (Figure 1B and 1C)

1. IX83 microscope (OLYMPUS; equipped with shutter (Sh1))
2. Spinning disk confocal unit (CSU) (Yokogawa, CSU-W1)
3. Objective lens (Obj2): UPLSAPO 60XW 1.2 N.A. (Olympus)
4. z-Piezo (Physik Instrumente, P-721)
5. Digital analog converter for regulating z-Piezo (USB-DAQ) (National Instruments, USB-6363)
6. Infrared (IR) laser for optical tweezers, 1,064 nm; 5 W (IPG Photonics, YLR-5-1064-LP-SF)
7. Blue laser for irradiation, 488 nm; 55 mW (Coherent, Sapphire)
8. FL1: red-right band-pass filter (Asahi, LV0630)

Cite as: Katoh, T. A. et al. (2023). Biophysical Analysis of Mechanical Signals in Immotile Cilia of Mouse Embryonic Nodes Using Advanced Microscopic Techniques. Bio-protocol 13(14): e4715. DOI: 10.21769/BioProtoc.4715.

9. FL2 (Asahi, SIX870)
10. DM1 (Chroma, zt405/488/561rpc)
11. DM2 (Chroma Technology, ZT1064rdc-sp-UF3). Note that we used ZT1064rdc-sp in Katoh et al. (2023), but that DM is better than this.
12. Beam expander for irradiation (Ex2 and 3) (Sigmakoki, LBED-5 and LBED-3)
13. Beam expander for optical tweezers (Ex4) (Sigmakoki, LBED-4Y)
14. Iris (Linos G061653000) (Opened)
15. Shutter (Sh2) (SURUGA SEIKI, model: F116)
16. Lens for irradiation (L1) (Thorlabs, AC254-300-A)
17. Lens for optical tweezers (L2) (Thorlabs, AC254-200-C)
18. Lens for optical tweezers (L2) (Thorlabs, AC254-150-C)
19. Neutral density (ND) filter for calibration of optical tweezers (only use for calibration measurement): NENIR13B (Thorlabs; transmission at 1064 nm is 3.81%)
20. Motorized XY stage (OptoSigma, BIOS-225T and FC-101G)
21. Stage top incubator (Tokai Hit, STXF-IX83WX and GM3000)
22. Optical table (Nippon Boushin Industry, AS-1809)

### C. Microscope for analyzing Pkd2 distribution

1. TCS SP8 STED 3 $\times$  (Leica)
2. HC PL APO 100 $\times$ /1.40 Oil STED white (Leica)

## Software

1. ImageJ, Fiji (version 1.52a, NIH)
2. Excel (Microsoft)
3. Software for deconvolution of STED microscopy image (Huygens; version 21.10; Scientific Volume Imaging)
4. Software for control of IX83 and CSU (iQ; Version 3.6.3; Andor)
5. Software for control of z-Piezo (LabView 2018; Version 18.0.1f4; National instruments)
6. Software for analyzing Pkd2 distribution (Igor; version 8.0.4.2; WaveMetrics)

## Procedure

### A. Measurement of flow-dependent changes in ciliary shape

1. Mouse E7.5 embryos harboring an *NDE4-hsp-5HT6-mNeonGreen-2A-tdKatushka2* (Katoh et al., 2023) transgene were isolated and roller-cultured as previously described (Behringer et al., 2014).
2. We prepared the medium for observation (see Recipes) by supplementing FluoroBrite DMEM with 75% rat serum. The medium was incubated in a CO<sub>2</sub> incubator.
3. The distal portion of each embryo, including the node, was excised and placed into a chamber, consisting of a glass slide fitted with a thick silicone rubber spacer (thickness of 400  $\mu$ m) to prevent disturbance of nodal flow, and covered with a coverslip (Figure 2). Setting the node region close to the glass surface is very important; however, do not deform the shape of the node to prevent disturbance of nodal flow.

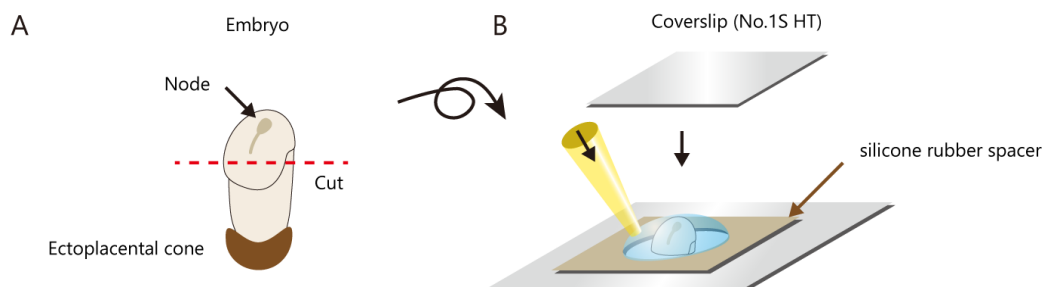


**Figure 2. Schematic of the mounting of the mouse embryonic node.** (A) For imaging, the distal portion of the embryo, including the node, was carefully cut. It is preferable to cut the tissue such that the node is located at the center top of the excised tissue. For immunostaining, the ectoplacental cone was removed (see section D). (B) A silicon rubber spacer was fitted on the glass slide. Excised tissue including the node was then placed in the center of the hole with the medium. The wide bore tip is preferable for usage (see Materials and Reagents). Lastly, it was covered with a coverslip.

4. We perform 3D live imaging using the microscope described above (see Table 1).
 

Setting of the objective: The correction ring was set at  $0.17\text{ }\mu\text{m}$  for  $37\text{ }^{\circ}\text{C}$ . A lens heater ( $37\text{ }^{\circ}\text{C}$ ) was used. Note that the deconvolution calculation (see Data analysis) is sensitive to aberrations.

Setting z-Piezo: the z-stack distance was set to  $200\text{ nm}$ . Typically,  $301$  z-stacks ( $60\text{ }\mu\text{m}$ ) were used.

Setting of the EM-CCD camera: EMGain and A/D were  $999$  and  $10\text{ MHz}$ , respectively.

*Note: When using a high level of EM gain, do not irradiate strong light to the EM-CCD camera to prevent damage to the image sensor.*

**Table 1. Equipment settings for 3D live imaging**

Device	Setting	Parameter
Objective lens	Correction ring	$0.17\text{ }\mu\text{m}$ ( $37\text{ }^{\circ}\text{C}$ )
z-Piezo	z-stack distance	$200\text{ nm}$
	Range	$301$ z-stacks ( $60\text{ }\mu\text{m}$ )
EM-CCD camera	EM gain	$999$
	A/D	$10\text{ MHz}$

5. The center of the node was irradiated with UV to stop the nodal flow (see Figure 1 in Katoh et al., 2023): a  $375\text{ nm}$  laser (set at  $70\text{ mW}$ ; laser power before the objective was  $23\text{ mW}$ ) was radiated for  $45\text{ s}$ . The irradiation duration was controlled by a shutter equipped with an IX83 microscope using iQ software. Laser protection goggles must be worn during this operation.
6. The procedure for 3D live imaging was repeated. The settings were identical to those of the previous imaging. In most embryos, the fluorescence intensity is weak; thus, the laser power for CSU is typically higher than before UV irradiation.  
The obtained 3D images were used for analysis for flow dependent change in angle of cilia and computational mesh generation for calculating membrane tension of cilia, as described below.
7. Measurement of PSF for deconvolution calculation (see Table 2).  
Sample: fluorescent beads were diluted  $1:1,250,000$  in phosphate-buffered saline [PBS(-)] solution. The beads were attached to the glass surface within several minutes.  
3D imaging of a fluorescent bead was performed using the same settings as described in step 4, excluding the use of the EM-CCD camera. To increase S/N, the EM gain and A/D of the EM-CCD camera were set to  $3$  and  $1\text{ MHz}$ , respectively.

**Table 2. Equipment settings for PSF measurement**

Device	Setting	Parameter
Objective lens	Correction ring	0.17 $\mu\text{m}$ (37 °C)
z-Piezo	z-stack distance	200 nm
	Range	301 z-stacks (60 $\mu\text{m}$ )
EM-CCD camera	EM gain	3
	A/D	1 MHz

## B. Manipulation of single cilium by optical tweezers

1. Mouse E7.5 embryos harboring *NDE4-hsp-dsVenus-Dand5-3'-UTR* (Minegishi et al., 2021) and *NDE4-hsp-5HT<sub>6</sub>-GCaMP6-2A-5HT<sub>6</sub>-mCherry* (Mizuno et al., 2020) were isolated and roller-cultured as previously described (Behringer et al., 2014).
2. The medium was prepared as described above.
3. The beads were prepared for trapping. Twenty microliters of polystyrene beads (diameter, 3.5  $\mu\text{m}$ ) were added to 980  $\mu\text{L}$  of FluoroBrite DMEM (1:50 dilution). After centrifugation at 20,300 $\times g$  for 15 min, isolated beads (pellets) were resuspended in 200  $\mu\text{L}$  of FluoroBrite DMEM.
4. A distal portion of each embryo, including the node, was excised and placed into a chamber consisting of a glass slide fitted with a thick silicone rubber spacer (thickness of 400  $\mu\text{m}$ ) to prevent any disturbance of nodal flow (see Figure 2). The embryo was carefully trimmed to obtain a node located parallel to the glass surface to prevent deformation of the embryo during observation.  
A portion of the diluted beads was carefully transferred to the medium above the node with a P2 pipette tip to expose the node to ~1–10 beads, and then carefully covered with a coverslip.
5. Live imaging was performed, and the target cilium was set using the ciliary GCaMP6/mCherry signal. A brightfield image was observed through a red channel of the CSU to check the shape of the embryo.
6. In the case of analysis by whole-cell FRAP later, 3D images of ciliary mCherry and cytoplasmic dsVenus were recorded (typically a z-axis depth of 1  $\mu\text{m}$  with 30 sections).
7. Mechanical stimuli were applied to cilia using the microscope described above. A polystyrene bead was trapped, placed in contact with a cilium, and forced to oscillate along the dorsoventral (D-V) axis for 1.5 h with the use of optical tweezers. Laser protection goggles must be worn during this operation.  
Setting of the objective: the correction ring was set at 0.17  $\mu\text{m}$  for 37 °C. A lens heater (37 °C) was used. Please note that optical tweezers are sensitive to aberrations.  
The setting of the IR laser was 400 mW for ZT1064rdc-sp-UF3 and 800 mW for ZT1064rdc-sp (condition in Katoh et al., 2023).  
Setting z-Piezo and USB-DAQ: a 2 Hz triangle wave with  $1.025 \pm 0.175$  V amplitude was generated using USB-DAQ controlled by the *simulate signal express* function in LabView and applied to the z-Piezo (Figure 3).  
Note that we manually tracked the cilium using a motorized XY stage because most embryos were displaced or deformed during 1.5 h of stimulation.
8. To measure mRNA degradation triggered by mechanical stimuli, we performed whole-cell fluorescence recovery after photobleaching (FRAP) analysis, as described below.
9. Measurement of trapping stiffness:  
Sample: polystyrene beads (diameter 3.5  $\mu\text{m}$ ) were diluted with distilled deionized water (MQ, typically 1:1,000) and placed into a flow chamber (Katoh et al., 2021) made up of a slide glass (24 mm  $\times$  60 mm, No. 1S), a coverslip (24 mm  $\times$  24 mm, No. 1S HT), and two pieces of double-sided tape for spacers (cut approximately 5 mm wide and 40 mm in length).  
Measurement: a single bead was weakly trapped by optical tweezers (typically 3.81 mW: laser power set at 100 mW and a 3.81% ND filter inserted into the optical pathway), and the restricted Brownian motion was measured. Motion of the bead was observed using a brightfield image with a CSU (using the bypass mode). Here, the frame rate needs to be faster than the cut-off frequency of the motion (we typically set this to ~200 fps).

Cite as: Katoh, T. A. et al. (2023). Biophysical Analysis of Mechanical Signals in Immotile Cilia of Mouse Embryonic Nodes Using Advanced Microscopic Techniques. Bio-protocol 13(14): e4715. DOI: 10.21769/BioProtoc.4715.

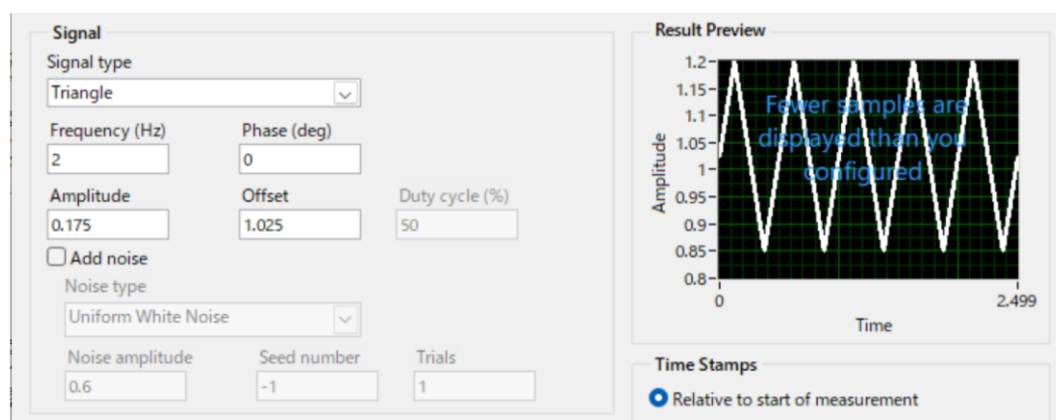


**Figure 3.** Setting of *simulate signal express* function in LabView. z-Piezo applied a 2 Hz triangle wave with an amplitude of  $1.025 \pm 0.175$  V using USB-DAQ.

### C. Measurement of *Dand5* mRNA degradation by whole-cell FRAP

- Whole-cell FRAP is a method for measuring mRNA levels using the level of fluorescence recovery after whole-cell bleaching (Katoh et al., 2023). Before bleaching, 3D images of ciliary mCherry and cytoplasmic dsVenus were recorded (typically, a *z*-axis depth of 1  $\mu\text{m}$  and 30 sections; Table 3).

**Table 3.** Setting of 3D live imaging for whole-cell FRAP

Device	Setting	Parameter
z-Piezo	<i>z</i> -stack distance	1 $\mu\text{m}$
	Range	30 <i>z</i> -stacks (29 $\mu\text{m}$ ; typically)
EM-CCD camera	EM gain	999 (typically)
	A/D	30 MHz (typically)
	Exposure time	200 ms (typically)
	Binning	1 $\times$ 1

- All cells in the node region were uniformly bleached by 3 min irradiation with a 488 nm laser (output power set at 55 mW). The irradiation duration was controlled by a shutter equipped with an IX83 microscope using iQ software (Figure 4A). Laser protection goggles must be worn during this operation.
- Fluorescence recovery was measured by 3D images using the microscope described above (Figure 4B). Setting z-Piezo: the distance of the *z*-stack was set to 1  $\mu\text{m}$ . Typically, 30 *z*-stacks (29  $\mu\text{m}$ ) were observed. Setting of the camera: the fluorescence intensity was quite low compared with that before bleaching. Therefore, we usually employed a  $2 \times 2$  binning mode with a 1 s exposure. 3D images were captured 15 times at 2 min time intervals (total observation duration is 30 min).
- Bleaching was repeated and fluorescence recovery was observed during the repeated process for 30 min (Figure 4A). The intensity in the second fluorescence recovery is low; thus, finally, we observed the 3D image with strong excitation (typically 30–55 mW) and long exposure times (1–4 s in each *z*-stack).
- Analysis of fluorescence recovery is described below (see “Analysis of *Dand5* mRNA levels for whole-cell FRAP experiments”).

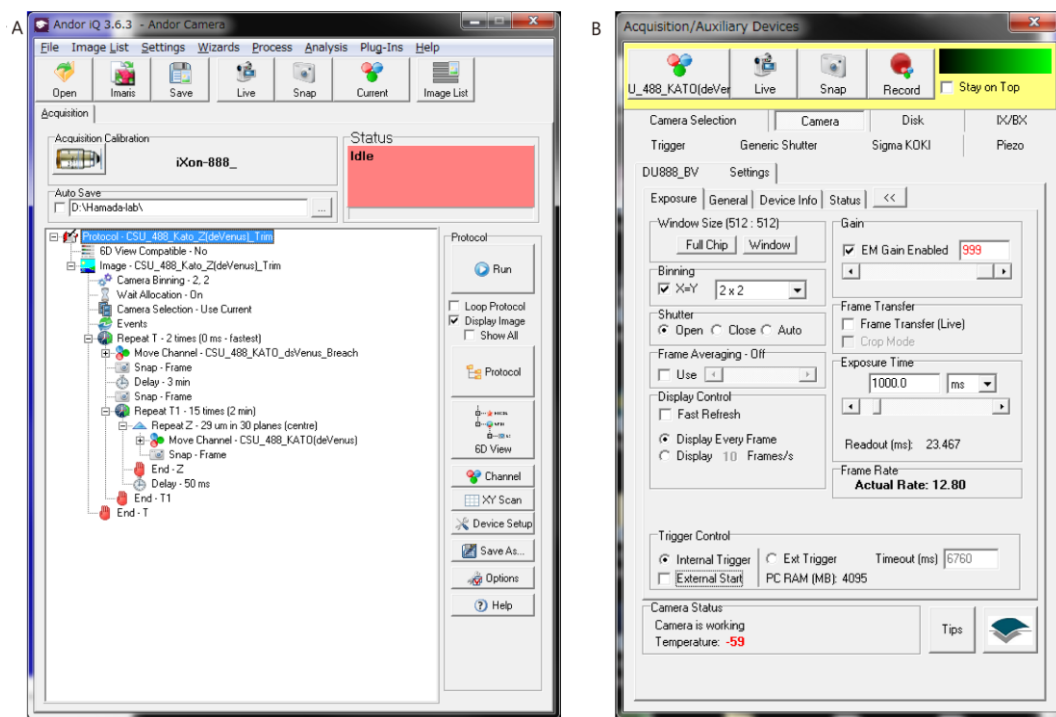


**Figure 4. Setting of iQ.** (A) Screenshot of *Protocol* in iQ. Steps 2–4 are automatically performed using this protocol. (B) Screenshot of *Channel* in iQ, representing the acquisition setting in Step 3.

#### D. Measurement of Pkd2 distribution by 3D-STED imaging

1. Immunostaining was performed as follows:
  - a. Dissection: mouse E7.5 embryos harboring *NDE2-hsp-Pkd2-Venus* (Yoshiba et al., 2012) were recovered in cold PBS(-). The ectoplacental cone was then removed from the embryo (see Figure 2A). For this procedure, we recommend using a 1.5 mL tube (although other sizes work equally well).
  - b. Fixation: embryos were immediately transferred to ice-cold PBS(-). When all embryos had been isolated, they were immediately fixed for 1 h at 4 °C in PBS containing 4% paraformaldehyde.
  - c. Rinse: embryos were washed three times with PBS containing 0.01% Triton X-100 (PBST; see Recipes).
  - d. Permeabilization: 30 min at room temperature in PBS containing 0.2% Triton X-100.
  - e. Rinse: embryos were washed three times with PBST.
  - f. Primary antibody: incubated overnight at 4 °C with acetylated tubulin (1:200 dilution) and green fluorescent protein (1:200 dilution) antibodies diluted in PBST.
  - g. Rinse and wash: antibodies were washed three times with PBST. During this, it is preferable to change the tube. Then, wash > 6 times with PBST at 1 h intervals.
  - h. Secondary antibody was incubated overnight at 4 °C with STAR RED (1:200 dilution, anti-mouse) and STAR ORANGE (1:200 dilution, anti-chick) antibodies diluted in PBST.
2. Mounting was performed as follows:  
Mounting solution: TDE-DABCO (see Recipes)
  - a. A distal portion of each embryo, including the node, was excised and the node region was placed in PBST containing 10% TDE-DABCO. In the final step, the node should be located close to the glass surface, as described below, to prevent resolution reduction—so, carefully trim the embryo.
  - b. The node region was transferred to PBST containing 20% TDE-DABCO.
  - c. The node region was transferred to PBST containing 50% TDE-DABCO.
  - d. The node region was transferred to TDE-DABCO.
  - e. The node region was placed into a chamber consisting of a glass slide fitted with a thin silicone rubber

Cite as: Katoh, T. A. et al. (2023). Biophysical Analysis of Mechanical Signals in Immotile Cilia of Mouse Embryonic Nodes Using Advanced Microscopic Techniques. Bio-protocol 13(14): e4715. DOI: 10.21769/BioProtoc.4715.

spacer (thickness 100  $\mu\text{m}$ ) and then carefully covered with a coverslip (see Figure 2). In this step, it is very important for the node to be close to the coverslip without deforming the shape of the node. Please note that we index-matched samples to minimize spherical aberration.

- f. Finally, it was sealed with nail polish. Samples were stored at 4 °C for approximately one week.
3. 3D-STED observation: 3D-STED imaging was performed as follows:  
Bit depth: 16 bit  
Channel 1: excitation wavelength 561 nm (white light laser pulse), detection wavelength for HyD 571–623 nm, gating 0.3–6 ns, depletion wavelength 775 nm (pulse)  
Channel 2: excitation wavelength 633 nm (white light laser pulse), detection wavelength for HyD 650–700 nm, gating 0.3–6 ns, depletion wavelength 775 nm (pulse)  
z-donut: 60%–80% (typically 80%)  
Pinhole setting: 0.5 AU at 640 nm  
Before observation, it is better to perform *Beam alignment*.  
Note that in STED microscopy, the excitation light is overlapped with the STED beam, quenching excited molecules in the excitation spot periphery. In this setting, we used the same wavelength of the STED beam for Channel 1 and Channel 2 (see depletion wavelength), so chromatic aberration does not occur.
4. Analysis of 3D images is described below in *Analysis of Pkd2 distribution for STED images*.

## Data analysis

### A. Analysis for flow dependent change in angle of cilia

1. Deconvolution calculation of 3D images: 3D deconvolution calculations were performed using DeconvolutionLab2 (Sage et al., 2017) (Figure 5A).  
Settings of DeconvolutionLab2:  
Algorithm: Richardson-Lucy Total Variation  
Iterations (N): 100  
Regularization parameter  $\lambda$ :  $10^{-12}$

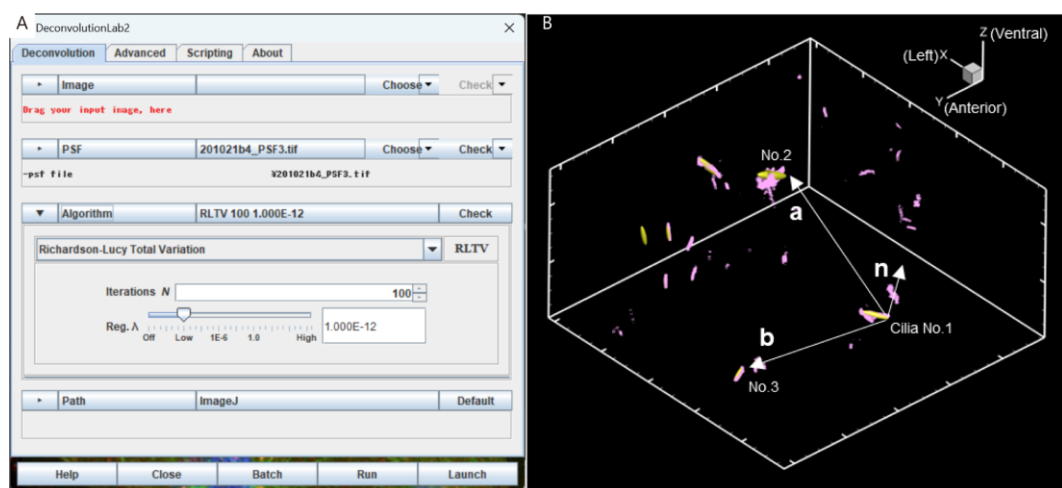


**Figure 5. Setting for deconvolution and correction of the three-dimensional orientation of the embryo.** (A) Screenshot of DeconvolutionLab2. (B) Define two vectors  $a$  and  $b$  from the base positions of the three cilia and calculate their outer product  $n = a \times b$ . The same process is applied to two different images (before and after UV irradiation) and the images are corrected so that the respective  $n$ -vectors match.

2. An 8-bit transformation of the image was performed and location information on the ciliated surface was extracted from ImageJ's *Gaussian Filter* and *Find Edges* convolution functions.
3. To quantify the three-dimensional orientation of the embryo, the basal positions of the three cilia were detected, which were defined as  $r_1$ ,  $r_2$ , and  $r_3$ .
4. Two vectors,  $a (= r_2 - r_1)$  and  $b (= r_3 - r_1)$ , were defined from the three basal positions, as shown in Figure 5B, and one normal vector,  $n = a \times b$ , was determined by the outer product of these vectors.
5. The  $n$ -vector in both the pre- and post-UV irradiation images was found, and these images were then rotated such that the two  $n$ -vectors coincide.
6. Ellipsoid fitting was performed on the ciliary geometry obtained from the microscopic images. The ciliary posture was defined by determining the declination of the ellipsoid major axis with respect to the dorsoventral axis.
7. Ciliary deformation was defined based on the change in the angle before and after UV irradiation.

## B. Computational mesh generation for calculating membrane tension of cilia

1. The cross-sectional centers of the cilia in the z-stack of each 3D image were determined.
2. Spline interpolation was applied to represent a smooth curve connecting the centers of each z-section.
3. We defined circles of radius 100 nm each in the direction normal to the centerline, as shown in Figure 6.

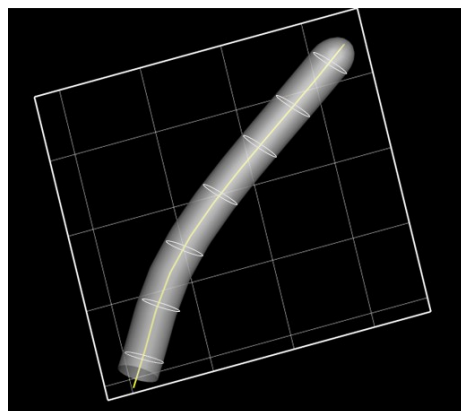


**Figure 6. Computational mesh generation to represent the ciliated membrane surface.** The ciliated surface is represented as a cylindrical surface with a series of circles of radius 100 nm normal to the centerline (yellow line). Grid size, 1.6  $\mu\text{m}$ .

4. The surface of the ciliary membrane was defined by connecting each circumference in the direction of the longitudinal axis.
5. A computational mesh was generated by discretizing the defined membrane surface by triangles.
6. The cilia shape after UV irradiation was defined as the reference shape and the shape before UV irradiation was used to calculate the elastic deformation of the cilia.

## C. Analysis of *Dand5* mRNA levels for whole-cell FRAP experiments

1. As described in Figure S6 and the Methods section in Katoh et al. (2023), our whole-cell FRAP system with *NDE4-hsp-dsVenus-Dand5-3'-UTR* transgene (Minegishi et al., 2021) can directly measure *Dand5* mRNA levels as the final (plateau) intensity. In this analysis, we used three 3D images: the image captured before stimuli, the last image of first fluorescence recovery, and the final image of second fluorescence recovery.
2. Measurement of intensity before stimulation:

- a. We first find a cell with a stimulated cilium and neighboring unstimulated ciliated cells (typically two unstimulated cells).
  - b. The suitable size of the region of interest (ROI) for these cells was set, and the average intensity in each of them was measured using ImageJ/Fiji.
  - c. The background intensity was measured using the region in the center of the node.
  - d. Finally, we calculated the following ratio:  $Ratio_0 = 2(I_S - I_B)/(I_{N1} + I_{N2} - 2I_B)$ , where  $I_S$ ,  $I_B$ ,  $I_{N1}$ , and  $I_{N2}$  are the intensity in stimulated cells, background intensity, intensity in neighboring unstimulated cell number #1, and intensity in neighboring unstimulated cell number #2, respectively.
3. Measurement of the intensity in the last image of first fluorescence recovery.
    - a. The stimulated cilium and the unstimulated cells were carefully identified. This was difficult because embryos are usually deformed during long-term observations. To identify target cells, we used movies taken during optical tweezer experiments, and 3D timelapse images during the FRAP experiment.
    - b. The intensity of each cell and the background intensity were measured as described above. We then calculated the  $Ratio_1$  as described above.
  4. Measurement of the intensity in the final image of second fluorescence recovery:  
The cells were carefully identified, the intensity of each cell was measured, and the background intensity was measured as described above. We then calculated  $Ratio_2$ , as described above.
  5. Finally, the normalized values were calculated: mRNA levels 30 min after stimuli (%) =  $Ratio_1/Ratio_0$ , mRNA levels 1 h after stimuli (%) =  $Ratio_2/Ratio_0$

## D. Analysis of Pkd2 distribution for STED imaging

1. Deconvolution calculation by Huygens software
  - a. Firstly, we directly read a .lif file by Huygens and then started the deconvolution wizard. The settings of the deconvolution wizard were as follows:  
Stabilization: On  
Deconvolution algorithm: classical maximum likelihood estimation (CMLE)  
PSF estimation: as close guess, Max detail
  - b. The calculated image was saved.  
A higher bit depth is better for subsequent analysis; therefore, we save the image as a .ome file in Huygens. The file was then opened by Fiji. When the image is opened by Fiji, it is flipped vertically, so we should reflip vertically. This image was saved as a .tiff file.
2. Analysis of angular distribution  
We used a custom-written macro that runs in Igor software. The details of this macro are as follows:
  - a. First, using ImageJ, the location of a single cilium in a 3D image was memorized as the width, depth, height,  $x$ ,  $y$ , and  $z$  values of the ROI. The threshold values in the red and green channels were measured to extract the signal. Then, the 3D tiff image was loaded with Igor.
  - b. When the cilium elongates along the  $z$ -axis, we calculated the center of gravity of the red channel in each  $xy$  plane (each z-stack). We typically use the threshold value for the red channel as the background. However, the background affects this calculation; therefore, it is preferable to carefully set the background. The resulting  $(x, y)$  coordinates represent the cilium center in each z-stack.  
When the cilium elongates along the  $x$ - or  $y$ -axis, we calculated the center in  $yz$  or  $xz$  planes using the same method.
  - c. The angle of the Pkd2 channel was calculated. If the  $z$ -plane had a Pkd2 signal above the threshold, we calculated the following and saved it as an array.  
Angle from the center of the cilia to the Pkd2 signal using arctangent function  $\theta$   
Distance from the center of cilia to the Pkd2 signal:  $r$   
Intensity:  $I$
  - d. The intensity was accumulated at each angle in each cilium. We extracted pixels whose  $r$  was close to the cilium (we usually set 500–1,000 nm) to exclude the non-ciliary signal. Then, all  $I$  values are accumulated at each  $\theta$  angle (typically a 45° sector) in every cilium.
  - e. All data from each cilium were plotted in one figure such as Figure 4B in Katoh et al. (2023).

Cite as: Katoh, T. A. et al. (2023). Biophysical Analysis of Mechanical Signals in Immotile Cilia of Mouse Embryonic Nodes Using Advanced Microscopic Techniques. Bio-protocol 13(14): e4715. DOI: 10.21769/BioProtoc.4715.

## Recipes

### 1. Medium for observation: FluoroBrite DMEM supplemented with 75% rat serum

We usually store 1 mL of 100% rat serum in sterile tubes at -80 °C and 10 mL of FluoroBrite DMEM in Corning tubes at 4 °C (long-term storage at -80 °C). Just before use, we mix 3 mL of rat serum with 1 mL of FluoroBrite DMEM on a clean bench.

### 2. PBST

100 µL of Triton X-100  
1 L of PBS(-)

### 3. TDE-DABCO

11.5 g of TDE  
250 µL of DABCO  
150 µL of 1 M Tris-HCl (pH 8.0)

## Acknowledgments

We thank K. Mizuno, K. Minegishi, X. Sai, and all members of the Laboratory for Organismal Patterning for improving the protocol; K. Kawaguchi and members of his laboratory for support in developing the analysis method for Pkd2 distribution for STED images; and D. Takao for support with STED imaging.

This study was supported by grants from the Ministry of Education, Culture, Sports, Science, and Technology (MEXT) of Japan (No. 17H01435) and Core Research for Evolutional Science and Technology (CREST) of the Japan Science and Technology Agency (JST) (No. JPMJCR13W5) to H.H.; by a Grant-in-Aid (No. 21K15096) from the Japan Society for the Promotion of Science (JSPS); by the RIKEN Special Postdoctoral Researcher Program to T.A.K.; by a grant from Precursory Research for Embryonic Science and Technology (PRESTO) of JST (No. JPMJPR2142) to T.O. 3D-STED microscopy was supported by grants from JST (Nos. JPMJMS2025-14, JPMJCR20E2, JPMJCR15G2, and JPMJCR1852), and JSPS (Nos. 19H05794 and 16H06280) to Y.O.

This protocol is derived from the original research paper (Katoh et al., 2023).

## Competing interests

The authors declare no competing interests.

## Ethical considerations

All animal experiments were approved by the Institutional Animal Care and Use Committee of RIKEN Kobe Branch.

## References

- Ashkin, A. (1970). [Acceleration and Trapping of Particles by Radiation Pressure](#). *Phys Rev Lett* 24(4): 156-159.
- Behringer, R., Gertsenstein, M., Nagy, K. V. and Nagy, A. (2014). [Manipulating the mouse embryo: a laboratory manual](#). Cold Spring Harbor Laboratory Press. ISBN: 9781936113002, 9781936113019.
- Ferreira, R. R., Fukui, H., Chow, R., Vilfan, A. and Vermot, J. (2019). [The cilium as a force sensor-myth versus reality](#). *J Cell Sci* 132(14): jcs213496.

Cite as: Katoh, T. A. et al. (2023). Biophysical Analysis of Mechanical Signals in Immobile Cilia of Mouse Embryonic Nodes Using Advanced Microscopic Techniques. Bio-protocol 13(14): e4715. DOI: 10.21769/BioProtoc.4715.

- Katoh, T. A., Daiho, T., Yamasaki, K., Danko, S., Fujimura, S. and Suzuki, H. (2021). [Angle change of the A-domain in a single SERCA1a molecule detected by defocused orientation imaging](#). *Sci Rep* 11(1): 13672.
- Katoh, T. A., Ikegami, K., Uchida, N., Iwase, T., Nakane, D., Masaike, T., Setou, M. and Nishizaka, T. (2018). [Three-dimensional tracking of microbeads attached to the tip of single isolated tracheal cilia beating under external load](#). *Sci Rep* 8(1): 15562.
- Katoh, T. A., Omori, T., Mizuno, K., Sai, X., Minegishi, K., Ikawa, Y., Nishimura, H., Itabashi, T., Kajikawa, E., Hiver, S., et al. (2023). [Immotile cilia mechanically sense the direction of fluid flow for left-right determination](#). *Science* 379(6627): 66-71.
- Klar, T. A., Jakobs, S., Dyba, M., Egner, A. and Hell, S. W. (2000). [Fluorescence microscopy with diffraction resolution barrier broken by stimulated emission](#). *Proc Natl Acad Sci USA* 97(15): 8206-8210.
- Minegishi, K., Rothe, B., Komatsu, K. R., Ono, H., Ikawa, Y., Nishimura, H., Katoh, T. A., Kajikawa, E., Sai, X., Miyashita, E., et al. (2021). [Fluid flow-induced left-right asymmetric decay of Dand5 mRNA in the mouse embryo requires a Bicc1-Ccr4 RNA degradation complex](#). *Nat Commun* 12(1): 4071.
- Mizuno, K., Shiozawa, K., Katoh, T. A., Minegishi, K., Ide, T., Ikawa, Y., Nishimura, H., Takaoka, K., Itabashi, T., Iwane, A. H., et al. (2020). [Role of Ca<sup>2+</sup> transients at the node of the mouse embryo in breaking of left-right symmetry](#). *Sci Adv* 6(30): eaba1195.
- Nauli, S. M., Alenghat, F. J., Luo, Y., Williams, E., Vassilev, P., Li, X., Elia, A. E., Lu, W., Brown, E. M., Quinn, S. J., et al. (2003). [Polycystins 1 and 2 mediate mechanosensation in the primary cilium of kidney cells](#). *Nat Genet* 33(2): 129-137.
- Omori, T., Winter, K., Shinohara, K., Hamada, H. and Ishikawa, T. (2018). [Simulation of the nodal flow of mutant embryos with a small number of cilia: comparison of mechanosensing and vesicle transport hypotheses](#). *R Soc Open Sci* 5(8): 180601.
- Praetorius, H. A. and Spring, K. R. (2001). [Bending the MDCK Cell Primary Cilium Increases Intracellular Calcium](#). *J Membr Biol* 184(1): 71-79.
- Rydholm, S., Zwart, G., Kowalewski, J. M., Kamali-Zare, P., Frisk, T. and Brismar, H. (2010). [Mechanical properties of primary cilia regulate the response to fluid flow](#). *Am J Physiol Renal Physiol* 298(5): F1096-1102.
- Sage, D., Donati, L., Soulez, F., Fortun, D., Schmit, G., Seitz, A., Guiet, R., Vonesch, C. and Unser, M. (2017). [DeconvolutionLab2: An open-source software for deconvolution microscopy](#). *Methods* 115: 28-41.
- Shinohara, K. and Hamada, H. (2017). [Cilia in Left-Right Symmetry Breaking](#). *Cold Spring Harb Perspect Biol* 9(10): a028282.
- Su, S., Phua, S. C., DeRose, R., Chiba, S., Narita, K., Kalugin, P. N., Katada, T., Kontani, K., Takeda, S. and Inoue, T. (2013). [Genetically encoded calcium indicator illuminates calcium dynamics in primary cilia](#). *Nat Methods* 10(11): 1105-1107.
- Vicidomini, G., Moneron, G., Han, K. Y., Westphal, V., Ta, H., Reuss, M., Engelhardt, J., Eggeling, C. and Hell, S. W. (2011). [Sharper low-power STED nanoscopy by time gating](#). *Nat Methods* 8(7): 571-573.
- Yoshiba, S., Shiratori, H., Kuo, I. Y., Kawasumi, A., Shinohara, K., Nonaka, S., Asai, Y., Sasaki, G., Belo, J. A., Sasaki, H., et al. (2012). [Cilia at the node of mouse embryos sense fluid flow for left-right determination via Pkd2](#). *Science* 338(6104): 226-231.

## Tracking the Subcellular Localization of Surface Proteins in *Staphylococcus aureus* by Immunofluorescence Microscopy

Salvatore J. Scalfidi<sup>#</sup>, Mac A. Shebes<sup>#</sup> and Wenqi Yu\*

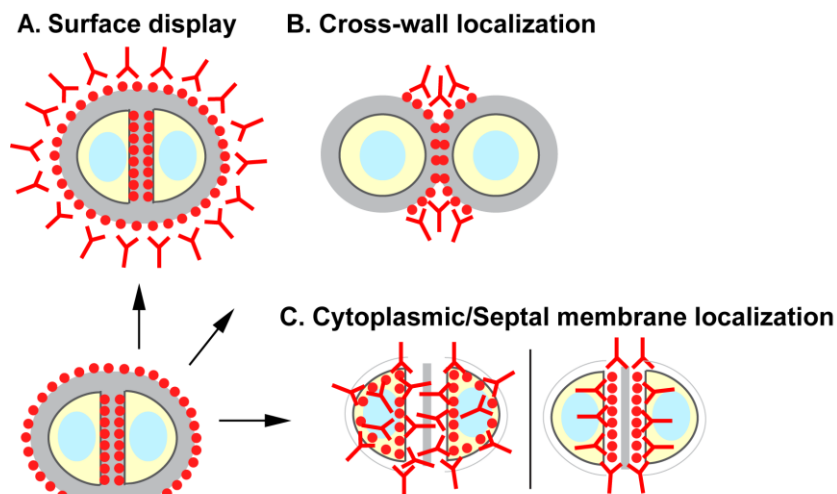
Department of Cell Biology, Microbiology and Molecular Biology, University of South Florida, Tampa, FL, USA

\*For correspondence: [wenqiyu@usf.edu](mailto:wenqiyu@usf.edu)

<sup>#</sup>Contributed equally to this work

**[Abstract]** Surface proteins of *Staphylococcus aureus* and other Gram-positive bacteria play essential roles in bacterial colonization and host-microbe interactions. Surface protein precursors containing a YSIRK/GXXS signal peptide are translocated across the septal membrane at mid-cell, anchored to the cell wall peptidoglycan at the cross-wall compartment, and presented on the new hemispheres of the daughter cells following cell division. After several generations of cell division, these surface proteins will eventually cover the entire cell surface. To understand how these proteins travel from the bacterial cytoplasm to the cell surface, we describe a series of immunofluorescence microscopy protocols designed to detect the stepwise subcellular localization of the surface protein precursors: surface display (protocol A), cross-wall localization (protocol B), and cytoplasmic/septal membrane localization (protocol C). Staphylococcal protein A (SpA) is the model protein used in this work. The protocols described here are readily adapted to study the localization of other surface proteins as well as other cytoplasmic or membrane proteins in *S. aureus* in general. Furthermore, the protocols can be modified and adapted for use in other Gram-positive bacteria.

### Graphic abstract:



### Tracking the subcellular localization of surface proteins in *S. aureus*

**Keywords:** Immunofluorescence microscopy, *Staphylococcus aureus*, Surface proteins, YSIRK/GXXS signal peptide, Protein A (SpA), SecA, Surface display, Cross-wall localization, Septal localization

**[Background]** *Staphylococcus aureus* is a Gram-positive bacterium and an opportunistic pathogen. It frequently colonizes human nares and skin and is a leading cause of both hospital- and community-acquired infections (von Eiff *et al.*, 2001; Tong *et al.*, 2015). The cell envelope of *S. aureus* consists of a cytoplasmic membrane and a thick cell wall peptidoglycan layer. To replicate, *S. aureus* undergoes binary fission by forming a division septum at the mid-cell. The cell wall biosynthesis machinery is recruited to the septum during cell division (Pinho and Errington, 2003). New cell wall peptidoglycan is synthesized to form a cross-wall ring and eventually a cross-wall disc coupled with the invagination of the septal membrane (Zhou *et al.*, 2015). Once the cross-wall disc is fully synthesized, specific cell wall hydrolases cleave at the outer edges of the cross-wall to split the two daughter cells (Oshida *et al.*, 1995; Sugai *et al.*, 1995; Yamada *et al.*, 1996; Kajimura *et al.*, 2005). Due to high internal turgor pressure, the two daughter cells separate from each other and the newly synthesized cross-wall discs become the new hemispheres of the daughter cells (Monteiro *et al.*, 2015; Zhou *et al.*, 2015).

Cell wall peptidoglycan-anchored surface proteins are key components of the Gram-positive bacterial cell envelope. Many of them perform virulence functions in *S. aureus*, such as adhesion, biofilm formation, nutrient acquisition, antibiotic resistance, and immune evasion (Foster *et al.*, 2014; Schneewind and Missiakas, 2019). Many surface protein precursors contain a specific N-terminal signal peptide with a highly conserved YSIRK/GXXS motif (Rosenstein and Götz, 2000; Tettelin *et al.*, 2001). The secretion, cell wall anchoring, and surface display of YSIRK/GXXS proteins are tightly coupled with the bacterial cell cycle (Carlsson *et al.*, 2006; Raz *et al.*, 2012; Yu *et al.*, 2018). In the early stages, the YSIRK/GXXS signal peptide promotes localized protein secretion at the division septum (Carlsson *et al.*, 2006; DeDent *et al.*, 2008). Subsequently, septal secreted surface proteins are covalently anchored to the cross-wall peptidoglycan by sortase A (Mazmanian *et al.*, 1999). Upon cell division and separation, cross-wall-anchored surface proteins are displayed on the surface of the new hemisphere of the daughter cells (Cole and Hahn, 1962; Swanson *et al.*, 1969; Raz *et al.*, 2012; Yu *et al.*, 2018). Eventually, surface proteins are displayed on the entire cell surface after several generations of cell division (DeDent *et al.*, 2008; Raz *et al.*, 2012; Yu *et al.*, 2018).

Proper imaging methods are essential in revealing the subcellular localization of proteins. Here, we describe a series of protocols to track the subcellular localization of surface proteins. While it is straightforward to localize proteins on bacterial cell surface (protocol A, Figure 1), a “pulse-chase” type of method is used to reveal the localization of newly anchored surface proteins. In their classical paper, Cole and Hahn (1962) described an immunofluorescence staining method in which streptococcal cells were incubated with fluorescently labeled surface protein M antibody and subsequently with non-fluorescent antibody. In another classical study, streptococci were trypsin-treated to digest the existing M protein on the bacterial surface; new surface-deposited M protein was observed after re-incubating the bacteria in fresh medium without trypsin (Swanson *et al.*, 1969). The method of trypsinization followed by regeneration has subsequently been used to localize newly anchored surface proteins on the cell surface of both streptococci and staphylococci (Carlsson *et al.*, 2006; DeDent *et al.*, 2008; Raz *et al.*, 2012; Yu *et al.*, 2018). Here, we provide a detailed description of the protocol that is specifically tailored to *S. aureus* (protocol B, Figure 1). The model protein we use is protein A (SpA), one of the major staphylococcal surface proteins that binds to host immunoglobulin and disrupts host immune responses (Forsgren and Sjöquist, 1966).

We have previously shown that SpA engages the SecA-mediated secretion pathway for translocation across the cytoplasmic membrane (Yu *et al.*, 2018). To reveal where SpA precursors accumulate in the cytoplasm upon *secA* depletion, we developed a protocol to detect the localization of intracellular proteins (protocol C, Figure 1) based on methods described earlier by Harry *et al.*, (1995) and Pinho and Errington (2003). In this protocol, staphylococcal cells are fixed with paraformaldehyde and glutaraldehyde, which adhere to the poly-L-lysine-coated glass slide. Cells are digested on the slide with a robust staphylococcal cell wall hydrolase, lysostaphin, to generate protoplasts (Schindler and Schuhardt, 1964). The protoplasts are fixed and permeabilized with methanol and acetone, respectively, and subsequently subjected to immunofluorescence staining. Depending on the genetic background of different strains, protocol C can be used to localize membrane-bound or cytoplasmic-localized surface protein precursors. Furthermore, protocol C is not restricted to surface proteins; it can be used to localize cytoplasmic or membrane proteins in *S. aureus* in general. The protocols described here can also be adapted for use in other Gram-positive bacteria.

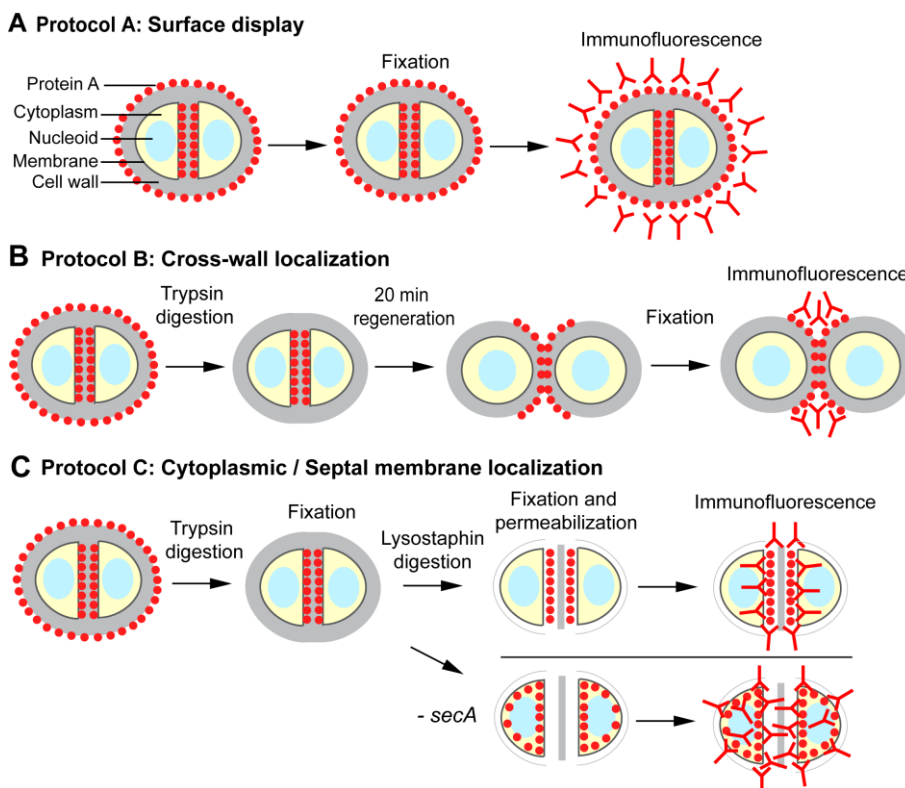


**Figure 1. Schematic overview of the protocols described in this work**

## **Materials and Reagents**

1. 8-well glass slides (MP Biomedicals/Thermo Fisher Scientific, catalog number: 096040805E)
2. Disposable borosilicate glass tubes, 16 mm diameter, 125 mm length (Thermo Fisher Scientific, catalog number: 1496130)
3. 1,250 µl XL graduated tips (USA Scientific, catalog number: 1112-1720)
4. 200 µl graduated tips (USA Scientific, catalog number: 1110-1700)

5. 10 µl graduated tips (USA Scientific, catalog number: 1111-3700)
6. 10 ml serological pipets (Thermo Fisher Scientific, catalog number: 1367811E)
7. 25 ml serological pipets (Thermo Fisher Scientific, catalog number: 13-678-11)
8. 1.5 ml microcentrifuge tubes (Thermo Fisher Scientific, catalog number: 05-408-129)
9. 2.0 ml microcentrifuge tubes (Thermo Fisher Scientific, catalog number: 05-408-138)
10. Scienceware microcentrifuge tube rack (Thermo Fisher Scientific, catalog number: 10029259)
11. 1.5 ml microcentrifuge tubes (Thermo Fisher Scientific, catalog number: 05-408-129)
12. 2.0 ml microcentrifuge tubes (Thermo Fisher Scientific, catalog number: 05-408-138)
13. Nunc 15 ml conical sterile tubes (Thermo Fisher Scientific, catalog number: 12565269)
14. Nunc 50 ml conical sterile tubes (Thermo Fisher Scientific, catalog number: 12565271)
15. Corning PES syringe filters (Thermo Fisher Scientific, catalog number: 09-754-29)
16. 20 ml filter syringes (Thermo Fisher Scientific, catalog number: 14-955-460)
17. Round Petri dishes (100 × 15 mm) (Thermo Fisher Scientific, catalog number: FB0875712)
18. Transfer pipettes (Thermo Fisher Scientific, catalog number: 13-711-7M)
19. Kimberly-Clark Professional™ Kimwipes™ Delicate Task Wipers (Thermo Fisher Scientific, catalog number: 06-666A)
20. BD Bacto™ Tryptic Soy Broth (TSB) (Thermo Fisher Scientific, catalog number: DF0370-07-5)
21. BD Tryptic Soy Agar (TSA) (Thermo Fisher Scientific, catalog number: DF0369-07-8)
22. Sodium chloride (NaCl) (Thermo Fisher Scientific, catalog number: S271-1)
23. Hydrochloric acid (HCl) (Thermo Fisher Chemical, catalog number: 187066)
24. Potassium chloride (KCl) (Thermo Fisher Scientific, catalog number: AM9640G)
25. Potassium phosphate dibasic (K<sub>2</sub>HPO<sub>4</sub>) (Thermo Fisher Scientific, catalog number: BP363-500)
26. Sodium phosphate dibasic, anhydrous (Na<sub>2</sub>HPO<sub>4</sub>) (Thermo Fisher Scientific, catalog number: BP332-1)
27. Ethylenediamine tetraacetic acid, EDTA (Thermo Fisher Scientific, catalog number: BP118-500)
28. Tris base (Thermo Fisher Scientific, catalog number: BP152-5)
29. D-(+)-glucose (Sigma-Aldrich, catalog number: G8270-1KG)
30. Acetone (Thermo Fisher Scientific, catalog number: A929-4)
31. Methanol (Thermo Fisher Scientific, catalog number: A454-4)
32. Ethanol (Thermo Fisher Scientific, catalog number: A405P-4)
33. Bovine Serum Albumin (BSA) (Thermo Fisher Scientific Bioreagents, catalog number: BP1600-100)
34. 0.1% poly-L-lysine solution (Sigma-Aldrich, catalog number: P8920-100ML)
35. Paraformaldehyde (PFA) 4% in PBS (Thermo Fisher Scientific, catalog number: AAJ19943K2)
36. Glutaraldehyde 50% in H<sub>2</sub>O (Sigma-Aldrich, catalog number: 340855-25ML)
37. Primary antibody: SpA<sub>KKAA</sub> antiserum (Kim *et al.*, 2010). Store at 4°C
38. Secondary antibodies:
  - a. Goat anti-rabbit IgG (H+L) Highly Cross-Adsorbed Secondary Antibody, Alexa Fluor 488 (Thermo Fisher Scientific, catalog number: A-11034). Store at 4°C
  - b. Goat anti-Rabbit IgG (H+L) Cross-Adsorbed Secondary Antibody, Alexa Fluor 647 (Thermo Fisher Scientific, catalog number: A-21244). Store at 4°C

39. Molecular Probes™ SlowFade™ Diamond Antifade Mountant (Invitrogen, catalog number: S36963)
40. Nile Red (Sigma-Aldrich, catalog number: 19123-10MG)
41. Hoechst 33342 DNA dye, 10 mg/ml (Thermo Fisher Scientific, catalog number: H3570), store at 4°C.
42. BODIPY™ Vancomycin-FL (Thermo Fisher Scientific, catalog number: V34850)
43. Corning™ Rectangular Cover Glasses No.1 (22 × 50 mm) (Thermo Fisher Scientific, catalog number: 12-553-461) (see Note 1)
44. Clear nail polish (cheapest one in any grocery store)
45. Trypsin, from bovine pancreas (Sigma-Aldrich, catalog number: T1426)
46. Trypsin inhibitor, from glycine max soybean (Sigma-Aldrich, catalog number: T9128)
47. Lysostaphin (AMBI, catalog number: LSPN-50)
48. Phosphate-buffered saline (PBS) (see Recipes)
49. Fixation solution (see Recipes)
50. GTE solution (see Recipes)
51. Trypsin stock solution (see Recipes)
52. Trypsin inhibitor stock solution (see Recipes)
53. BSA blocking solution (see Recipes)
54. Lysostaphin stock solution (see Recipes)
55. Nile Red stock solution (see Recipes)
56. BODIPY™ Vancomycin-FL stock solution (see Recipes)

## **Equipment**

1. Eppendorf pipettes 100–1,000 µl, 20–200 µl, 2–20 µl, 0.1–2.5 µl (Eppendorf, catalog number: 2231000714)
2. Eppendorf Easypet®3 (Eppendorf, catalog number: 4430000018)
3. Fisherbrand™ Traceable™ Multi-Colored Timer (Thermo Fisher Scientific, catalog number: 02-261-840)
4. Forceps (MilliporeSigma™ Filter Forceps/Thermo Fisher Scientific, catalog number: XX6200006P)
5. In-house vacuum
6. Shaker (Eppendorf New Brunswick™ Innova® 42 shaker, catalog number: EPM1335-0010)
7. Table centrifuge (Eppendorf, model: Centrifuge 5425, catalog number EP5405000441)
8. Spectrophotometer (Thermo Scientific Genesys GENESYS™ 30 Visible Light Spectrophotometer, catalog number: 14-380-442)
9. Mini-tube rotator (Fisherbrand™ Mini Tube Rotator, catalog number: 88-861-051)
10. Incubator microbiological (Fisher Scientific, catalog number: 51030513)
11. -20°C freezer
12. 4°C refrigerator
13. LP Vortex Mixer (Thermo Fisher Scientific, catalog number: 88880017)
14. Leica SP5 2-photon Laser Scanning Confocal microscope (Leica Microsystems, product name: Leica TCS SP5 Confocal)

## Software

1. Image J (Rasband W.S./U. S. NIH, Bethesda, Maryland, USA, <https://imagej.nih.gov/ij/>)
2. Leica microscope software LAS\_AF Leica (Leica microscopes)
3. Prism GraphPad Software for statistical analysis (<https://www.graphpad.com/scientific-software/prism/>)
4. Adobe Illustrator to assemble figures

## Procedure

### A. Slide preparation

1. Add 50 µl 0.1% poly-L-lysine to each well of an 8-well glass slide and allow to sit for 5 min at room temperature (see Note 2).
2. Briefly rinse the wells with ddH<sub>2</sub>O, remove the excess liquid using a vacuum, and allow the slide to air dry completely (see Notes 3 and 4).

### B. Bacterial cultures

1. Prepare an overnight culture: inoculate one single colony from a streaked agar plate to 3 ml TSB in a glass test tube; add the appropriate antibiotics, if needed.
2. Grow the overnight culture at 37°C with rigorous shaking at 220 rpm.
3. The next morning, inoculate 30 µl overnight culture to 3 ml fresh TSB (1:100 dilution).
4. Grow the cultures at 37°C with rigorous shaking at 220 rpm.
5. Measure the optical density OD<sub>600</sub> of the culture every hour in a spectrophotometer.
6. Place the cultures on ice when OD<sub>600</sub> reaches 0.8–1.0 (see Note 5).
7. Continue the sample preparation in Part C below according to the different protocols (A, B, or C).

### C. Sample preparation

#### Protocol A – Surface display:

1. Transfer 2 ml bacterial culture into a 2 ml microcentrifugation tube.
2. Spin at 18,000 × g for 3 min in a tabletop centrifuge to pellet the bacterial cells.
3. Remove the supernatant without disturbing the pellet.
4. Resuspend the pellet in 1 ml PBS and vortex well.
5. Spin at 18,000 × g for 3 min and remove the supernatant (steps 4–5 are “wash with PBS” steps).
6. Resuspend the pellet in 1 ml PBS, vortex thoroughly; mix 250 µl bacterial suspension with 250 µl fixation solution (see Recipes) in a clean 1.5 ml microcentrifuge tube, briefly vortex to mix, and incubate for 20 min at room temperature (fixation step).
7. Wash twice with PBS, as described in steps 4–5 (see Note 6).
8. Resuspend the pellet in 150 µl PBS, vortex thoroughly (see Note 7).
9. Add 50 µl bacterial suspension to poly-L-lysine-coated glass slides and allow to sit for 5 min.
10. Remove the excess liquid (non-adherent cells) using a vacuum.

11. Add one drop of PBS to each well using a plastic disposable transfer pipette and remove using a vacuum (this is the “drop and remove on-slide wash” step).
12. Repeat the drop and remove on-slide wash step.
13. Continue with immunofluorescence in Part D.

**Protocol B – Cross-wall localization:**

1. Transfer 2 ml bacterial culture into a 2 ml microcentrifugation tube.
2. Spin at 18,000 × g for 3 min in a tabletop centrifuge to pellet the bacterial cells.
3. Remove the supernatant without disturbing the pellet.
4. Wash once with PBS.
5. Resuspend the pellet in 900 µl PBS, vortex thoroughly; add 100 µl 5 mg/ml trypsin stock solution (see Recipes) and briefly vortex (trypsin final concentration: 0.5 mg/ml).
6. Incubate the tubes in a Mini-tube rotator at 37°C for 1 h at a rotation speed of 16 (medium speed).
7. Wash twice with PBS.
8. Resuspend the pellet in 900 µl fresh TSB, vortex thoroughly; add 100 µl 10 mg/ml soybean trypsin inhibitor stock solution (see Recipes) and briefly vortex to mix (final concentration of soybean trypsin inhibitor: 1 mg/ml).
9. Incubate the tubes in a Mini-tube rotator at 37°C for exactly 20 min at a rotation speed of 16 (see Note 8).
10. Add 250 µl fixation solution to a clean 1.5 ml microcentrifuge tube during the 20 min incubation.
11. At the 20-min timepoint, quickly transfer 250 µl bacterial sample to the microcentrifuge tubes prepared in the previous step.
12. Vortex to mix and allow the sample to sit at room temperature for 20 min.
13. Wash twice with PBS.
14. Resuspend the pellet in 150 µl PBS and vortex thoroughly (adjust the volume depending on the pellet size).
15. Add 50 µl bacterial suspension to a glass slide coated with poly-L-lysine and allow to sit for 5 min.
16. Remove the liquid (non-adherent cells) using a vacuum.
17. Perform the drop and remove on-slide wash twice for each well as described above.
18. Continue with immunofluorescence in Part D.

**Protocol C – Cytoplasmic/septal membrane localization:**

1. Place two 50 ml tubes containing approximately 25 ml methanol and 25 ml acetone, respectively, into a -20°C freezer.
2. Normalize all the bacterial cultures to OD<sub>600</sub> = 1.
3. Transfer 2 ml normalized bacterial culture to a 2 ml microcentrifuge tube (this step is to have same cell numbers for the following enzymatic digestion step).
4. Spin at 18,000 × g for 3 min in a tabletop centrifuge to pellet the bacterial cells.
5. Remove the supernatant without disturbing the pellet.

6. Wash once with PBS.
7. Resuspend the pellet in 900 µl PBS and vortex thoroughly; add 100 µl 5 mg/ml trypsin stock solution and briefly vortex (see Note 9).
8. Incubate in a Mini-tube rotator at 37°C for 1 h at a rotation speed of 16.
9. Wash twice with PBS.
10. Resuspend the pellet in 500 µl PBS, vortex thoroughly; add 500 µl fixation solution and vortex to mix.
11. Incubate the sample for 15 min at room temperature and then on ice for 15 min to fix.
12. Wash three times with PBS.
13. Resuspend the pellet in 1 ml freshly made GTE buffer (see Recipes) and vortex thoroughly (see Note 10).
14. Add 50 µl cell suspension to poly-L-lysine-coated glass slides (this is the control without lysostaphin digestion) (see Note 11).
15. Prepare a timer, add 10 µl lysostaphin working solution (see Recipes) to the rest of the cell suspension; quickly vortex and immediately add 50 µl to the glass slides (see Note 12).
16. Incubate for 2 min on the slide (see Note 13).
17. Remove the liquid using a vacuum until completely dry.
18. Immediately place the slide into prechilled methanol at -20°C for 5 min.
19. Take out the slide using forceps and place into prechilled acetone at -20°C for 30 s (see Note 14).
20. Take out the slide using forceps and allow to air-dry completely.
21. Once the slide is dry, apply 50 µl PBS to the sample well to rehydrate.
22. Perform the drop and remove on-slide wash twice for each well.
23. Continue with immunofluorescence in Part D.

#### D. Immunofluorescence

1. Remove PBS, add BSA blocking solution (see Recipes), and incubate for 30 min at room temperature.
2. Remove the blocking solution, add 50 µl primary antibody solution (rabbit serum SpA<sub>KKAA</sub> 1:4,000 dilution in BSA blocking solution), and incubate overnight at 4°C or at room temperature for 1 h (see Note 15).
3. Remove the unbound primary antibody solution and wash 8 times with PBS with the last wash step for 5 min.
4. Remove the washing solution, add 50 µl secondary antibody diluted in BSA blocking solution (*e.g.*, Alexa Fluor 647-IgG or Alexa Fluor 488-IgG, 1:500 dilution), and incubate in the dark for 1 hour at room temperature (see Note 16).
5. Perform the on-slide wash 10 times with PBS.
6. Take a clean 1.5 ml microcentrifuge tube, add 1 ml PBS, 5 µl Hoechest stock solution (1:200 dilution), 2 µl Van-FL stock solution (1:500 dilution), or 5 µl Nile Red stock solution (1:200 dilution) (see Recipes) and mix well; add 50 µl staining solution to each well.
7. Incubate in the dark for 10 min at room temperature.
8. Perform the on-slide wash three times with PBS.
9. After the last wash, remove all the excess liquid from the well.

10. Add a 5- $\mu$ l drop of Slow Fade Diamond Antifade Mountant at 3 different places between the sample wells (see Note 17).
11. Brush a thin layer of nail polish around the edges of the slide and seal with a cover slip; gently press the cover slip and use a Kim wipes to remove the excess antifade solution around the edges (see Note 18).
12. Image the samples using a microscope with the appropriate fluorescent channels (Part E).
13. The prepared slides can be stored at 4°C for a few days and at -20°C for a longer period; however, immediate imaging is recommended.

#### E. Imaging

1. The samples prepared above are suitable to be imaged by different imaging systems, including epifluorescence microscopy, confocal microscopy, or deconvolution microscopy. However, to reveal bacterial cellular features and define protein localization in tiny bacterial cells, a microscope with high resolution is recommended. A 60 $\times$  or 100 $\times$  objective lens with a higher numerical aperture is needed. We used a Leica DM 2000 coupled with a sensitive CCD camera, a Leica SP5 2-photon Laser Scanning Confocal microscope, and a Leica SP8 3X STED Laser Confocal Microscope. All showed good imaging results.
2. Representative images of protocols A, B, and C are displayed in Figure 2. The images were captured using a Leica SP5 2-photon Laser Scanning Confocal microscope.

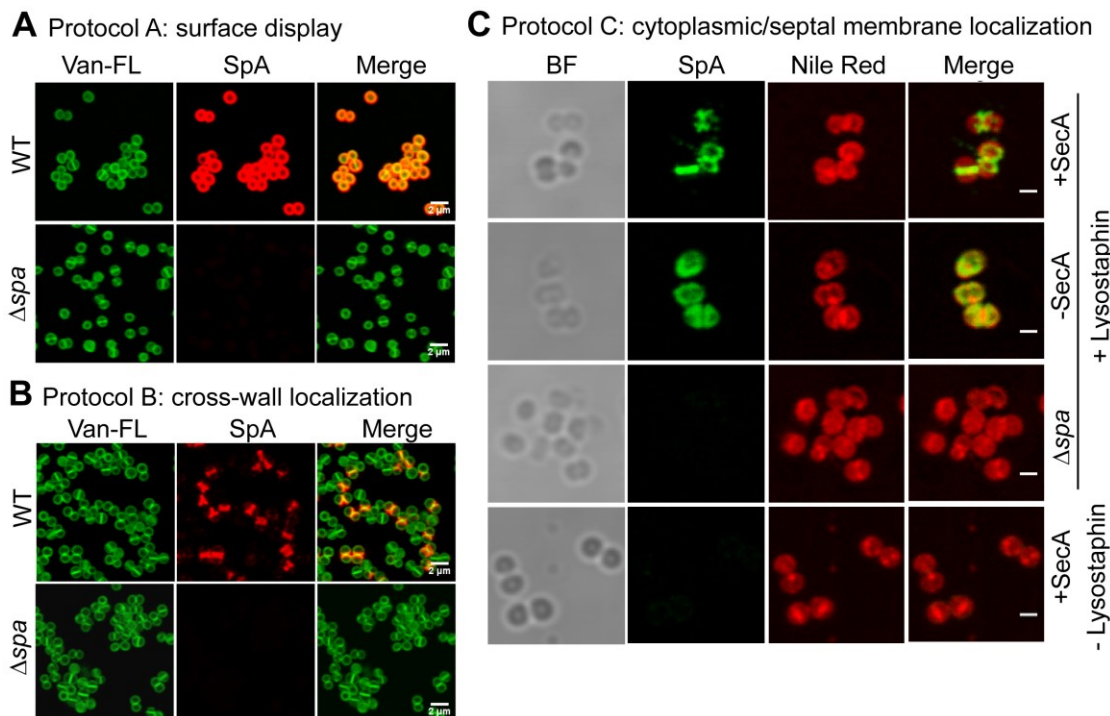


**Figure 2. Representative images from (A) protocol A, showing surface display of SpA; (B) protocol B, showing cross-wall localization of SpA; and (C) protocol C, showing septal localization of SpA in the presence of SecA and cytoplasmic localization of SpA precursors in the absence of SecA. Van-**

FL: BODIPY™ Vancomycin-FL cell wall staining; BF: brightfield images; Nile Red: membrane staining; scale bar: 2  $\mu$ m in panels A and B and 1  $\mu$ m in panel C. Images are adapted from Yu *et al.* (2018).

## Data analysis

1. Take at least three images with random views for each sample in each experiment. One has to take more random images, especially when there are only a few cells on the slides or when there are different phenotypes on one slide.
  2. Perform the experiment independently at least three times.
  3. To quantitate the percentage of SpA cross-wall localization, open images from protocol B in ImageJ, split the channels, and enlarge the images to allow better visualization.
  4. Open the “cell counter” tool in ImageJ.  
Select cell type 1, manually count pairs of diplococci in Van-FL-stained images, and record the number. Count at least 50 pairs of diplococci per image. Diplococci are defined as two connecting daughter cells that have just been split but not yet separated (see sample images in Figure 3) (see Note 19).
  5. Select cell type 2, manually count cross-wall localized SpA signals in the merged images, and record the number. Cross-wall localized SpA signals are defined as clear lines at the cross-wall. To be rigorous, dots are not counted.
  6. Calculate the average of three images per experiment.
  7. Input the average values of three independent experiments to GraphPad Prism.
  8. In GraphPad Prism, use a *t*-test to statistically analyze significant differences between two groups; use one-way ANOVA for multiple group comparisons; and use Tukey’s multiple comparison test to analyze differences among multiple groups.

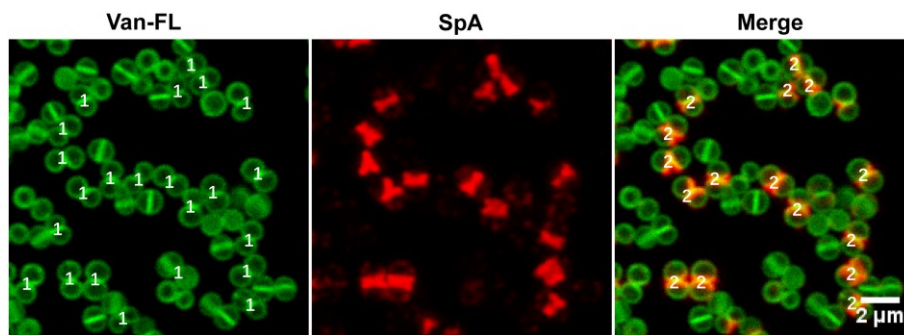


**Figure 3.** Sample images with the cell counting window, demonstrating how to quantitate the percentage of SpA cross-wall localization. Images are adapted from Yu *et al.* (2018).

## Notes

1. The choice of thickness of the cover slip depends on the imaging system.

2. A 1:10 dilution of poly-L-lysine to 0.01% also works.
3. It takes about 15 min to air-dry the poly-L-lysine-coated slides. One can also use a vacuum to dry the slides.
4. To assemble the vacuum system, connect an in-house vacuum to a tube, cut the extremity off a 200  $\mu$ l pipette tip, and insert the tip into the tube. It is important not to touch the samples on the glass slides during drying.
5. It usually takes about 2–3 h for *S. aureus* to reach an OD<sub>600</sub> of 0.8–1.0 under standard lab culture conditions.
6. Cells tend to clump after fixation; a longer vortex may be needed.
7. The volume can be adjusted according to the pellet size; if unsure, one can add less PBS and make dilutions. The key point here is to have a proper number of cells on the slide so that most of the cells are well separated. Too many cells will lead to bacterial clumping and cause artifacts in immunostaining; too few cells will not provide reliable results.
8. The time of re-generation was determined experimentally in our protocol. It should be tested and optimized depending on different growth conditions and antigens.
9. This step is not critical for protocol C, as lysostaphin digestion will remove most of the cell wall as well as the existing SpA. We include this step in our protocol to minimize any potential background caused by existing SpA.
10. GTE buffer is an osmotic stabilizing buffer. Lysostaphin is a zinc-dependent endopeptidase (Sabala *et al.*, 2014). Although EDTA in the GTE buffer can chelate zinc, it does not have any obvious negative effects in our experiments. We have tried other osmotic stabilizing buffers without EDTA, such as TSM [50 mM Tris-HCl (pH 7.5), 0.5 M sucrose, 10 mM MgCl<sub>2</sub>], which also works.
11. It is important to have this control. Staphylococcal cells after lysostaphin digestion will become more translucent in brightfield images, whereas undigested cells have a dark cell contour. Moreover, the two closely attached daughter cells will separate after lysostaphin digestion (see Figure 2C).
12. Other cell wall hydrolases can substitute lysostaphin if this protocol is to be adapted for another bacterium. Lysozyme, for example, has been used in *Bacillus subtilis* (Harry *et al.*, 1995). Most *S. aureus* strains are lysozyme-resistant, which limits its use in *S. aureus*. The digestion time and buffer will have to be adjusted experimentally for a different enzyme or bacterium.
13. It is critical to perform on-slide digestion to stabilize the protoplasts.
14. This step stabilizes the protoplast after lysostaphin digestion and permeabilizes the cytoplasmic membrane. Depending on the bacterial strain and abundance of antigens, Triton X-100 can be used to further permeabilize the cytoplasmic membrane.
15. For any new antigen, serial dilution of primary antibody is necessary to determine the optimal concentration. A negative control that does not express the antigen is an essential control. If there is no mutant available, one should include at least a control without primary antibody. Minimal background signals should be seen in the negative control.
16. Depending on the microscope system, one can choose different fluorescent-labeled secondary antibodies. We consistently use the secondary antibody at a 1:500 dilution.

17. Different kinds of antifade solution are commercially available. One should choose the antifade solution compatible with the imaging system.
18. Make sure that the antifade solution covers every well as a very thin layer without bubbles, and that the cover slip is leveled on the slide.
19. The reason for counting diplococci is because cross-wall localized SpA signals can only be detected at the cross-wall of these diplococci under our experimental conditions; however, as defining diplococci may be subjective, it can introduce bias. Thus, one can count total cell numbers instead of diplococci.

## **Recipes**

1. Phosphate-buffered saline (PBS)  
137 mM NaCl  
2.7 mM KCl  
10 mM Na<sub>2</sub>HPO<sub>4</sub>  
1.8 mM K<sub>2</sub>HPO<sub>4</sub>  
pH 7.4
  - a. Dissolve 8 g NaCl, 0.2 g KCl, 1.44 g Na<sub>2</sub>HPO<sub>4</sub>, and 0.24 g K<sub>2</sub>HPO<sub>4</sub> in 1 L ddH<sub>2</sub>O
  - b. Adjust the pH to 7.4 with HCl and autoclave at 121°C for 20 min
2. Fixation solution  
2.4% paraformaldehyde and 0.01% glutaraldehyde in PBS  
Mix 30 ml 4% PFA and 10 µl 50% glutaraldehyde and add PBS to a 50-ml total volume. Store at 4°C (stable for at least two weeks).
3. GTE solution  
50 mM glucose  
10 mM EDTA  
20 mM Tris-HCl pH 7.5  
*Note: Make fresh and filter-sterilize before use.*
  - a. Make stock solutions of 0.5 M EDTA (pH 8) and 1 M Tris-HCl (pH 7.5)
  - b. Add 0.9 g D-glucose, 2 ml 0.5 M EDTA, and 2 ml 1 M Tris-HCl to a final volume of 80 ml ddH<sub>2</sub>O
  - c. Adjust the pH to 7.5 with HCl, add ddH<sub>2</sub>O to 100 ml, filter-sterilize, and store at 4°C
4. Trypsin stock solution  
5 mg/ml trypsin in PBS, filter-sterilize, and store at -20°C
5. Trypsin inhibitor stock solution  
10 mg/ml trypsin inhibitor in ddH<sub>2</sub>O, filter-sterilize, store at -20°C
6. BSA blocking solution: 3% BSA in PBS  
Dissolve 0.3 g BSA powder in 10 ml PBS; make fresh and filter-sterilize before use, store at 4°C
7. Lysostaphin stock solution
  - a. Make a stock solution of 10 mg/ml in 20 mM sodium acetate (pH 4.5), store at -20°C
  - b. Dilute with 200 mM Tris-HCl (pH 8) to 2 mg/ml as a working solution, store at 4°C

8. Nile Red stock solution
  - a. Dissolve in 100% ethanol to make a 0.5 mg/ml stock solution, store at -20°C
  - b. Add 5 µl Nile Red stock solution to 1 ml PBS (1:200 dilution) to stain the samples
9. BODIPY™ Vancomycin-FL stock solution
  - a. Dissolve 100 µg in 100 µl DMSO to make a 1 µg/µl stock solution, store at -20°C
  - b. Add 2 µl Van-FL stock solution to 1 ml PBS (1:500 dilution) to stain the samples

### **Acknowledgments**

This work was supported by the start-up funds to W.Y. from the University of South Florida. We thank Olaf Schneewind and Dominique Missiakas for their mentorship during the initial development of the protocols. We thank Vytas Bindokas, Robert Hill, and Byeong Cha for their assistance with microscope facilities. We thank lab members for suggestions regarding the manuscript. This work reports the fluorescence microscopy methods used in our previous paper (Yu *et al.*, 2018). Images from Yu *et al.* (2018) have been adapted in this report to demonstrate the methods.

### **Competing interests**

The authors declare that there are no conflicts of interest or competing interests.

### **References**

1. Carlsson, F., Stalhammar-Carlemalm, M., Flardh, K., Sandin, C., Carlemalm, E. and Lindahl, G. (2006). [Signal sequence directs localized secretion of bacterial surface proteins](#). *Nature* 442(7105): 943-946.
2. Cole, R. M. and Hahn, J. J. (1962). [Cell wall replication in \*Streptococcus pyogenes\*](#). *Science* 135(3505): 722-724.
3. DeDent, A., Bae, T., Missiakas, D. M. and Schneewind, O. (2008). [Signal peptides direct surface proteins to two distinct envelope locations of \*Staphylococcus aureus\*](#). *EMBO J* 27(20): 2656-2668.
4. Forsgren, A. and Sjöquist, J. (1966). ["Protein A" from \*S. aureus\*. I. Pseudo-immune reaction with human gamma-globulin](#). *J Immunol* 97(6): 822-827.
5. Foster, T. J., Geoghegan, J. A., Ganesh, V. K. and Hook, M. (2014). [Adhesion, invasion and evasion: the many functions of the surface proteins of \*Staphylococcus aureus\*](#). *Nat Rev Microbiol* 12(1): 49-62.
6. Harry, E. J., Poglano, K. and Losick, R. (1995). [Use of immunofluorescence to visualize cell-specific gene expression during sporulation in \*Bacillus subtilis\*](#). *J Bacteriol* 177(12): 3386-3393.
7. Kajimura, J., Fujiwara, T., Yamada, S., Suzawa, Y., Nishida, T., Oyamada, Y., Hayashi, I., Yamagishi, J., Komatsuzawa, H. and Sugai, M. (2005). [Identification and molecular characterization of an N-acetylmuramyl-L-alanine amidase Sle1 involved in cell separation of \*Staphylococcus aureus\*](#). *Mol Microbiol* 58(4): 1087-1101.

8. Kim, H. K., Cheng, A. G., Kim, H. Y., Missiakas, D. M. and Schneewind, O. (2010). [Nontoxigenic protein A vaccine for methicillin-resistant \*Staphylococcus aureus\* infections in mice](#). *J Exp Med* 207(9): 1863-1870.
9. Mazmanian, S. K., Liu, G., Ton-That, H. and Schneewind, O. (1999). [Staphylococcus aureus sortase, an enzyme that anchors surface proteins to the cell wall](#). *Science* 285(5428): 760-763.
10. Monteiro, J. M., Fernandes, P. B., Vaz, F., Pereira, A. R., Tavares, A. C., Ferreira, M. T., Pereira, P. M., Veiga, H., Kuru, E., VanNieuwenhze, M. S., Brun, Y. V., Filipe, S. R. and Pinho, M. G. (2015). [Cell shape dynamics during the staphylococcal cell cycle](#). *Nat Commun* 6: 8055.
11. Oshida, T., Sugai, M., Komatsuzawa, H., Hong, Y. M., Suginaka, H. and Tomasz, A. (1995). [A Staphylococcus aureus autolysin that has an N-acetylmuramoyl-L-alanine amidase domain and an endo-beta-N-acetylglucosaminidase domain: cloning, sequence analysis, and characterization](#). *Proc Natl Acad Sci U S A* 92(1): 285-289.
12. Pinho, M. G. and Errington, J. (2003). [Dispersed mode of Staphylococcus aureus cell wall synthesis in the absence of the division machinery](#). *Mol Microbiol* 50(3): 871-881.
13. Raz, A., Talay, S. R. and Fischetti, V. A. (2012). [Cellular aspects of the distinct M protein and SfbI anchoring pathways in Streptococcus pyogenes](#). *Mol Microbiol* 84(4): 631-647.
14. Rosenstein, R. and Götz, F. (2000). [Staphylococcal lipases: biochemical and molecular characterization](#). *Biochimie* 82(11): 1005-1014.
15. Sabala, I., Jagielska, E., Bardelang, P. T., Czapinska, H., Dahms, S. O., Sharpe, J. A., James, R., Than, M. E., Thomas, N. R. and Bochtler, M. (2014). [Crystal structure of the antimicrobial peptidase lysostaphin from Staphylococcus simulans](#). *FEBS J* 281(18): 4112-4122.
16. Schindler, C. A. and Schuhardt, V. T. (1964). [Lysostaphin: A New Bacteriolytic Agent for the Staphylococcus](#). *Proc Natl Acad Sci U S A* 51: 414-421.
17. Schneewind, O. and Missiakas, D. (2019). [Sortases, Surface Proteins, and Their Roles in Staphylococcus aureus Disease and Vaccine Development](#). *Microbiol Spectr* 7(1).
18. Sugai, M., Komatsuzawa, H., Akiyama, T., Hong, Y. M., Oshida, T., Miyake, Y., Yamaguchi, T. and Suginaka, H. (1995). [Identification of endo-beta-N-acetylglucosaminidase and N-acetylmuramyl-L-alanine amidase as cluster-dispersing enzymes in Staphylococcus aureus](#). *J Bacteriol* 177(6): 1491-1496. Swanson, J., Hsu, K. C. and Gotschlich, E. C. (1969). [Electron microscopic studies on streptococci. I. M antigen](#). *J Exp Med* 130(5): 1063-1091.
19. Tettelin, H., Nelson, K. E., Paulsen, I. T., Eisen, J. A., Read, T. D., Peterson, S., Heidelberg, J., DeBoy, R. T., Haft, D. H., Dodson, R. J., Durkin, A. S., Gwinn, M., Kolonay, J. F., Nelson, W. C., Peterson, J. D., Umayam, L. A., White, O., Salzberg, S. L., Lewis, M. R., Radune, D., Holtzapple, E., Khouri, H., Wolf, A. M., Utterback, T. R., Hansen, C. L., McDonald, L. A., Feldblyum, T. V., Angiuoli, S., Dickinson, T., Hickey, E. K., Holt, I. E., Loftus, B. J., Yang, F., Smith, H. O., Venter, J. C., Dougherty, B. A., Morrison, D. A., Hollingshead, S. K. and Fraser, C. M. (2001). [Complete genome sequence of a virulent isolate of Streptococcus pneumoniae](#). *Science* 293(5529): 498-506.

20. Tong, S. Y., Davis, J. S., Eichenberger, E., Holland, T. L. and Fowler, V. G., Jr. (2015). [\*Staphylococcus aureus\* infections: epidemiology, pathophysiology, clinical manifestations, and management.](#) *Clin Microbiol Rev* 28(3): 603-661.
21. von Eiff, C., Becker, K., Machka, K., Stammer, H. and Peters, G. (2001). [Nasal carriage as a source of \*Staphylococcus aureus\* bacteremia.](#) Study Group. *N Engl J Med* 344(1): 11-16.
22. Yamada, S., Sugai, M., Komatsuzawa, H., Nakashima, S., Oshida, T., Matsumoto, A. and Suginaka, H. (1996). [An autolysin ring associated with cell separation of \*Staphylococcus aureus\*.](#) *J Bacteriol* 178(6): 1565-1571.
23. Yu, W., Missiakas, D. and Schneewind, O. (2018). [Septal secretion of protein A in \*Staphylococcus aureus\* requires SecA and lipoteichoic acid synthesis.](#) *Elife* 7.
24. Zhou, X., Halladin, D. K., Rojas, E. R., Koslover, E. F., Lee, T. K., Huang, K. C. and Theriot, J. A. (2015). [Bacterial division. Mechanical crack propagation drives millisecond daughter cell separation in \*Staphylococcus aureus\*.](#) *Science* 348(6234): 574-578.

## Super-resolution Imaging of the T cell Central Supramolecular Signaling Cluster Using Stimulated Emission Depletion Microscopy

Sin Lih Tan<sup>1, \$,\*</sup>, Dominic Alibhai<sup>2</sup>, Stephen J. Cross<sup>2</sup>, Harry Thompson<sup>3</sup> and Christoph Wülfing<sup>1,\*</sup>

<sup>1</sup>School of Cellular and Molecular Medicine, University of Bristol, Bristol, United Kingdom; <sup>2</sup>Wolfson BioImaging Facility, University of Bristol, Bristol, United Kingdom; <sup>3</sup>School of Biochemistry, University of Bristol, Bristol, United Kingdom; <sup>\$</sup>Present address: Horizon Discovery, Cambridge Research Park, Cambridge, United Kingdom

\*For correspondence: [christoph.wuelfing@bris.ac.uk](mailto:christoph.wuelfing@bris.ac.uk); [sinlih.tan@horizondiscovery.com](mailto:sinlih.tan@horizondiscovery.com)

**[Abstract]** Supramolecular signaling assemblies are of interest for their unique signaling properties. A  $\mu\text{m}$  scale signaling assembly, the central supramolecular signaling cluster (cSMAC), forms at the center interface of T cells activated by antigen presenting cells (APC). The adaptor protein linker for activation of T cells (LAT) is a key cSMAC component. The cSMAC has widely been studied using total internal reflection fluorescence microscopy of CD4 $^{+}$  T cells activated by planar APC substitutes. Here we provide a protocol to image the cSMAC in its cellular context at the interface between a T cell and an APC. Super resolution stimulated emission depletion microscopy (STED) was utilized to determine the localization of LAT, that of its active, phosphorylated form and its entire pool. Agonist peptide-loaded APCs were incubated with TCR transgenic CD4 $^{+}$  T cells for 4.5 min before fixation and antibody staining. Fixed cell couples were imaged using a 100x 1.4 NA objective on a Leica SP8 AOBS confocal laser scanning microscope. LAT clustered in multiple supramolecular complexes and their number and size distributions were determined. Using this protocol, cSMAC properties in its cellular context at the interface between a T cell and an APC could be quantified.

**Keywords:** Immune Synapse, cSMAC, STED, LAT, T cell activation

**[Background]** T cell activation in response to antigen presenting cells (APCs) is controlled by engagement of the T cell receptor (TCR) in combination with co-inhibitory and co-stimulatory receptors and orchestrated by the integrated function of multiple signaling intermediates. Dynamic recruitment of signaling intermediates into microscopically detectable structures at T cell interface is an important element of signal integration.  $\mu\text{m}$  scale signaling assemblies were first described at the center and periphery of T cells activated by antigen presenting cells (APC) for the TCR, PKC $\theta$  and LFA-1, talin, respectively, as central and peripheral supramolecular activation clusters (cSMAC and pSMAC) (Monks *et al.*, 1997 and 1998; Grakoui *et al.*, 1999).  $\mu\text{m}$  scale of assemblies, in particular in the form of supramolecular protein complexes, provides unique biophysical and signaling properties (Li *et al.*, 2012; Banani *et al.*, 2016; Shin and Brangwynne, 2017). Such complexes are readily observed by fluorescence microscopy, held together by a network of multivalent protein interactions and often have distinct phase properties (Li *et al.*, 2012; Banani *et al.*, 2016; Shin and Brangwynne, 2017). The cSMAC has many properties of such supramolecular protein complexes: It contains various multivalent signaling intermediates (Balagopalan *et al.*, 2015), prominently LAT (linker for activation of T cells), components of this complex including LAT and PKC $\theta$  exchange with the remainder of the cell to a moderate extent and slowly (Roybal *et al.*,

2015), and components of this complex can be assembled into supramolecular structures *in vitro* (Su *et al.*, 2016). Therefore, understanding biophysical properties of the cSMAC is of substantial importance.

The cSMAC has been imaged using confocal microscopy of fixed T cell APC couples (Monks *et al.*, 1997 and 1998; Freiberg *et al.*, 2002), spinning disk confocal live cell imaging of T cell APC couples (Singleton *et al.*, 2009; Clark *et al.*, 2019), and using total internal reflection (TIRF) imaging of T cells activated on planar APC substitutes (Yokosuka *et al.*, 2005; Varma *et al.*, 2006). Resolution in confocal imaging is limited by the Abbe diffraction limit. Therefore, only overall cSMAC formation can be detected but not details of cSMAC structure. The use of planar APC substitutes allows more efficient diffraction limited imaging but does not reflect the membrane topology of T cell APC couples well (Roybal *et al.*, 2015) and, therefore, may result in altered structural details of  $\mu\text{m}$  scale signaling complexes (Clark *et al.*, 2019). To overcome these experimental restrictions, we imaged single z planes of fixed T cell APC couples stained for the critical cSMAC component LAT with STED super-resolution microscopy on a microscope capable of 50 nm lateral resolution. In STED imaging, a doughnut shaped laser beam silences fluorescence around a central excitation spot and thereby diminishes the excitation volume of a confocal laser scanning microscopy system to below the conventional diffraction limit. Using automated object detection, we quantified structural properties of LAT signaling complexes.

This protocol provides access to structural features of supramolecular signaling complexes that form in T cells activated in a cellular interaction with antigen presenting cells.

## **Materials and Reagents**

1. 1 ml syringe plunger (such as VWR, catalog number: NSCAS7510-1)
2. 24-well plate (such as BD Biosciences, catalog number: 353047)
3. 50 ml Falcon tube
4. 15 ml Falcon tube
5. 1.5 ml Eppendorf tube
6. 40  $\mu\text{m}$  cell strainer
7. Petri dish
8. Coverslips (Carl Zeiss<sup>TM</sup>, catalog number: 10474379), store at room temperature
9. PEP pen (ImmEdge, Vector Laboratories: H-4000), store at room temperature
10. Microscope Slide (VWR, SuperFrost Plus, catalog number: 631-0108, store at room temperature)
11. 5C.C7 TCR transgenic mice (Davis Lab, Stanford [Seder *et al.*, 1992], RRID:MGI:3799371)
12. CH27 Cell Line (RRID:CVCL\_7178)
13. Anti-LAT pY191 (Cell Signaling, catalog number: 3584), store at 4 °C
14. Anti-LAT (Cell Signaling, catalog number: 9166), store at 4 °C
15. Anti-rabbit IgG, Alexa Fluor 488 (Molecular Probes, catalog number: R37118), store at 4 °C
16. Anti-CD19 antibody (BD Biosciences, Biotin Rat Anti-mouse CD19, Clone 1D3, catalog number: 553784), store at 4 °C
17. Paraformaldehyde (Sigma-Aldrich, catalog number: P6148), store at 4 °C
18. Ammonium Chloride (Sigma-Aldrich, catalog number: 213330), store at room temperature

19. Triton X-100 (Sigma-Aldrich, catalog number: T8787), store at room temperature
20. PBS (Thermo Fisher, catalog number: 14200075), store at room temperature
21. Fc block, Rat Anti-Mouse CD16/CD32 (BD Bioscience, catalog number: 53141), store at 4 °C
22. ProLong Gold (Thermo Fisher, catalog number: P36930), store at room temperature
23. Moth cytochrome C (MCC) peptide, recombinant peptide (ANERADLIAYLKQATK), store at -20 °C
24. SDS (Sigma, catalog number: 71729), store at room temperature
25. Biotinylated BSA (Thermo Fisher, catalog number: 29130), store at -20 °C
26. T50 solution (10 mM Tris-Cl pH = 8.0, 50 mM NaCl), store at 4 °C
27. Neutravidin (0.2 mg/ml diluted in ddH<sub>2</sub>O, Thermo Scientific, catalog number: 31000), store at 4 °C
28. Sodium orthovanadate (Na<sub>3</sub>VO<sub>4</sub>) (20 mM working stock in ddH<sub>2</sub>O, Sigma-Aldrich, catalog number: S6508), store at -20 °C
29. Hydrogen Peroxide (H<sub>2</sub>O<sub>2</sub>) (30% solution, Sigma, catalog number: H1009), store at 4 °C
30. 100% Ethanol (Sigma-Aldrich, catalog number: 459835), store at room temperature
31. RPMI with L-glutamine (Lonza, catalog number: BE12-702F)
32. FBS (SLS LAB PRO, catalog number: S-001A-BR)
33. 100 U/ml Penicillin plus 100 µg/ml streptomycin (Gibco, catalog number: 15140122)
34. 2-mercaptoethanol (Gibco, catalog number: 31350010)
35. T cell Culture Components (see Recipes)
  - Complete medium
  - Interleukin-2 medium
  - Moth cytochrome C (MCC) agonist peptide for the stimulation of 5C.C7 TCR transgenic T cells
36. 2x Pervanadate components (see Recipes)
37. Imaging buffer (see Recipes)

## Equipment

1. P2, P20, P200 pipettes
2. Centrifuge
3. Incubator
4. Confocal laser scanning microscope (Leica, SP8 AOBS) equipped with pulsed white light laser 470-670 nm with 2.5 mW/nm, 592 nm continuous wave STED depletion laser, Leica STED White 100x 1.4 NA objective and time gated Leica SMD HyD detectors

## Software

1. Huygens Professional (SVI, [www.svi.nl](http://www.svi.nl))
2. ImageJ plugin (Modular Image Analysis, version 0.5.22), available on GitHub as <https://github.com/SJCross/MIA> with .mia settings file provided as [supplementary material](#).

## Procedure

### A. T cell and APC Culture (Ambler *et al.*, 2017)

1. T cell culture: Cull a 5C.C7 T cell receptor transgenic mouse over 6-week-old using approved procedures such as those listed in Schedule One of the UK Animals (Scientific Procedures) Act 1986. All animal breeding, maintenance and handling needs to be approved by the appropriate authorities.
2. Dissect lymph nodes and collect them in a 15 ml Falcon tube containing 5 ml of complete medium.
3. Place a 40  $\mu$ m cell strainer over a 50 ml Falcon tube. Pour all lymph nodes onto the cell strainer and mechanically dissociate lymph nodes by gently forcing through the filter once using a 1 ml syringe plunger. Wash the plunger and cell strainer using 5 ml of complete medium.
4. Centrifuge the cells for 3 min at 200  $\times g$ . Remove supernatant, resuspend the cell pellet in 1 ml of complete medium and count the cells.
5. Dilute cells to a density of  $4 \times 10^6$  cells/ml.
6. Culture 1 ml of cell suspension in one well of a 24-well plate and add 0.65  $\mu$ l of 5 mM MCC peptide to achieve a final MCC concentration of 3  $\mu$ M. Incubate at 37 °C, 6% CO<sub>2</sub> overnight.
7. Split 5C.C7 T cells with interleukin-2 medium as necessary, usually 1:1 every day. The MCC peptide is only used to prime the culture. T cell maintenance is achieved using interleukin-2.
8. Experiments need to be repeated with at least two independent primary T cell cultures.
9. APC culture: CH27 B cell lymphoma cells are used as antigen presenting cells and are maintained in complete medium by splitting 1:10 every two days.

### B. T cell stimulation using Pervanadate

1. As a positive control, T cells can be stimulated with the phosphatase inhibitor Pervanadate to induce generalized and extensive tyrosine phosphorylation.
2. On day 5 of T cell culture, collect T cells from as many wells of the 24-well plate as needed ( $4 \times 10^6$  cells/well) into a 15 ml Falcon tube, centrifuge at 200  $\times g$  for 3 min. Resuspend T cell pellet in 150  $\mu$ l of imaging buffer per well.
3. Count T cells and collect required cell number (40,000 per experimental replicate) in a 1.5 ml Eppendorf tube.
4. Add freshly prepared 2x pervanadate at a ratio of 1:1 to cells with complete medium in a 1.5 ml Eppendorf tube. Incubate for 5 min at 37 °C and stain (Procedure D).

### C. Coating of STED compatible coverslips

1. Wash STED compatible coverslips (high performance, thickness no. 1.5, 0.170 ± 0.005 mm, Zeiss) with 10% SDS for 10 min followed by one wash with ddH<sub>2</sub>O.
2. Submerge the washed coverslips in 100% ethanol for 30 min in a Petri dish.
3. Wash the coverslips once with ddH<sub>2</sub>O and bake on a heat block at 60 °C for 30 min until dry.
4. When dry, draw a circular boundary (~10 mm diameter) using a PEP pen and allow it to dry.
5. Resuspend biotinylated BSA in T50 solution at a concentration of 1 mg/ml.

6. Add 50 µl of biotinylated BSA on the middle of a coverslip and incubate at 37 °C for 7 min.
7. Wash the coverslip once with 50 µl T50 solution.
8. Add 50 µl of Neutravidin solution (final concentration of 0.2 mg/ml in ddH<sub>2</sub>O) onto the coverslip for 1 min at 37 °C.
9. Wash once with T50 solution followed by two washes with PBS.
10. Dilute anti-CD19 antibody to a final concentration of 10 µg/ml in imaging buffer.
11. Add 50 µl of diluted anti-CD19 onto the coverslip and incubate at 37 °C for 10 min.
12. Wash the coverslip twice with 50 µl of imaging buffer and add a further 50 µl of imaging buffer to keep the coverslip moist.
13. Store the coated coverslips in a parafilm sealed dish at 4 °C until use.
14. **ΔCRITICAL STEP** Use the coated coverslips within 3 days of coating.

#### D. Cell staining

1. Primary 5C.C7 T cells are activated by interaction with CH27 APCs presenting the MCC agonist peptide recognized by the 5C.C7 T cell receptor. As a control, T cells are additionally activated with the phosphatase inhibitor Pervanadate.
2. Remove the imaging buffer that is used to keep the cover slide moist using a P200 pipette.
3. Prime APCs, CH27 cells (from Step A9), with 10 µM MCC peptide by incubation in complete medium for at least 4 h (Ambler *et al.*, 2017) and resuspend to 40,000 cells/50 µl of imaging buffer. Resuspend 5C.C7 TCR transgenic T cells (from Step A7) (Ambler *et al.*, 2017) to 40,000 cells per 5 µl of imaging buffer.
4. Seed 50 µl of APCs (40,000 cells) onto the coated cover slide and allow to settle for 10 min at room temperature.
5. Add 5 µl of T cells (40,000 cells) or 10 µl of Pervanadate-treated T cells (40,000 cells) for 4.5min at room temperature.
6. **ΔCRITICAL STEP** Gently remove the volume using a P200 pipette and add 50 µl of 4% PFA for 20 min at 4 °C.
7. Gently wash the cover slide once with 50 µl PBS using a P200 pipette.
8. Quench by adding 50 µl of 50 mM of NH<sub>4</sub>Cl for 10 min at 4 °C and wash the cover slide three times with 50 µl of PBS.
9. Permeabilize the cells using 50 µl of 0.02% Triton X-100 in PBS for 20 min at 4 °C.
10. Wash the coverslip three times with 50 µl of PBS followed by incubation with 50 µl of blocking solution (1% BSA in PBS) for 30 min at room temperature.
11. Remove the solution and add 50 µl of primary antibody, anti-phospho-LAT (Tyr 191) at a dilution of 1:50 or anti-LAT at a dilution of 1:100, in 1% BSA in PBS with Fc Block (Rat Anti-Mouse CD16/CD32) at the same dilution and incubate overnight at 4 °C.
12. Remove primary antibodies and wash the cover slide three times with 50 µl of PBS.
13. Incubate the cover slide with 50 µl of secondary antibody (Donkey anti-Rabbit IgG, Alexa Fluor 488) diluted 1:1,000 in 1% BSA in PBS with Fc Block at 1:500 for 1 h at room temperature.

14. Wash the cover slide with 50 µl of PBS for three times and remove the PBS from the coverslip.
15. After adding one drop of ProLong Gold mount a coverslip on the slide (VWR, SuperFrost Plus) and allow to cure for 24 h.

#### E. STED microscopy

1. First, image the slide with the Leica SP8X STED microscope in confocal mode using the following settings:
  - a. 100x 1.4 NA HC PL APO CS2 STED white oil objective.
  - b. 512 x 512 pixels.
  - c. 400 Hz scan speed.
  - d. 488 nm excitation selected on white light laser with corresponding NF488 filter.
  - e. Default 70% white laser power is to be adjusted with the acousto-optic tunable filter to as low as 10%.
  - f. HyD1 hybrid detector collection range 498-520 nm.
  - g. Hybrid detector gain 100%.
  - h. Hybrid detector gating 0.3-8 ns.
  - i. Line average 2.
  - j. Output image bit size 8 bit.
2. Whilst in confocal mode, place your sample and select a region of interest.
3. To image your region of interest with STED, duplicate sequence 1, *i.e.*, the sequence of imaging steps used to choose the region of interest, and modify the duplicated sequence as follows:
  - a. Switch 592 nm STED laser ON. The 592 nm depletion laser generates a donut shaped depletion area for fluorophore excitation at 488 nm. Set it to 30-50%, *i.e.*, 50-70% depletion, using the acousto-optic tunable filter depending on your Alexa Fluor 488 staining brightness. Excessive depletion may photodamage the sample.
  - b. Increase 488 nm laser power as needed to maintain good signal.
  - c. Select optimized frame size for STED with optimized pixel size as calculated automatically by the software using the ‘optimized pixel size’ function.
  - d. Hybrid detector collection range 498-510 nm.
  - e. Hybrid detector gain 200%.
  - f. Hybrid detector gating 1.5-8 ns. A longer start gate time before acquisition ensures efficient depletion of the majority of molecules to improve resolution.
4. **ΔCRITICAL STEP** If the data are to be deconvolved after acquisition ensure no/minimal saturation in the acquired image and adjust laser power and gain as necessary.
5. **ΔCRITICAL STEP** Once the STED sequence has been set, go to Configuration to align STED beams.
6. STED beams need to be aligned every 15 min for the first hour to minimize temperature drift.
7. Start scan and acquire STED images.

## **Data analysis**

1. For deconvolution open STED .lif images with the Huygens Professional software.
2. Select image series to be deconvolved.
3. Right click on image and select microscope parameters. Check the auto read metadata is correct, *e.g.*, embedding media was ProLong Gold (1.47 RI).
4. Set all parameters as verified and accepted.
5. Right click on image, select deconvolution wizard.
6. Draw three lines across the background in each image for the background intensity.
7. Key in the average background intensity value.
8. Click go and then max iterations set to 40 as the default value. Verify convergence of the deconvolution routine and adjust the number of iterations if necessary.
9. Once the deconvolution is complete, save the image as .TIFF file and analyze deconvolved image in Fiji (NIH) (Schindelin *et al.*, 2012; Rueden *et al.*, 2017).
10. Automated puncta analysis with Fiji (NIH). LAT puncta were detected and measured using a Wolfson Bioimaging ImageJ-Fiji plugin (Modular Image Analysis, version 0.5.22). This can be installed and used with the following steps:
  - a. Download v0.5.22 of the plugin from <https://github.com/sjcross/MIA/releases/tag/v0.5.22> and place the “Modular\_Image\_Analysis-0.5.22.jar” file in the Fiji “plugins” folder.
  - b. To install required third-party libraries, launch Fiji and go to “Help > Update...”, then select “Manage update sites” and add the “Biomedgroup” and “IJPB-plugins” update sites. Restart Fiji when prompted.
  - c. Start MIA within Fiji by going to “Plugins > Wolfson Bioimaging > Modular image analysis”.
  - d. Click “Load” and select the “MIA object detection workflow.mia” workflow file provided as a supplement to this protocol. This contains all the instructions for MIA to perform the analysis. There are a few user-accessible settings to select files to process and to control the analysis:
    - “Input control > Input mode”: In “batch” all files within a selected folder will be processed, whereas in “single file” only one image file will be processed.
    - “Input control > Single file path”: Select the batch-processing folder or single file to be analyzed.
    - “Input control > Series mode”: For multi-series files (*e.g.*, Leica LIFs), all series can be processed, or a sub-set of series can be selected.
    - “Input control > Series number”: If processing a subset of available series the series to process can be specified as a comma-separated list of series indices.
    - “Threshold image > Threshold multiplier”: Adjusts the automatically detected threshold prior to application. Values <1 will lower the threshold and values >1 will increase it.
    - “Remove objects smaller than...”: Applies an optional size filter to detected objects. Sizes are specified in  $\mu\text{m}^3$  units. Disable using the power icon.
    - “Remove objects darker than...”: Applies an optional object intensity filter. Intensities are measured from the raw image stack. Disable using the power icon.

- “Remove blobs not in a cluster”: Applies an optional filter, which removes any objects not identified as part of a cluster using DBSCAN. Disable using the power icon.
  - “Add cluster outlines to overlay”: Render the cluster outlines on the output overlay images (showing what was detected).
  - “Show outlines image”: Display the outlines image as soon as it is generated.
  - “Save outlines image”: Save the outlines image to the same folder as the input files, but with the suffix “\_outlinesNew”.
- e. Click “Run” to start processing. When finished, the message window at the bottom of the plugin will display “Complete!”. Results will be saved in the same folder as the input file.
11. Puncta were identified using the Otsu algorithm with a threshold multiplier of 3.5 followed by a watershed 3D method to separate close objects. The volume of each punctum was determined.
  12. Small puncta detected in the APCs that don't express LAT were used to derive a detection size threshold for LAT complexes such that all puncta smaller than the 95 percentile of the APC puncta size distribution were excluded from the analysis (Figure 1). Thus, complexes smaller than  $0.04/0.06 \mu\text{m}^3$  in the LAT/pLAT data were excluded from the analysis. Repeating the analysis with a 99-percentile cut-off didn't change the conclusions reached.
  13. The closest distance between adjacent puncta that could be resolved was 100 nm.

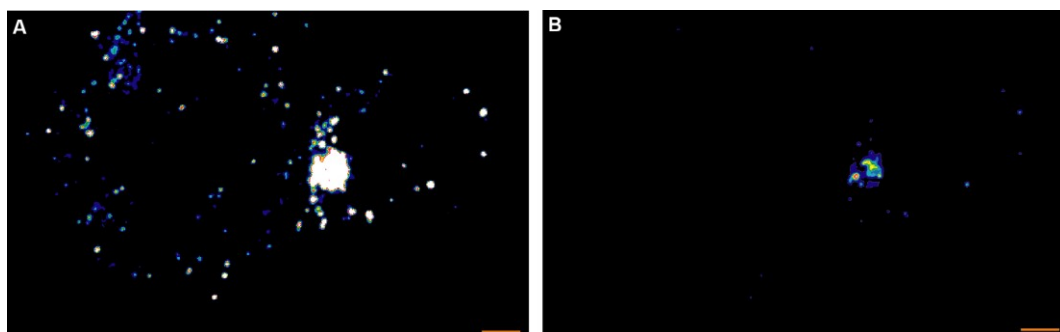


**Figure 1. Two versions of one representative STED midplane image are given of 5C.C7 T cells activated by CH27 APCs (10  $\mu\text{M}$  MCC agonist peptide) and stained with  $\alpha$ -LAT pY191.** Staining fluorescence intensity is given in rainbow-like false-color scale (increasing from blue to red). A. The Otsu algorithm with a threshold of 3.5 A.U. identifies large phospho-LAT clusters at the cellular interface and small, unspecific puncta in both APC and CD4 $^{+}$  T cell. B. The bright LAT cluster formed a ‘central’ pattern as more readily seen in B where the same data are displayed on a different intensity scale. Scale bars = 1  $\mu\text{m}$ .

14. LAT puncta could be clustered at the center of the T cell APC interface (Figures 1-2) or could be distributed across the entire interface (Figures 2-3). Such ‘central’ or ‘diffuse’ distributions correspond to the formation or lack of a formation of the cSMAC complex, respectively. Patterns were determined using established pattern classification methods (Singleton *et al.*, 2009). Puncta numbers and sizes were quantified as a function of this pattern classification in Figure 3B of Clark *et al.* (2019).

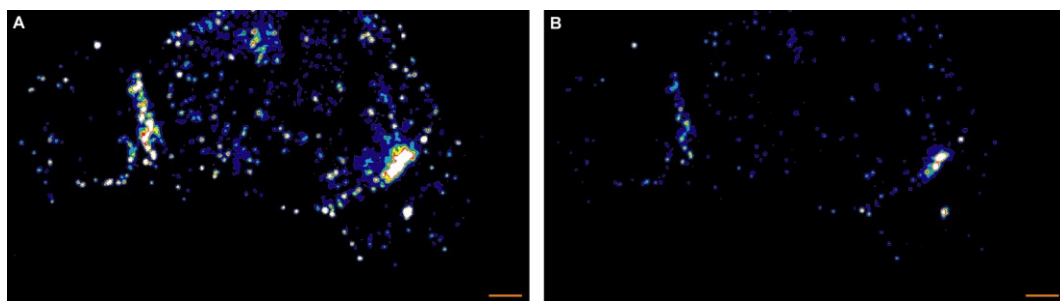


**Figure 2. Two versions of a representative STED midplane image are given showing two different LAT patterns in 5C.C7 T cells activated by one CH27 APC (10  $\mu\text{M}$  MCC, the middle cell) and stained with  $\alpha$ -LAT pY191.** Staining fluorescence intensity is given in rainbow-like false-color scale (increasing from blue to red). A. The 5C.C7 T cell on the left shows ‘diffuse’ patterning of phospho-LAT. The 5C.C7 T cell on the right show ‘central’ patterning. As in Figure 1 small, unspecific puncta in both APC and CD4 $^{+}$  T cells are visible. B. The patterns are more readily seen in B where the same data are displayed on a different intensity scale. Scale bars = 1  $\mu\text{m}$ .

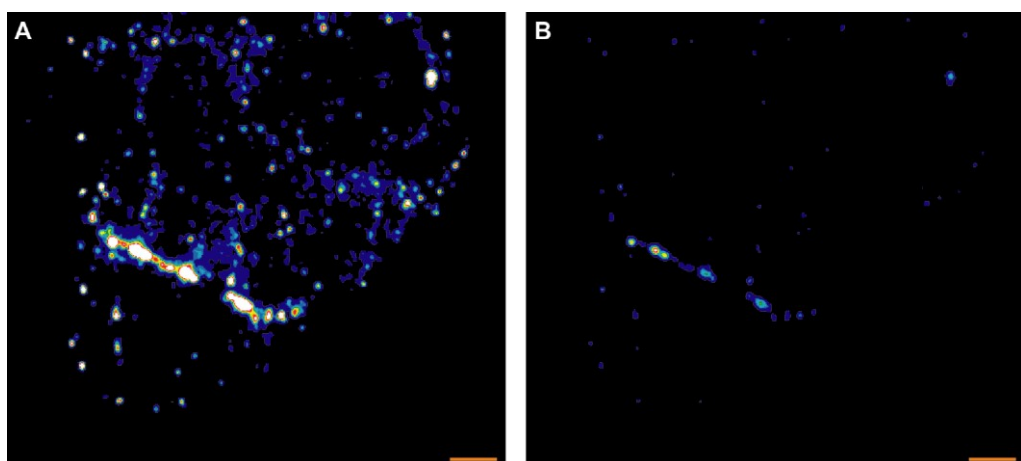


**Figure 3. Two versions of a representative STED midplane image showing diffuse LAT protein patterning in a 5C.C7 T cells activated by one CH27 APC (10  $\mu\text{M}$  MCC, the cell on the top).** Staining fluorescence intensity is given in rainbow-like false-color scale (increasing from blue to red). A. The 5C.C7 T shows ‘diffuse’ patterning of phospho-LAT. As in Figure 1 small, unspecific puncta in both APC and CD4 $^{+}$  T cell are visible. B. The pattern is more readily seen in B where the same data are displayed on a different intensity scale. Scale bars = 1  $\mu\text{m}$ .

## Recipes

### 1. T cell Culture Components

#### Complete medium

RPMI with L-glutamine, 10% FBS, 100 U/ml Penicillin plus 100  $\mu\text{g}/\text{ml}$  streptomycin, 50  $\mu\text{M}$  2-mercaptoethanol

#### Interleukin-2 medium

complete medium with 50 U/ml of rhIL-2

**Moth cytochrome C (MCC) agonist peptide for the stimulation of 5C.C7 TCR transgenic T cells**

5 mM solution in ddH<sub>2</sub>O

2. 2x Pervanadate components

- a. Dilute 30% H<sub>2</sub>O<sub>2</sub> stock solution 1:10 in ddH<sub>2</sub>O to make up a 3% solution of H<sub>2</sub>O<sub>2</sub>
- b. Make up 2x pervanadate stock by adding 4 µl of 3% H<sub>2</sub>O<sub>2</sub> solution with 20 µl of 20 mM Na<sub>3</sub>VO<sub>4</sub> in 976 µl of ddH<sub>2</sub>O in a 1.5 ml Eppendorf tube
- c. Incubate 2x pervanadate for 10 min in the dark at RT and ready to use

3. Imaging buffer

PBS without calcium and magnesium, 10% FBS, 1 mM calcium chloride, 0.5 mM magnesium chloride

**Acknowledgments**

We acknowledge the University of Bristol FACS and Wolfson BioImaging facilities for providing equipment and technical support as well as BrisSynBio, a BBSRC/EPSRC-funded Synthetic Biology Research Centre (grant number: L01386X). The work was supported by a grant from the BBSRC (BB/P011578/1 to C.W.) and the EPSRC and BBSRC Centre for Doctoral Training in Synthetic Biology (EP/L016494/1 to H. T.). The procedure described in detail in this protocol paper was derived from Clark *et al.* (2019).

**Competing interests**

The authors declare no competing interests.

**Ethics**

All animals were maintained in pathogen-free animal facilities at the University of Bristol under the University mouse breeding Home Office License P10DC2972.

**References**

1. Ambler, R., Ruan, X., Murphy, R. F. and Wulffing, C. (2017). [Systems imaging of the immune synapse](#). *Methods Mol Biol* 1584: 409-421.
2. Balagopalan, L., Kortum, R. L., Coussens, N. P., Barr, V. A. and Samelson, L. E. (2015). [The linker for activation of T cells \(LAT\) signaling hub: from signaling complexes to microclusters](#). *J Biol Chem* 290(44): 26422-26429.
3. Banani, S. F., Rice, A. M., Peeples, W. B., Lin, Y., Jain, S., Parker, R. and Rosen, M. K. (2016). [Compositional control of phase-separated cellular bodies](#). *Cell* 166(3): 651-663.
4. Clark, D. J., McMillan, L. E., Tan, S. L., Bellomo, G., Massoue, C., Thompson, H., Mykhaylechko, L., Alibhai, D., Ruan, X., Singleton, K. L., Du, M., Hedges, A., Schwartzberg, P. L., Verkade, P., Murphy, R.

- F. and Wulffing, C. (2019). [Transient protein accumulation at the center of the T cell antigen-presenting cell interface drives efficient IL-2 secretion](#). *Elife* 8: 45789.
5. Freiberg, B. A., Kupfer, H., Maslanik, W., Delli, J., Kappler, J., Zaller, D. M. and Kupfer, A. (2002). [Staging and resetting T cell activation in SMACs](#). *Nat Immunol* 3(10): 911-917.
6. Grakoui, A., Bromley, S. K., Sumen, C., Davis, M. M., Shaw, A. S., Allen, P. M. and Dustin, M. L. (1999). [The immunological synapse: A molecular machinery controlling T cell activation](#). *Science* 285: 221-226.
7. Li, P., Banjade, S., Cheng, H. C., Kim, S., Chen, B., Guo, L., Llaguno, M., Hollingsworth, J. V., King, D. S., Banani, S. F., Russo, P. S., Jiang, Q. X., Nixon, B. T. and Rosen, M. K. (2012). [Phase transitions in the assembly of multivalent signalling proteins](#). *Nature* 483(7389): 336-340.
8. Monks, C. R., Freiberg, B. A., Kupfer, H., Sciaky, N. and Kupfer, A. (1998). [Three-dimensional segregation of supramolecular activation clusters in T cells](#). *Nature* 395(6697): 82-86.
9. Monks, C. R., Kupfer, H., Tamir, I., Barlow, A. and Kupfer, A. (1997). [Selective modulation of protein kinase C-theta during T-cell activation](#). *Nature* 385(6611): 83-86.
10. Roybal, K. T., Mace, E. M., Mantell, J. M., Verkade, P., Orange, J. S. and Wulffing, C. (2015). [Early signaling in primary T cells activated by antigen presenting cells is associated with a deep and transient lamellar actin network](#). *PLoS One* 10(8): e0133299.
11. Rueden, C. T., Schindelin, J., Hiner, M. C., DeZonia, B. E., Walter, A. E., Arena, E. T. and Eliceiri, K. W. (2017). [ImageJ2: ImageJ for the next generation of scientific image data](#). *BMC Bioinformatics* 18(1): 529.
12. Schindelin, J., Arganda-Carreras, I., Frise, E., Kaynig, V., Longair, M., Pietzsch, T., Preibisch, S., Rueden, C., Saalfeld, S., Schmid, B., Tinevez, J. Y., White, D. J., Hartenstein, V., Eliceiri, K., Tomancak, P. and Cardona, A. (2012). [Fiji: an open-source platform for biological-image analysis](#). *Nat Methods* 9(7): 676-682.
13. Seder, R. A., Paul, W. E., Davis, M. M. and Fazekas de St. Groth, B. (1992). [The presence of interleukin 4 during in vitro priming determines the lymphokine-producing potential of CD4<sup>+</sup> T cells from T cell receptor transgenic mice](#). *J Exp Med* 176(4): 1091-1098.
14. Shin, Y. and Brangwynne, C. P. (2017). [Liquid phase condensation in cell physiology and disease](#). *Science* 357(6357).
15. Singleton, K. L., Roybal, K. T., Sun, Y., Fu, G., Gascoigne, N. R., van Oers, N. S. and Wulffing, C. (2009). [Spatiotemporal patterning during T cell activation is highly diverse](#). *Sci Signal* 2(65): ra15.
16. Su, X., Ditlev, J. A., Hui, E., Xing, W., Banjade, S., Okrut, J., King, D. S., Taunton, J., Rosen, M. K. and Vale, R. D. (2016). [Phase separation of signaling molecules promotes T cell receptor signal transduction](#). *Science* 352(6285): 595-599.
17. Varma, R., Campi, G., Yokosuka, T., Saito, T. and Dustin, M. L. (2006). [T cell receptor-proximal signals are sustained in peripheral microclusters and terminated in the central supramolecular activation cluster](#). *Immunity* 25(1): 117-127.
18. Yokosuka, T., Sakata-Sogawa, K., Kobayashi, W., Hiroshima, M., Hashimoto-Tane, A., Tokunaga, M., Dustin, M. L. and Saito, T. (2005). [Newly generated T cell receptor microclusters initiate and sustain T cell activation by recruitment of Zap70 and SLP-76](#). *Nat Immunol* 6(12): 1253-1262.

## Optical Clearing and Index Matching of Tissue Samples for High-resolution Fluorescence Imaging Using SeeDB2

Meng-Tsen Ke<sup>1</sup> and Takeshi Imai<sup>1, 2, \*</sup>

<sup>1</sup>Laboratory for Sensory Circuit Formation, RIKEN Center for Developmental Biology, Kobe, Japan; <sup>2</sup>Graduate School of Medical Sciences, Kyushu University, Fukuoka, Japan

\*For correspondence: [t-imai@med.kyushu-u.ac.jp](mailto:t-imai@med.kyushu-u.ac.jp)

**[Abstract]** Tissue clearing techniques are useful for large-scale three-dimensional fluorescence imaging of thick tissues. However, high-resolution imaging deep inside tissues has been challenging, as it is extremely sensitive to light scattering and spherical aberrations. Here, we present a water-based optical clearing and mounting media, SeeDB2, which is designed for high numerical aperture (NA) objective lenses with oil or glycerol immersion. Using quick and simple soaking procedures, the refractive indices of samples can be matched either to that of immersion oil (1.52) or glycerol (1.46), thus minimizing light scattering and spherical aberrations. Fine morphology and various fluorescent proteins are highly preserved during the clearing and imaging process. Our method is useful for the three-dimensional fluorescence imaging of neuronal circuitry at synaptic resolution using confocal and super-resolution microscopy. SeeDB2 is also useful as a mounting media for the super-resolution imaging of fluorescent proteins.

**Keywords:** Tissue clearing, Fluorescence imaging, Confocal imaging, Super-resolution imaging, Connectome, SeeDB2

**[Background]** Biological tissues are organized in 3D. In addition, many of important cellular machineries, *e.g.*, synapses in neurons, are at sub-micron scale. Therefore, there have been increasing demands for a method for sub-micron-scale 3D imaging. Serial electron microscopy techniques (*e.g.*, FIB-SEM or SBF-SEM) are promising, but they cannot make the best use of the genetic fluorescent labeling tools available in modern life science. To facilitate 3D imaging with fluorescence microscopy, a number of tissue clearing techniques have been developed in recent years (Richardson and Lichtman, 2015 and 2017). They are designed for large-scale 3D imaging, and some of them allow for whole-brain, and even whole-body-scale fluorescence imaging of fixed samples combined with confocal, two-photon, or light-sheet microscopy. However, many of them have not been fully optimized for high-resolution imaging.

In fluorescence microscopy, lateral resolution ( $d$ ) is given as:

$$d = 0.61\lambda/\text{NA}$$

where  $\lambda$  is the wavelength of the light and NA represents the numerical aperture. The resolution improves as  $d$  decreases. Therefore, we need to use high NA objective lenses for high-resolution imaging.

NA is defined as:

$$\text{NA} = n \sin\alpha$$

where  $n$  is the refractive index (RI) of the immersion media, and  $\alpha$  is the half angular aperture. Therefore, many of the high NA objective lenses are designed for oil (RI = 1.52) or glycerol (RI = 1.46) immersion for the best

resolution. Previously, high NA objective lenses are intended to image thin sections or just the surface of samples. However, if we try to image deeper in the samples with these objective lenses, image quality will be easily impaired due to “spherical aberrations”. As RI of tissue samples are lower than that of immersion oil (RI = 1.52) and a glass coverslip (RI ~1.52), the excitation light will refract at the interface between the coverslip and samples, and it will no longer converge onto a small focal spot. This is known as spherical aberrations, reducing resolution and brightness in microscopy.

To minimize spherical aberrations, index matching of samples is crucial. However, many of the existing mounting media and clearing solutions have low RI, ranging from 1.33 (water) to 1.46 (glycerol-based mounting media). Even our previous clearing agent, SeeDB (RI = 1.49), did not reach RI 1.52 (Ke *et al.*, 2013, 2014). 2,2'-thiodiethanol (TDE, RI = 1.52) has been previously proposed for index matching for oil-immersion objective lenses and has been widely used for synthetic fluorescent dyes (Staudt *et al.*, 2007). However, a major drawback of TDE is that most of fluorescent proteins are totally quenched in TDE. To overcome this limitation, we developed a new tissue clearing agent, SeeDB2S, that has a high refractive index (RI = 1.52), but also highly preserves fluorescent proteins (Ke *et al.*, 2016). We also formulated SeeDB2G (RI = 1.46) for glycerol-immersion objective lenses. As fluorescent proteins are better preserved than in commercialized mounting media, SeeDB2G/S are also useful as mounting media for high-resolution imaging. SeeDB2G/S is particularly powerful for high-resolution confocal microscopy and super-resolution microscopy of fluorescent proteins in tissues, sections, and cells.

## **Materials and Reagents**

1. 1.5 ml Eppendorf tube (Eppendorf, for 1 ml solution)
2. 5 ml Eppendorf tube (Eppendorf, catalog number: 0030119401; optional for 3 ml solution, for thick brain slices or whole-mount samples)
3. Paint brush (for thin brain slices, No. 1-2, see Figure 1)
4. Silicone rubber sheet (translucent, 0.2 mm thick; *e.g.*, AS ONE, catalog number: 6-9085-13; see Figure 1)

*Note: Various thickness of silicone rubber sheets are available from Togawa Rubber (AS ONE), Professional Plastics, CS Hyde, etc., ranging from 0.1 mm to 8.0 mm. The thickness should match that of brain slices.*

5. Glass slide (76 mm x 26 mm; MATSUNAMI Glass; Figure 1)
6. Coverslips (18 x 18 mm, No 1.5H; *e.g.*, Paul Marienfeld, catalog number: 0107032 or ZEISS, catalog number: 474030-9000-000; Figure 1)

*Note: No 1.5H (170 ± 5 µm thick) is highly recommended for super-resolution imaging.*

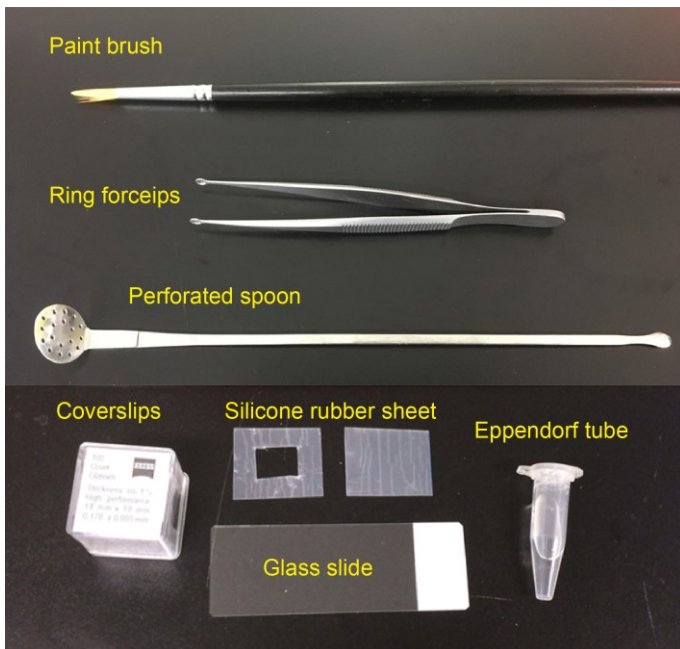


**Figure 1. Materials required for preparing imaging chamber and slice mounting**

7. Sodium chloride (NaCl)
8. Sodium hydrogen phosphate dodecahydrate ( $\text{Na}_2\text{HPO}_4 \cdot 12\text{H}_2\text{O}$ )
9. Potassium chloride (KCl)
10. Potassium dihydrogen phosphate ( $\text{KH}_2\text{PO}_4$ )
11. 4% paraformaldehyde (PFA; *e.g.*, NACALAI TESQUE, catalog number: 26126-25) in PBS
12. 20% Saponin (NACALAI TESQUE, catalog number: 30502-42) in ddH<sub>2</sub>O with filter sterilization

*Note: Different vendors prepare saponin from different species of plants. We strongly recommend NACALAI TESQUE. Brownish lots (often found in Sigma-Aldrich) should be avoided.*
13. Low-melting point agarose (*e.g.*, Thermo Fisher Scientific, catalog number: 16520100)
14. Omnipaque 350 (*e.g.*, DAIICHI SANKYO, Omnipaque 350 Injection, 50 ml in 1 bottle; also available from GE healthcare)
15. Histodenz (*e.g.*, Sigma-Aldrich, catalog number: D2158)
16. Sodium azide (*e.g.*, Sigma-Aldrich, catalog number: 13412)
17. 1 M stock of Tris-HCl, pH 7.6 (*e.g.*, NACALAI TESQUE, catalog number: 35436-01), used to prepare Tris-EDTA buffer
18. 0.5 M stock of EDTA, pH 8.0 (*e.g.*, Dojindo, catalog number: 347-07481), used to prepare Tris-EDTA buffer
19. Immersion media:

Glycerol (*e.g.*, Type G Immersion Liquid, Leica Microsystems, catalog number: 11513910; Glycerine solution, Leica Microsystems, catalog number: 11513872) for SeeDB2G  
Oil (Type F, Olympus, MOIL-30; also available from Leica, Zeiss, *etc.*) for SeeDB2S
20. (Optional) SeeDB2 Trial Kit (Wako Pure Chemical Industries, catalog number: 294-80701)
21. Phosphate-buffered saline (PBS) (see Recipes)

22. Tris-EDTA buffer, pH 7.6 (see Recipes)
23. Permeabilization solution (see Recipes)
24. Solution 1 (see Recipes)
25. Solution 2 (see Recipes)
26. SeeDB2 solutions (see Recipes)
  - a. SeeDB2G with saponin (clearing)
  - b. SeeDB2G (mounting)
  - c. SeeDB2S with saponin (clearing)
  - d. SeeDB2S (mounting)

## **Equipment**

1. Perforated spoon (optional for handling thick brain slices, custom-ordered, flat head, head diameter = 15 mm, see Figure 1 and Video 1)
2. Ring forceps (optional for whole-mount samples, *e.g.*, Natsume Seisakusho, NAPOX, catalog number: A-26, see Figure 1)
3. Vibratome (*e.g.*, LinearSlicer, DOSAKA, model: PRO7N)
4. Seesaw shaker (*e.g.*, Bio Craft, model: BC-700)
5. Rotator (*e.g.*, TAITEC, model: RT-30mini, catalog number: 0057154-000)
6. Fluorescence microscope
  - a. Confocal microscope (*e.g.*, Olympus, model: FV3000; Leica Microsystems, model: Leica TCS SP8; Nikon, model: A1+)
  - b. Super-resolution microscope (*e.g.*, Zeiss, model: LSM 880 with Airyscan; Leica Microsystems, model: Leica TCS SP8 with Hyvolution 2; Leica Microsystems, model: Leica TCS SP8 STED)
7. Objective lenses  
Examples: 63x oil-immersion (NA = 1.4, WD = 0.14 mm) (Leica Microsystems, model: HC PL APO 63x/1.4 Oil CS2, catalog number: 15506350); 100x oil-immersion (NA = 1.4, WD = 0.13 mm) (Leica Microsystems, model: HC PL APO 100x/1.4 Oil CS2, catalog number: 15506325); 63x glycerol-immersion (NA = 1.3, WD = 0.28 mm) (Leica, model: HCX PL APO 63x/1.30 GLYC CORR, catalog number: 11506193); 63x oil-immersion (NA = 1.4, WD = 0.19 mm) (Carl Zeiss, model: Plan-Apochroamt 63x/1.40 Oil DIC, catalog number: 440762-9904-000)

## **Procedure**

- A. Choice of optical clearing protocol
  1. SeeDB2G (RI = 1.46): SeeDB2G is optimized for glycerol-immersion lenses to achieve the highest resolution, but water- and multi-immersion objective lenses are also useful with reasonable resolution. SeeDB2G is useful for larger tissues due to lower viscosity.
  2. SeeDB2S (RI = 1.52): SeeDB2S is optimized for high-NA oil-immersion objective lenses. Since

SeeDB2S is viscous and oil-immersion lenses typically have a short W.D. (0.1-0.2 mm), we recommend using relatively thin samples (< 300 µm thick slices) for SeeDB2S.

In this protocol, we describe the protocol for high-resolution/super-resolution imaging of mouse brain slices. However, SeeDB2 is also useful for high-resolution imaging of other organisms (*e.g.*, *Drosophila*), other organs and sample types (mouse oocytes), cultured cells, and frozen sections. See the original paper (Ke *et al.*, 2016) and [SeeDB Resources](#) for details.

*Note:* SeeDB Resources (<https://sites.google.com/site/seedbresources/>) provide updated information from the authors, see Ke *et al.*, 2014.

#### B. Choice of objective lenses and slice thickness

Because of the working distance limitations in high-NA lenses, only one-fourth to half of the depth accessible by 20x lens can be reached by 63x or 100x lenses. Be sure to select neurons located close to the surface. See Table 1 showing examples of objective lenses used for confocal imaging.

**Table 1. Examples of objective lenses**

Objective lens	10x air	20x multi	40x oil	63x glycerol	63x oil	100x oil
N.A.	0.4	0.75	1.3-1.4	1.3	1.4	1.4-1.46
W.D. (mm)	2.2-3.1	0.68	0.21-0.24	0.3	0.14-0.19	0.11-0.13
Immersion	-	Water/glycerol/oil	Oil	Glycerol	Oil	Oil
Lateral resolution	2 µm	0.5 µm	0.3 µm	0.25 µm	0.21 µm	0.2 µm
Confocal	+	+	+	+	+	+
Super-resolution	-	-	±	±	+	+
SeeDB2G	±	+	±	+	±	±
SeeDB2S	±	±	+	±	+	+
Suitable sample thickness	< 2 mm	< 1 mm	< 500 µm	< 500 µm	< 300 µm	< 200 µm

+, optimal; ±, non-optimal; -, not suitable. Data based on Leica and Zeiss objective lenses.

#### C. SeeDB2G (Figure 2)

1. Dissect the mouse brain after an intracardiac perfusion of 4% PFA in PBS. Post-fix the brain sample in 4% PFA at 4 °C with gentle shaking overnight.
2. Wash the sample in PBS three times with gentle shaking (10 min each).
3. Embed the sample in 4% low-melting point agarose/PBS with desired orientation and then cut the brain with a vibratome.
4. Transfer the sample into the permeabilization solution and incubate with shaking overnight (> 16 h) at 4 °C. Antibody staining and counterstaining should be performed prior to the clearing process.

Optional: Perform antibody staining in 3 ml using 5 ml Eppendorf tubes on a rotator. After blocking with blocking buffer (0.5% skim milk, 0.25% fish gelatin, 2% saponin in PBS) for 24 h at 4 °C, incubate samples with primary antibodies in washing buffer (2% saponin in PBS) for 24 h. After three washes with washing buffer, incubate samples with secondary antibodies and DAPI for 12-16 h. Wash

samples three times (2 h each) in washing buffer.

*Note: We recommend 2% saponin for thick mouse brain samples; however, for the thinner slices, lower concentrations of Triton X-100 are also workable. Antibodies are able to penetrate up to 200-300 µm in depth.*

5. Transfer the sample into a new tube filled with solution 1 and place it on a rotator. Incubate for 6-10 h for whole-mount samples, 2-4 h for slice samples (200-500 µm).
6. Transfer the sample into a new tube filled with solution 2 and place it on a rotator. Incubate for 6-10 h for whole-mount samples, 2-4 h for slice samples (200-500 µm).
7. Transfer the sample into a new tube filled with SeeDB2G with saponin and place it on a rotator. Incubate for 6-10 h for whole-mount samples, 2-4 h for slice samples (200-500 µm). An example of transmission images is shown in Figure 4.

*Notes:*

- a. *Do not store samples in solutions containing saponin. For thin slice or neonate samples, prolonged incubation (> 24 h) in solutions containing saponin may cause damage to the sample.*
- b. *Store the sample in SeeDB2G (without saponin) till mounting and imaging.*  
*SeeDB2-cleared samples can be stored in Eppendorf at 4 °C for up to 6 months. Sodium azide (0.05%) should be added for the long-term storage.*

#### D. SeeDB2S (Figure 2)

1. Dissect the mouse brain after intracardiac perfusion of 4% PFA in PBS. Post-fix the brain sample in 4% PFA at 4 °C with gentle shaking overnight.
2. Wash the sample in PBS three times with gentle shaking (10 min each).
3. Embed the sample in 4% low-melting point agarose/PBS with desired orientation and then cut the brain with a vibratome.
4. Transfer the sample into permeabilization solution and incubate with shaking overnight (> 16 h) at 4 °C. Antibody staining and counterstaining should be performed prior to the clearing process.

*Note: We recommend 2% saponin for thick mouse brain samples; however, for the thinner slices, lower concentrations of Triton X-100 are also workable. Antibodies penetrate up to 200-300 µm depth.*

5. Transfer the sample into a new tube filled with solution 1 and place it on a rotator. Incubate for 2-4 h for slice samples (200-500 µm).
6. Transfer the sample into a new tube filled with solution 2 and place it on a rotator. Incubate for 2-4 h for slice samples (200-500 µm).
7. Transfer the sample into a new tube filled with SeeDB2G with saponin and place it on a rotator. Incubate for 2-4 h for slice samples (200-500 µm).
8. Transfer the sample into a new tube filled with SeeDB2S with saponin and place it on a rotator. Incubate for 2-4 h for slice samples (200-500 µm).
9. Transfer the sample into a new tube filled with SeeDB2S (without saponin, 0.01% sodium azide can be added for long-term storage) for mounting. An example of transmission images are shown in Figure 4.

*Note: Do not store samples in solutions containing saponin. For thin slice or neonate samples,*

prolonged incubation (> 24 h) in solutions containing saponin may cause damages to the sample.

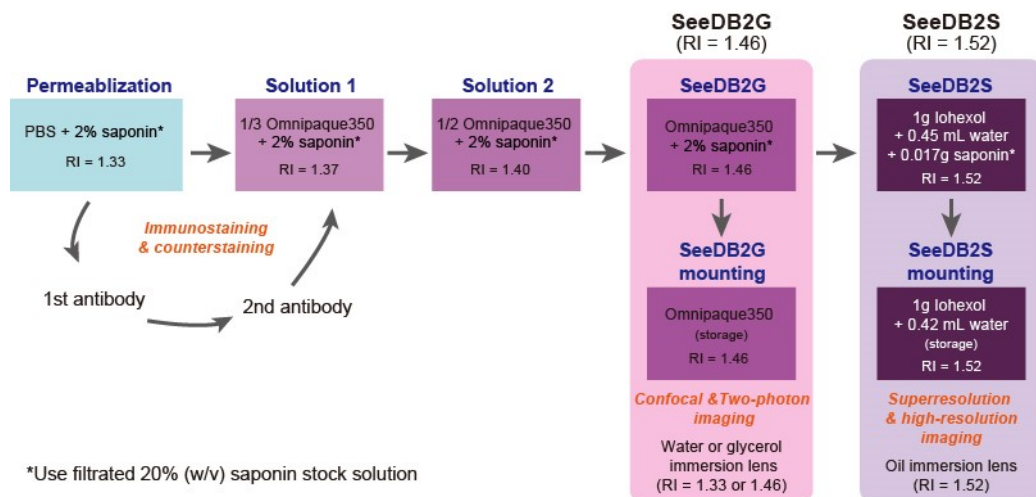


**Figure 2. Graphic protocol for SeeDB2**

E. Imaging chamber preparation and sample mounting (Video 1 and Figure 3)

1. (Optional) Stand the sample in SeeDB2G/S for 2–4 h to remove the air bubbles.

*Note: If air bubbles are heavily accumulated in the tube, transfer the sample to a new tube filled with SeeDB2G/S and incubate it for 2–4 h.*

2. Cut the silicone rubber sheet into appropriate size using scissors or a utility knife.
3. Remove the protection sheets (stuck to both sides, only found in 0.2 mm silicone sheet) and press the sheet onto the glass slide. Push the rubber sheet to remove air bubbles between the glass slide and the rubber sheet.
4. Leave a drop of SeeDB2G/S (from the storage tube, not a fresh one) into the chamber, and pick up the brain slice with a perforated spoon and a paint brush to mount the sample.

*Note: Do not place the brain slices onto a dry surface. Do not expose SeeDB2S solution or SeeDB2S-cleared samples to the air for long time (> 5 min).*

5. (Optional) Remove the air bubbles in the imaging chamber with a paint brush.
  6. Gently press the cover glass onto the imaging chamber and use the spillover of SeeDB2G/S to seal the cover glass. See Figure 3 for mounted samples on a glass slide.
- Note: Do not use nail polish to seal the sample. The excess amount of SeeDB2G/S will form a tight film after air drying.*
7. Use an appropriate immersion media for high-resolution fluorescence imaging. Use glycerol (Refractive index = 1.46) for SeeDB2G, and oil (Refractive index = 1.52; Type F) for SeeDB2S. SeeDB2G/S cannot be used as an immersion media. Figure 5 shows an example of confocal images. Figure 6 shows super-resolution images (Airyscan and STED).



**Video 1. Imaging chamber preparation and sample mounting.** Cut a silicone rubber sheet (1 mm-thick and 0.2 mm-thick are shown in this video) into an appropriate size with scissors or a utility knife. A silicone rubber sheet will adhere to a glass slide, by removing air between the rubber sheet and the glass slide. Mount cleared samples (cleared samples are often difficult to find) using a perforated spoon and a paint brush. Use No. 1.5H coverslips to seal the samples.

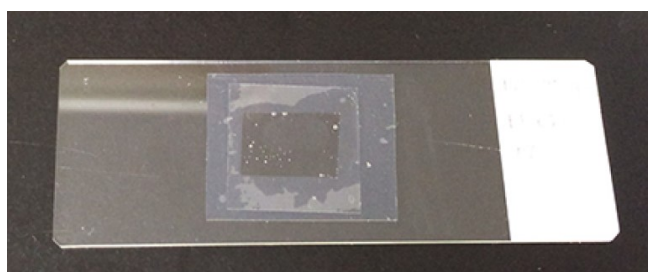


**Figure 3. Slice sample ready for imaging.** A 220  $\mu\text{m}$  brain slice was mounted within the imaging chamber. A silicone rubber sheet (0.2 mm thick) was used for the spacer, and a coverslip is placed to seal the sample. The silicone rubber sheet will adhere to the glass slide and coverslip without adhesive. The spill-over of the SeeDB2G/S will form a tight film after air drying.

#### F. Anticipated Results (Figure 4)



**Figure 4. Transmission images of 500  $\mu\text{m}$  adult mouse brain slices after optical clearing with SeeDB2G and SeeDB2S (Ke *et al.*, 2016).** Grids are 2.6 x 3.2 mm.

## Data analysis

Data analysis procedures have been described in the original publication (Ke *et al.*, 2016). No statistical analysis was performed in this protocol paper. We used Neurolucida (MBF Bioscience) for the 3D rendering in Figure 5.

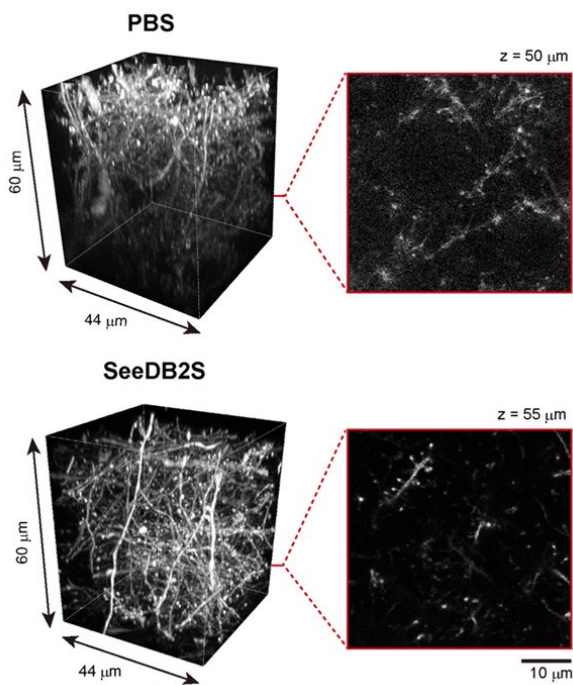


**Figure 5. Confocal imaging of adult brain slices (*Thy1-YFP-H* mouse).** Adult brain slices (220  $\mu\text{m}$  thick) were imaged with 63x oil-immersion lens under confocal microscopy (Leica TCS SP8). In the PBS sample (uncleared), due to light scattering and spherical aberrations, the resolution and fluorescence signals intensity were damped. The highest resolution was maintained throughout all depths when cleared with SeeDB2S.

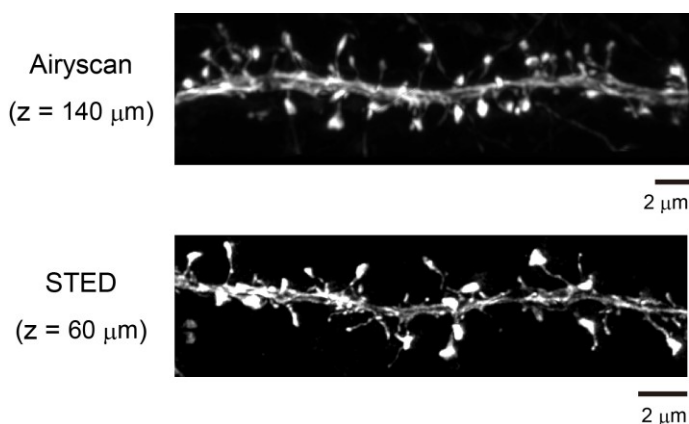


**Figure 6. Super-resolution imaging of adult brain slices (*Thy1-YFP-H* mouse).** Due to the minimized spherical aberrations, SeeDB2S is also useful for various kinds of super-resolution

microscopy, such as STED (Leica), Airyscan (Zeiss), Hyvolution2 (Leica), and SpinSR (Olympus). For large-scale super-resolution imaging, we first imaged with a 20x objective lens. Then, we focused on a particular neuron and obtained super-resolution images along the target neuron to save imaging time and data volume. We used Neurolucida (MBF Bioscience) for the quantification and reconstruction of neuronal morphology. Images adapted from Ke *et al.* (2016).

## **Notes**

1. The saponin solution is brownish

We strongly recommend saponin from NACALAI TESQUE. Different vendors prepare saponin from different species of plants. Brownish lots should be avoided. Alternatively, a low concentration of Triton X-100 can be used.

2. Histodenz does not dissolve completely

Prepare ~10 ml SeeDB2S solution in a 50 ml conical tube to prevent insufficient mixing of iohexol powder and Tris buffer. Use rotator for gentle mixing.

3. White or yellow aggregations in SeeDB2 solutions

To avoid bacterial contamination, filter and sterilize the 20% saponin stock solution. Add 0.01%-0.1% of sodium azide to each clearing solution and store the solutions containing saponin at 4 °C.

4. Water evaporation

The surface of SeeDB2 forms a film as the water evaporates from the surface. SeeDB2 should be sealed in the imaging chamber during imaging.

5. Sealing samples in the imaging chambers/glass slides

Nail polish should not be used to seal the samples. For thick samples, we routinely use a silicone rubber. To seal samples on glass slides, we use an excess amount of SeeDB2, which then forms a tight film after water evaporation.

6. Samples are floating within SeeDB2

To avoid movement artifacts during imaging, we prepared brain slices that are slightly thicker than the thickness of the spacer (translucent silicone rubber sheet). For example, we prepared 220 µm brain slices when we used 200 µm-thick rubber sheets. For small samples, it is also useful to prepare SeeDB2 with 0.1% low-melting agarose to immobilize the sample; we used low-melting agarose to image mouse oocyte samples. Embedding small samples in agarose may also be useful to avoid the loss of samples during clearing, as it is often difficult to find invisible samples from clearing solution.

7. Movement artifacts

Because SeeDB2 allows for imaging up to the limit of the working distance (W.D.) of the objective lens, glass slides are often pushed up by the objective lenses as you get closer to the upper limit, which leads to movement artifacts. We recommend using a clamp or placing a weight on the glass slide in order to avoid the movement of samples during imaging.

8. Detecting sample surface

Because the refractive index of SeeDB2 is the same as that of coverslips, it is difficult to determine the

surface of the sample when you perform the fluorescence imaging. Make sure to attach the sample to the coverslip (see Note 6).

#### 9. Photo-bleaching

Various fluorescent proteins (*e.g.*, TagBFP2, ECFP, mTurquoise2, EGFP, EYFP, CyOFP, tdTomato, tdKatushka2) are very stable and resistant to photo-bleaching in SeeDB2 solution. Indeed, SeeDB2 performs much better than commercialized mounting media for fluorescent proteins. However, some Alexa dyes and DAPI are easily photo-bleached in SeeDB2. In these situations, we suggest 2,2'-Thiodiethanol (TDE, refractive index up to 1.52) as an alternative for chemical dyes (Staudt *et al.*, 2007), however, fluorescent proteins are quenched in TDE.

### Recipes

#### 1. Phosphate-buffered saline (PBS)

80 g NaCl

29 g Na<sub>2</sub>HPO<sub>4</sub>·12H<sub>2</sub>O

2 g KCl

2 g KH<sub>2</sub>PO<sub>4</sub>

Add ddH<sub>2</sub>O to prepare 1 L PBS

#### 2. Tris-EDTA buffer, pH 7.6

10 mM Tris-HCl

0.25 mM EDTA

#### 3. Permeabilization solution

100 µl 20% saponin solution + 900 µl PBS

#### 4. Solution 1

100 µl 20% saponin solution + 333 µl Omnipaque350 + 567 µl ddH<sub>2</sub>O

#### 5. Solution 2

100 µl 20% saponin solution + 500 µl Omnipaque350 + 400 µl ddH<sub>2</sub>O

#### 6. SeeDB2 solutions

*Notes:*

- a. *Tris-EDTA buffer pH 7.6 (Recipe 2) is used to prepare SeeDB2S from Histodenz powder. Do not use PBS. Phosphate buffer will generate white precipitates after long-term storage and impair imaging quality.*
- b. *The solution of 0.01% sodium azide can be included in the buffer for long-term preservation. Do not store clearing solution for long time.*
- c. *Pre-made SeeDB2 solutions are also commercialized from FUJIFILM Wako Pure Chemical.*

Solutions	Composition
SeeDB2G with saponin (clearing)	2% saponin in Omnipaque350
SeeDB2G (mounting)	Use Omnipaque350 directly

	Or 7,500 µl Tris-EDTA (pH 7.6) + 10 g Histodenz
SeeDB2S with saponin (clearing)	3,780 µl Tris-EDTA (pH 7.6) + 420 µl 20% saponin solution + 10 g Histodenz
SeeDB2S (mounting)	4,200 µl Tris-EDTA (pH 7.6) + 10 g Histodenz Add 4,200 µl Tris-EDTA to a 50 ml conical tube, and then add 10 g Histodenz. Use a rotator to fully dissolve the Histodenz in the conical tube

### **Acknowledgments**

This protocol was adapted from our original publication of the protocol (Ke *et al.*, 2016). We thank J.R. Sanes for providing the Thy1-YFP-H mouse line, R. Sakaguchi for help with video, and M. Leiwe for proofreading. This work was supported by grants from the PRESTO program of the Japan Science and Technology Agency (JST), the Brain/MINDS project of the Japan Agency for Medical Research and Development (AMED), the Mitsubishi Foundation, the Strategic Programs for R&D (President's Discretionary Fund) of RIKEN, the JSPS KAKENHI (grant numbers 23680038, 15K14336, 16K14568, 16H06456, 17H06261), and RIKEN CDB intramural grant. M.-T.K. was supported by RIKEN Foreign Postdoctoral Researcher program. The imaging experiments were supported by the RIKEN Kobe Light Microscopy Facility. Animal experiments were supported by Laboratory for Animal Resources and Genetic Engineering (LARGE) at the RIKEN Center for Life Science Technologies.

### **Competing interests**

M.-T.K. and T.I. have filed a patent application on SeeDB2, assigned to RIKEN.

### **References**

1. Ke, M. T., Fujimoto, S. and Imai T. (2013). [SeeDB: a simple and morphology-preserving optical clearing agent for neuronal circuit reconstruction](#). *Nat Neurosci* 16(8): 1154-1161.
2. Ke, M. T., Fujimoto, S. and Imai T. (2014). [Optical clearing using SeeDB](#). *Bio-protocol* 4(3): e1042.
3. Ke, M. T., Nakai, Y., Fujimoto, S., Takayama, R., Yoshida, S., Kitajima, T. S., Sato, M. and Imai, T. (2016). [Super-resolution mapping of neuronal circuitry with an index-optimized clearing agent](#). *Cell Rep* 14(11): 2718-2732.
4. Richardson, D. S. and Lichtman, J. W. (2015). [Clarifying tissue clearing](#). *Cell* 162(2):246-257.
5. Richardson, D. S. and Lichtman, J. W. (2017). [SnapShot: tissue clearing](#). *Cell* 171(2): 496-496.e1.
6. Staudt, T., Lang, M. C., Medda, R., Engelhardt, J., Hell, S. W. (2007). [2,2'-thiodiethanol: a new water soluble mounting medium for high resolution optical microscopy](#). *Microsc Res Tech*. 70(1):1-9.

## Multicolor Stimulated Emission Depletion (STED) Microscopy to Generate High-resolution Images of Respiratory Syncytial Virus Particles and Infected Cells

Masfique Mehedi<sup>1, #, \*</sup>, Margery Smelkinson<sup>2, #</sup>, Juraj Kabař<sup>2</sup>, Sundar Ganesan<sup>2</sup>, Peter L. Collins<sup>1</sup> and Ursula J. Buchholz<sup>1</sup>

<sup>1</sup>RNA Viruses Section, Laboratory of Infectious Diseases, National Institute of Allergy and Infectious Diseases, National Institutes of Health, Bethesda, Maryland, USA; <sup>2</sup>Biological Imaging Section, Research Technologies Branch, National Institute of Allergy and Infectious Diseases, National Institutes of Health, Bethesda, Maryland, USA

\*For correspondence: [masfique.mehedi@nih.gov](mailto:masfique.mehedi@nih.gov)

#Contributed equally to this work

**[Abstract]** Human respiratory syncytial virus (RSV) infection in human lung epithelial A549 cells induces filopodia, cellular protrusions consisting of F-actin, that extend to neighboring uninfected cells (Mehedi *et al.*, 2016). High-resolution imaging via stimulated emission depletion (STED) microscopy revealed filamentous RSV particles along these filopodia, suggesting that filopodia facilitate RSV cell-to-cell spread (Mehedi *et al.*, 2016). In this protocol, we describe how to fix, permeabilize, immunostain, and mount RSV-infected A549 cells for STED imaging. We show that STED increases resolution compared to confocal microscopy, which can be further improved by image processing using deconvolution software.

**Keywords:** RSV, A549, STED microscopy, Filopodia, Cell-to-cell spread, Immunofluorescence, Confocal microscopy

**[Background]** RSV forms pleomorphic virus particles, with a predominance of long filaments about 100 nm in diameter and up to about 10  $\mu$ m in length (Bachi and Howe, 1973; Mehedi *et al.*, 2016). High-resolution light microscopy techniques are key to visualizing the interactions between RSV infected cells and virus particles. In a recent study, we used super-resolution fluorescence microscopy to study RSV cell-to-cell spread in human lung epithelial A549 cells.

STED microscopy is one of the super-resolution microscopy techniques that have been developed to circumvent the limitations imposed by the ~200 nm diffraction barrier of light (Hell and Wichmann, 1994; Westphal *et al.*, 2008). STED is based on confocal fluorescence microscopy and employs a pair of lasers, namely a pulsed excitation source and a photon depletion source. The excitation pulse is focused on the sample and excites the fluorescent dye therein. The excitation laser is superimposed with a doughnut-shaped STED depletion laser that quenches excited dye molecules except for the doughnut hole at the very center of the excitation focus, so that emission occurs only from the narrow center. Narrowing the excitation focal point in this way allows for images to be taken at resolutions far below the diffraction limit, *e.g.*, typically 30-80 nm. While STED imaging relies on efficient dye depletion, image resolution and intensity are limited by photobleaching inflicted upon the dye. To address these two contrasting, yet key issues that arise with STED imaging, optimal sample preparation, most notably dye selection and signal intensity optimization, are crucial. STED enabled us to state conclusively

that RSV was attached to filopodia rather than merely in the vicinity, and to precisely enumerate viral particles. Here, we describe how samples were prepared for multicolor STED imaging including dye selection, fixation procedure, imaging parameters, and deconvolution. We show how STED and STED deconvolution can improve lateral resolution both qualitatively and quantitatively.

## **Materials and Reagents**

1. Aerosol resistant pipette tips  
20 µl (Thermo Fisher Scientific, catalog number: 21-402-551)  
200 µl pipette tips (Thermo Fisher Scientific, catalog number: 02-682-255)  
1,000 µl pipette tips (Thermo Fisher Scientific, catalog number: 21-402-582)
2. T225 cm<sup>2</sup> flask with canted neck (Corning, Costar®, catalog number: 3001)
3. Microscope slides (super clean) (Scientific Device Laboratory, catalog number: 022)
4. Sterile 12 mm circle untreated cover glasses; thickness 0.13-0.17 mm (Carolina Biological Supply, catalog number: 633029)
5. 50 ml conical tube
6. 24-well cell culture plate (Corning, Costar®, catalog number: 3524)
7. The cell line of interest (human respiratory epithelial A549 cells [ATCC, catalog number: CCL-185])
8. Recombinant wild type RSV (A2 strain, GenBank KT992094) (virus stock with known virus titer, see Notes)
9. TryLE Select cell dissociation reagent, stored at room temperature (Thermo Fisher Scientific, Gibco™, catalog number: 12563)
10. Bovine serum albumin (BSA) standard (Thermo Fisher Scientific, Thermo Scientific™, catalog number: 23210)
11. Anti-RSV F protein mouse monoclonal antibody (mAb) (Abcam, catalog number: ab43812)
12. Anti-beta-tubulin (9F3) rabbit mAb (Cell Signaling Technology, catalog number: 2128)
13. Goat anti-mouse Alexa Fluor 488 (AF488) (Thermo Fisher Scientific, catalog number: A11029)
14. Goat anti-rabbit IgG-Atto 647N (Sigma-Aldrich, catalog number: 40839)
15. Rhodamine phalloidin (CYTOSKELETON, catalog number: PHDR1)
16. ProLong Gold Antifade Mountant (Thermo Fisher Scientific, Invitrogen™, catalog number: P36930)
17. Ultrapure methanol free formaldehyde prepared from paraformaldehyde (PFA) 16% solution, EM Grade (Polysciences, catalog number: 18814)
18. F-12 medium without additives, which is sold commercially as Ham's F-12 nutrient mix (Thermo Fisher Scientific, Gibco™, catalog number: 11765054)
19. Fetal bovine serum (FBS) (GE Healthcare, HyClone™, catalog number: SH30071.03)
20. L-Glutamine 200 mM (Thermo Fisher Scientific, Gibco™, catalog number: 25030081)
21. Dulbecco's phosphate buffer saline (DPBS) (Thermo Fisher Scientific, catalog number: 14190)
22. Triton X-100 (BioUltra, ~10% in H<sub>2</sub>O, Sigma-Aldrich, catalog number: 93443)
23. Trypan blue 0.4% solution (Lonza, catalog number: 17-942E)

24. F-12 complete medium (see Recipes)
25. 4% PFA (see Recipes)
26. 0.05% Triton X-100 (see Recipes)
27. 3% BSA (see Recipes)

## **Equipment**

1. Pipettes (Mettler-Toledo, RAININ, model: Pipet-Lite XLS)
2. Humidified CO<sub>2</sub> incubator (Thermo Fisher Scientific, Thermo Scientific™, model: Forma™ Steri-Cult™)
3. Centrifuge (Beckman Coulter, model: Allegra 25R)
4. Leica TCS SP8 STED 3X system (Leica Microsystems, model: Leica TCS SP8 STED 3X) equipped with:
  - a. A white light excitation laser
  - b. 592 nm, 600 nm, 775 nm depletion lasers
  - c. HC PL APO 100x/1.40 oil STED white objective
  - d. Gated HyD hybrid detectors
5. Hemocytometer (Marienfeld-Superior, catalog number: 0680030)
6. Dumont NOC tweezer (Electron Microscopy Sciences, catalog number: 0103-NOC-PO-1)

## **Software**

1. Images were acquired using LAS X software (version 3.1.1.15751) (Leica Microsystems)
2. Images were deconvolved using Huygens deconvolution software (Huygens Essentials version 16.10.1.p3, Scientific Volume Imaging BV, Hilversum, The Netherlands)
3. PRISM software version 7

## **Procedure**

### A. Virus infection

1. Maintain A549 cells in T225 flasks, following the ATCC's culturing recommendations, with the following modifications:
  - a. Use F-12 complete medium to maintain the line (see Recipes); use TrypLE Select cell dissociation reagent; use FBS to deactivate the TrypLE Select.
  - b. To seed A549 cells onto coverslips, remove the F12 complete cell culture medium from a T225 flask containing a monolayer of about 80% confluent A459 cells. Gently rinse the monolayer with 10 ml pre-warmed (37 °C) 1x DPBS, and remove the DPBS.
  - c. To dissociate cells, add 5 ml TrypLE Select cell dissociation reagent, and incubate for 5 min at 37 °C in a standard humidified CO<sub>2</sub> incubator. Inactivate TrypLE Select by adding 10 ml of cold FBS.

Detach and dissociate A549 cells by gentle pipetting, and transfer the single-cell suspension to a 50 ml conical tube.

- d. Pellet the cells by centrifugation at 300  $\times$  g for 5 min at 4 °C in a tabletop centrifuge. Resuspend the cell pellet in 10 ml of pre-warmed (37 °C) F-12 complete medium. Dilute 10  $\mu$ l of the resuspended A549 cells 1:10 in DPBS with 0.04% trypan blue (80  $\mu$ l DPBS, 10  $\mu$ l trypan blue [0.4%], 10  $\mu$ l aliquot of A549 cells, resuspended in complete F-12 medium) and determine the concentration of the resuspended cells per ml using a hemocytometer as recommended by the manufacturer.
  - e. Dilute the resuspended A549 cells from the 50 ml conical tube with F-12 complete medium to 3  $\times$  10<sup>4</sup> cells per ml, and seed cells by adding 1 ml of F-12 complete medium with 3  $\times$  10<sup>4</sup> cells to each well of a 24-well plate containing a coverslip.
  - f. Incubate the cells overnight in a cell culture incubator at 37 °C, 5% CO<sub>2</sub>.
2. To infect A549 cells, replace the medium with 150  $\mu$ l F-12 medium without additives, containing sucrose-purified RSV (Collins *et al.*, 1995 and Le Nouen *et al.*, 2009; see Notes) at a multiplicity of infection (MOI) of 1 plaque forming unit (PFU) per cell (see Notes).
  3. Incubate A549 cells with virus inoculum for 1 h at 37 °C in a CO<sub>2</sub> incubator.
  4. Remove virus inoculum and wash infected cells 2 x with 1 ml F-12 medium without additives.
  5. Incubate infected cells in 1 ml of F-12 medium with 2% FBS and 1% L-glutamine for 24 h at 37 °C in a CO<sub>2</sub> incubator.

#### B. Slide preparation

1. Remove cell culture medium and wash monolayers 3 x with 1 ml DPBS.
2. To fix infected cells, incubate cells with 1 ml of a freshly prepared 1:4 dilution of PFA (4% final concentration) in DPBS for 30 min at room temperature.
3. Remove PFA solution and wash cells 3 x each with 1 ml DPBS.
4. To permeabilize fixed cells, incubate with 1 ml 0.05% Triton X-100 in DPBS for 10 min at room temperature.
5. Remove Triton X-100 solution and wash cells 3 x each with 1 ml DPBS.
6. To block unspecific protein binding, incubate coverslip with 1 ml 3% BSA in PBS for 3 h at 4 °C.
7. Wash cells 1 x with 1 ml DPBS.
8. Incubate cells overnight at 4 °C with primary antibody mix: mouse anti-RSV F mAb (1:500) and rabbit anti-tubulin mAb (1:100) in PBS with 0.1% BSA.
9. Wash cells 3 x each with 1 ml DPBS.
10. Incubate cells with secondary antibody mix: goat anti-mouse AF488 (1:200) and goat anti-rabbit Atto 647N (1:100) in DPBS with 0.1% BSA for 3 h at 4 °C in the dark.
11. Wash cells 3 x each with 1 ml DPBS.
12. For actin cytoskeleton staining, incubate cells with rhodamine phalloidin (1:500) in DPBS for 30 min at 4 °C in the dark.
13. Wash cells 2 x each with 1 ml DPBS.
14. Wash cells 2 x each with 1 ml deionized H<sub>2</sub>O.

15. To mount the coverslip on a glass slide, first place 10  $\mu$ l of ProLong Gold Antifade mounting medium onto a glass slide. Pick up the coverslip with Dumont #NO forceps and lower the cover slip cell-side down onto the mounting medium, taking care to avoid trapping air bubbles.
16. Dry slide overnight in the dark.

### C. Imaging procedure

1. In Figure 1, all images were collected in a single focal plane with a 30 nm pixel size using a bidirectional scan speed of 600 Hz.

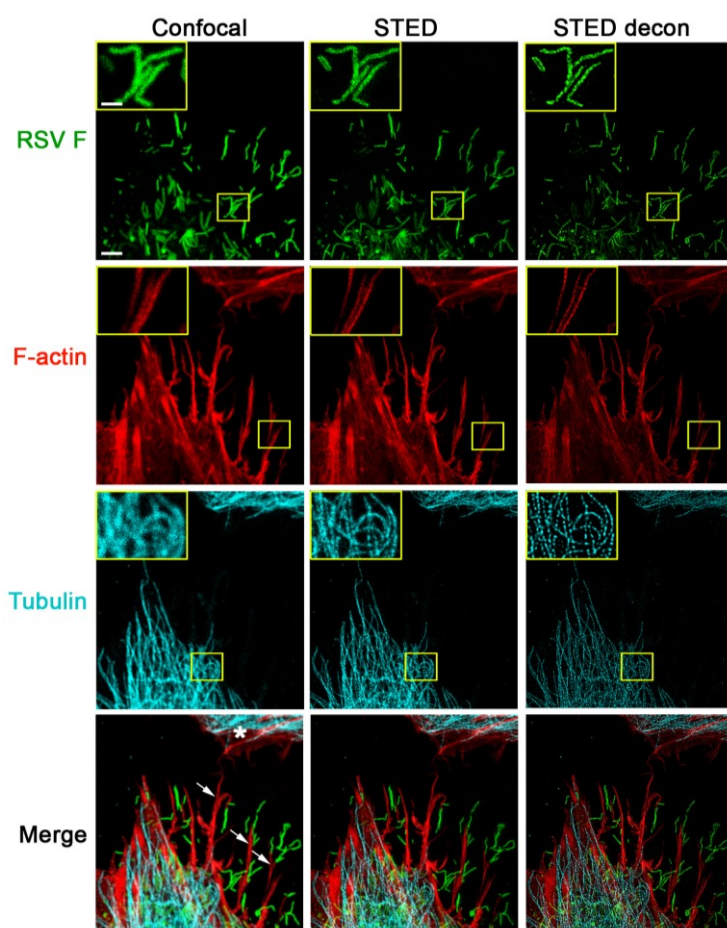


**Figure 1. STED imaging of RSV viral particles along filopodia.** A549 cells were infected with RSV (MOI = 1 PFU/cell) for 24 h. Cells were fixed, permeabilized, and immunostained with antibodies for RSV F (green); the cellular tubulin network was visualized by staining for beta tubulin (cyan). These cells were further stained with rhodamine phalloidin to detect F-actin (red). All images were collected in a single focal plane as described in the imaging procedure. For confocal image acquisition (left panel), excitation wavelengths for the detection of RSV F (AF488), F-actin (rhodamine phalloidin), and tubulin (Atto 647N) were 488 nm, 561 nm, and 647 nm, respectively. The subsequent STED acquisition (middle panel) was done in the following order: first, the Atto 647N conjugate used for tubulin immunostaining was excited with 647 nm and depleted with 775 nm; then, to visualize F-actin, rhodamine phalloidin was excited with 561 nm and depleted with 660 nm; and finally, the AF488

conjugate used for RSV F specific immunostaining was excited with 488 nm and depleted with 592 nm. Filopodia (indicated by arrows on the bottom left image) appear to shuttle RSV particles towards a neighboring cell (marked with a \* in the bottom left image). An increase in resolution of all channels is apparent with STED imaging, which can be further improved by deconvolution using Huygens software (STED decon, right panel). Scale bar = 3  $\mu$ m, inset scale bar = 1  $\mu$ m.

2. Gated HyD detectors were used to collect an emission bandwidth of approximately 40 nm. All fluorophores were excited with a pulsed white light laser tuned to the appropriate wavelength.
3. For confocal channel acquisition, AF488 was excited with 488 nm; rhodamine phalloidin was excited with 561 nm; and Atto 647N was excited with 647 nm. All HyD detector gating was set to 0.3-6 nsec. High intensity signals enabled the usage of low laser power settings, and single color controls were used to confirm the absence of background fluorescence. Of note, the laser power for confocal acquisition was set 3-5 fold lower than for STED acquisition. Photobleaching during confocal acquisition was negligible.
4. Photon depletion occurs when some overlap exists between the STED laser wavelength and the emission spectrum of the fluorophore. Thus, for STED channel acquisition (subsequent to confocal acquisition), AF488 was excited with 488 nm and photon depleted with 592 nm with 1.2-6 nsec HyD gating; rhodamine phalloidin was excited with 561 nm and depleted with 660 nm with 1-6 nsec HyD gating; and Atto 647N was excited with 647 nm and depleted with 775 nm with 0.6-6 nsec HyD gating.
5. Caution needs to be taken to limit exposure of fluorophores to a depletion laser if they can absorb energy at that specific wavelength (*i.e.*, fluorophores that have excitation spectra encompassing the wavelengths of the depletion lasers, 592 nm, 660 nm, or 775 nm). This is because the depletion laser output at the imaging plane is ~500-1,000 times greater than the excitation source, which will rapidly result in photobleaching. For example, Atto 647N will be photobleached by the 660 nm depletion laser, Alexa 594 will be photobleached by the 592 nm depletion laser, *etc.* Therefore, to avoid photobleaching, the collection order of the STED channels is of utmost importance, with longer wavelength fluorophores collected first and the shorter wavelengths collected last. In this experiment, the collection order of the STED channels was Atto 647N, followed by rhodamine phalloidin, and then AF488.
6. Using single color controls, we confirmed that only the intended fluorophore was excited per each channel, and that neither cellular autofluorescence nor non-specific binding of the primary or secondary antibodies were detected.
7. While confocal images were collected with a pinhole set to 1 Airy Unit (AU), this was reduced to 0.7 AU for STED imaging to reduce optical sectioning and increase the signal-to-noise ratio.
8. Additionally, due to the strong depletion power, excitation powers were increased approximately 3-5 fold compared to confocal to compensate for signal loss. A frame accumulation of 2 was also used to further amplify the signal.

#### D. Image processing

1. STED images were deconvolved using Huygens deconvolution software (Huygens Essentials v.17.040.p5, SVI BV, The Netherlands) to reverse the optical distortion created during image acquisition (Figure 2). Within this software package, we used the Deconvolution Wizard with automatic background subtraction and microscopic parameters recognition with a continued maximum likelihood estimate (CMLE) iterative algorithm. Processing parameters included microscopic and deconvolution parameters, which are important for proper point spread function (PSF) calculation necessary for successful deconvolution. Microscopic parameters were verified and corrected if necessary to avoid processing artifacts. The deconvolution parameters were adjusted in this Huygens deconvolution package as described below. This Huygens Essentials package was the only STED deconvolution package available at that time. However, there now are a number of software packages or free plug-ins available for classical confocal, multiphoton, or wide-field deconvolution applications.

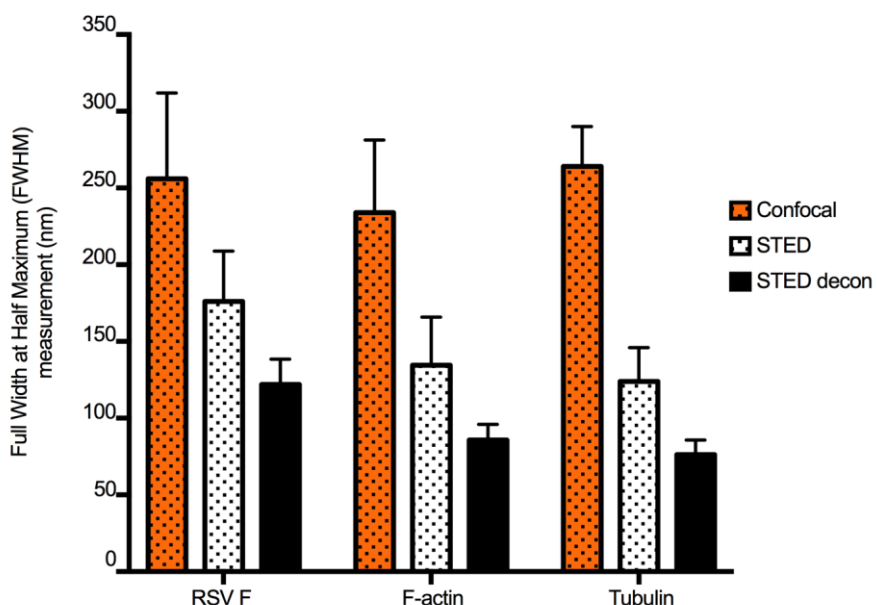


**Figure 2. STED and deconvolution improve lateral resolution.** To quantify the improvement in image resolution shown in Figure 1, we took the Gaussian profiles (bell curves) of signal intensity for a number of representative narrow structures and measured the width of the curve at the intensity level that is half of the maximum, which provided ‘full-width at half-maximum’ (FWHM) values. Smaller values of FWHM indicate improved resolution. This was done for five structures from each channel (green: virus filaments (RSV F), red: actin filaments, and cyan: tubulin filaments). The same structures were measured in confocal, STED, and STED deconvolved (STED decon) images. For each stain, STED significantly improved resolution compared to confocal microscopy, and resolution was further improved by deconvolution. Error bars represent standard deviation.

2. STED resolution was improved in Huygens Essentials by using settings for background subtraction, for the number of iterations, and for the desired signal-to-noise ratios that were determined empirically

after several rounds of iterations. For RSV F, these values were 0.0316 for background subtraction, 54 for the number of iterations, and 18 for the signal-to-noise ratio. For F-actin, these values were 0.0695, 46, and 19, respectively. For tubulin, these values were 0.0835, 49, and 20, respectively. Deconvolved images were thoroughly compared with the original raw image to avoid artifacts such as striping, ringing, or discontinuous staining.

3. Additional deconvolution parameters were set in Huygens Essentials to account for the expected amount by which the fluorescence is suppressed by the STED beam (STED saturation factor) and the expected fraction of fluorescent molecules that is photoresistant to the depletion beam (STED immunity fraction). The STED saturation factor is the absolute intensity of the STED laser divided by the saturation intensity. For the maximum intensity STED laser, the saturation factor is 30, and it is scaled based on the STED laser intensity. The STED immunity fraction is the fraction of the fluorophores that has not been depleted by the STED laser. It is described as an additional confocal PSF component that is added to the pure STED PSF and is estimated in percentage of the maximum saturation. It has only a minor influence on the quality of deconvolved images, and typical values are around 10%. For RSV F, these values were 30 for the STED saturation factor, and 14 for the STED immunity fraction. For F-actin, these values were 27 and 10, respectively. For tubulin, these values were 5 and 11, respectively.

## **Notes**

1. To avoid disturbing the cell monolayer while pipetting, tilt the plate slightly (at an angle less than 45°) and direct the pipette tip towards the side wall of each well during dispensing.
2. Pipette slowly to preserve fragile cellular structures and viral filaments.
3. To prevent possible interfering effects on cell biology, do not include antibiotic and anti-fungal agents when culturing A549 cells
4. It is not essential that sucrose purified recombinant RSV be used for these studies.
5. Prior to these studies, the titer of the RSV stock should be determined by immunoplaque assay on 24-well plates of Vero 76 cells (ATCC CRL-1587). In short, prepare serial tenfold dilutions of the RSV stock of interest in cell culture medium. Discard the growth medium from 24-well plates of subconfluent Vero cell monolayers, and transfer 100 µl per well of the serial RSV dilutions to duplicate wells of 24-well plates. To allow for virus adsorption, incubate for 2 h in a cell culture incubator; gently rocking the plates every 20 min to prevent the monolayers from drying out. After adsorption, overlay the monolayers with 1 ml of 0.8% methyl cellulose overlay (prepared using cell culture medium) per well, and incubate the cultures for 5-6 days. Then discard the methyl cellulose overlay by inverting the plates, and fix with ice-cold 80% methanol. Visualize RSV plaques by immunostaining using an RSV specific primary antibody preparation (for example a commercially available mouse monoclonal antibody to RSV), followed by a species-specific secondary antibody (for example, a peroxidase-conjugated goat anti-mouse IgG(H+L), KPL #074-18064), and a detection system of choice (for example, CN Peroxidase substrate, KPL #50-73-02, and peroxidase substrate solution B, KPL #50-65-02). Select wells of a dilution that yielded well-separated plaques, count virus plaques per well,

and calculate the titer of the virus stock (plaque forming units per ml) by multiplying the average number of plaques by the dilution factor.

### **Data analysis**

Images were deconvolved and FWHM measurements were made using Huygens deconvolution software. Standard deviation was calculated using PRISM software version 7. STED microscopic observation of filopodia-driven RSV cell-to-cell spread has previously been described in detail in (Mehedi *et al.*, 2016). Here, we include an additional channel to visualize the tubulin network in the RSV infected cells.

### **Recipes**

1. F-12 complete medium  
500 ml F-12 nutrient mix  
10% FBS  
1% L-glutamine
2. 4% PFA  
30 ml 1x DPBS  
10 ml 16% PFA
3. 0.05% Triton X-100  
50 ml 1x DPBS  
250 µl Triton X-100
4. 3% BSA  
50 ml 1x DPBS  
1,500 µl BSA (1 mg/ml)

### **Acknowledgments**

This study was supported by the Intramural Research Program of NIAID, NIH. All authors have declared that no competing interest exists. This protocol was adapted from previously published work (Mehedi *et al.*, 2016).

### **References**

1. Bachi, T. and Howe, C. (1973). [Morphogenesis and ultrastructure of respiratory syncytial virus](#). *J Virol* 12(5): 1173-1180.
2. Collins, P. L., Hill, M. G., Camargo, E., Grosfeld, H., Chanock, R. M. and Murphy, B. R. (1995). [Production of infectious human respiratory syncytial virus from cloned cDNA confirms an essential role for the transcription elongation factor from the 5' proximal open reading frame of the M2 mRNA](#)

- [in gene expression and provides a capability for vaccine development.](#) *Proc Natl Acad Sci U S A* 92(25): 11563-11567.
3. Hell, S. W. and Wichmann, J. (1994). [Breaking the diffraction resolution limit by stimulated emission: stimulated-emission-depletion fluorescence microscopy.](#) *Opt Lett* 19(11): 780-782.
  4. Le Nouen, C., Munir, S., Losq, S., Winter, C. C., McCarty, T., Stephany, D. A., Holmes, K. L., Bukreyev, A., Rabin, R. L., Collins, P. L. and Buchholz, U. J. (2009). [Infection and maturation of monocyte-derived human dendritic cells by human respiratory syncytial virus, human metapneumovirus, and human parainfluenza virus type 3.](#) *Virology* 385(1): 169-182.
  5. Mehedi, M., McCarty, T., Martin, S. E., Le Nouen, C., Buehler, E., Chen, Y. C., Smelkinson, M., Ganesan, S., Fischer, E. R., Brock, L. G., Liang, B., Munir, S., Collins, P. L. and Buchholz, U. J. (2016). [Actin-related protein 2 \(ARP2\) and virus-induced filopodia facilitate human respiratory syncytial virus spread.](#) *PLoS Pathog* 12(12): e1006062.
  6. Westphal, V., Rizzoli, S. O., Lauterbach, M. A., Kamin, D., Jahn, R. and Hell, S. W. (2008). [Video-rate far-field optical nanoscopy dissects synaptic vesicle movement.](#) *Science* 320(5873): 246-249.

## Staining of Membrane Receptors with Fluorescently-labeled DNA Aptamers for Super-resolution Imaging

Maria Angela Gomes de Castro<sup>1,\*</sup>, Claudia Höbartner<sup>2</sup> and Felipe Opazo<sup>1,3,\*</sup>

<sup>1</sup>Institute of Neuro- and Sensory Physiology, University Medical Center Göttingen, Göttingen, Germany;

<sup>2</sup>Institute for Organic and Biomolecular Chemistry, Georg-August-University, Göttingen, Germany; <sup>3</sup>Center for Biostructural Imaging of Neurodegeneration (BIN), University Medical Center Göttingen, Göttingen, Germany

\*For correspondence: [macdani@gwdg.de](mailto:macdani@gwdg.de); [fopazo@gwdg.de](mailto:fopazo@gwdg.de)

**[Abstract]** One of the most prominent applications of fluorescent super-resolution microscopy is the study of nanodomain arrangements of receptors and the endocytic pathway. Staining methods are becoming crucial for answering questions on the nanoscale, therefore, the use of small and monovalent affinity probes is of great interest in super-resolution microscopy with biological samples. One kind of affinity probe is the aptamer. Aptamers are single DNA or RNA sequences that bind with high affinity to their targets and due to their small size they are able to (i) place the fluorophore in close proximity to the protein of interest and (ii) bind to most of the protein of interest overcoming the steric hindrance effect, resulting in better staining density. Here we describe a detailed protocol with which to stain live cells using aptamers and to image them with Stimulated Emission Depletion (STED) microscopy. In this protocol, the stainings were performed with commercially available aptamers that target the epidermal growth factor receptor (EGFR), the human epidermal growth factor receptor 2 (HER2 or ErbB2) and the ephrin type-A receptor 2 (Epha2). Since aptamers can be coupled to most of the popular fluorophores, we believe that the procedure presented here can be extended to the large majority of the current super-resolution microscopy techniques.

**Keywords:** Microscopy, Super-resolution, STED, Aptamers, Affinity probes

**[Background]** Recent advances in super-resolution imaging techniques have led to the search for more accurate methodologies to tag cellular elements. Diffraction unlimited imaging instruments provide excellent resolutions, however standard sample staining methodologies, such as immunostaining, lack the necessary precision for the detection of cellular elements. Due to their large dimension (~15 nm in length) and high molecular weight (~150 kDa), antibodies can poorly penetrate into biological samples. Additionally, the primary/secondary antibody complex places the fluorophores at approximately 25 nm away from the target, compromising the detection accuracy. Moreover, due to the large size of the primary/secondary antibody complex, a smaller fraction of the targets can be labelled due to the steric hindrance (Fornasiero and Opazo, 2015). This leads to lower labelling density, a crucial parameter for super-resolution microscopy, especially in recognizing and describing nanostructures. To circumvent these problems, small affinity probes that bind to single targets (monovalently) such as aptamers, affibodies or nanobodies have been tested in recent years (Rothbauer *et al.*, 2006; Opazo *et al.*, 2012; Ries *et al.*, 2012) and are becoming valuable tools for super-resolution microscopy. Nanobodies, affibodies and aptamers have a relatively small linear size (~3 nm, ~2 nm and ~3 nm, respectively). This property allows them to place the fluorescent dye in close proximity to the target, penetrate samples in a more

efficient manner and bind to a higher fraction of target proteins, bypassing the effect of steric hindrance observed by antibodies (Ries *et al.*, 2012; Mikhaylova *et al.*, 2015). In a previous study we made a systematic comparison between three commercially available aptamers and antibodies that target the epidermal growth factor receptor (EGFR), the human epidermal growth factor receptor 2 (HER2 or ErbB2) and the ephrin type-A receptor 2 (Epha2). Our results showed that aptamers were able to find more epitopes (resulting in higher labeling density). As a consequence, several structural features of the subcellular components that were imaged became more apparent. Among these, the inner lumen and the complex morphology of endocytic organelles were visible. For these reasons, smaller imaging tools are becoming the preferred choice over antibodies, in order to improve the quality of an immunolabeling super-resolution approach and allow a more precise description the localization and the distribution of membrane receptors (Gomes de Castro *et al.*, 2017).

## **Materials and Reagents**

1. Biospin 6 column (Micro Bio-Spin™ P-6 Gel Columns, Tris Buffer) (Bio-Rad Laboratories, catalog number: 7326222)
2. Cell culture 12-well plates (Thermo Fisher Scientific, catalog number: 150628)
3. 18 mm diameter round glass coverslips (Gerhard Menzel, catalog number: CB00180RA1)
4. 15 ml tubes
5. PCR tubes
6. Parafilm M
7. Soft paper tissue
8. Gloves
9. Microscopy glass slides
10. 2 ml tubes
11. Vacuum filtration (*e.g.*, VWR® Vacuum Filtration Systems, Standard Line) (VWR, catalog number: 10040-436)
12. 0.2 µm syringe filter
13. Transfer pipette
14. The images shown in Figure 1 are from aptamers against human:  
EGFR (5'-SH-EGFR aptamer-3', seq # 2369-27-02, 50 mer)  
ErbB2 (5'-SH-ErbB2 aptamer-3', seq # 1194 ± 35, 40 mer)  
Epha2 (5'-SH-EphA2 aptamer-3', seq # 2176-01-01, 76 mer)  
*Note: They were produced by Aptamer Sciences, Inc., South Korea and supplied by AMS Biotechnology, Europe. All three aptamers contain the chemical modification 5-(N-benzylcarboxyamide)-2'-deoxyuridine (5-Bzdu) in unrevealed locations.*
15. Triethylammonium acetate buffer pH 7.0, 1 M (TEAA) (AppliChem, catalog number: A3846)
16. Maleimide Atto647N dye (Atto-TEC, catalog number: AD 647N-41)
17. Dimethyl sulfoxide, anhydrous (DMSO) (Sigma-Aldrich, catalog number: 276855)
18. Sodium chloride (NaCl)

19. Ethanol
20. 1x Dulbecco's phosphate buffered saline (1x DPBS) (Sigma-Aldrich, catalog number: D8662)
21. Acetonitrile
22. Trypsin-EDTA solution (Lonza, catalog number: 17-161E)
23. Ultrapure DNase- and RNase-free distilled water (Carl Roth, catalog number: T143.2)
24. Tris (2-carboxyethyl) phosphine hydrochloride (TCEP) (Sigma-Aldrich, catalog number: C4706)
25. Sodium hydroxide (NaOH)
26. DMEM, high glucose medium, no glutamine (Thermo Fisher Scientific, Gibco<sup>TM</sup>, catalog number: 11960044)
27. Fetal bovine serum (FBS) (Biochrom, catalog number: S 0615)
28. L-Glutamine 200 mM (Lonza, catalog number: BE17-605E)
29. Penicillin/streptomycin 10,000 U/ml, each (Lonza, catalog number: 17-602E)
30. RPMI 1640 medium, no glutamine (Thermo Fisher Scientific, Gibco<sup>TM</sup>, catalog number: 21870076)
31. Poly-L-lysine (PLL) (Sigma-Aldrich, catalog number: P5899-5MG)
32. Sodium phosphate dibasic ( $\text{Na}_2\text{HPO}_4$ )
33. Potassium phosphate monobasic ( $\text{KH}_2\text{PO}_4$ )
34. Potassium chloride (KCl)
35. Magnesium chloride hexahydrate ( $\text{MgCl}_2 \cdot 6\text{H}_2\text{O}$ )
36. Salmon sperm DNA, sheared, 10 mg/ml (Thermo Fisher Scientific, catalog number: AM9680)
37. Dextran sulfate sodium salt (Sigma-Aldrich, catalog number: 31404)
38. Paraformaldehyde (PFA) (Sigma-Aldrich, catalog number: P6148)
39. Glycine (Sigma-Aldrich, catalog number: G8898)
40. Mowiol<sup>®</sup> (Sigma-Aldrich, catalog number: 81381)
41. 1 M Tris (2-carboxyethyl) phosphine hydrochloride stock solution (TCEP) (see Recipes)
42. Complete DMEM medium (see Recipes)
43. Complete RPMI medium (see Recipes)
44. Poly-L-lysine (PLL) stock solution (see Recipes)
45. 5x phosphate buffer saline (5x PBS) (see Recipes)
46. 25 mM MgCl<sub>2</sub> solution (5x MgCl<sub>2</sub>) (see Recipes)
47. Blocking solution (see Recipes)
48. 4% paraformaldehyde (PFA) (see Recipes)
49. Quenching solution (see Recipes)
50. Mowiol<sup>®</sup> (see Recipes)
51. (Optional) Buffer A (see Recipes)
52. (Optional) Buffer B (see Recipes)

## **Equipment**

1. Microcentrifuge (*e.g.*, Eppendorf, model: 5415 or similar)

2. Nucleosil 100-5 C18 column
3. (Optional) Dionex DNAPac PA200 4 x 250 mm column
4. Hemocytometer
5. Cell culture hood
6. Thermal cycler
7. Aluminum metal plate (length x width x thickness [cm]: *e.g.*, 20 x 12 x 2)
8. Cell culture incubator
9. Half-curved-forceps
10. Oven
11. STED microscope, Leica pulsed STED setup composed by a True Confocal System (TCS) STED SP5 (Leica Microsystems, model: Leica TCS SP5) fluorescence microscope equipped with a 100x 1.4 NA HCX PL APO oil objective (Leica Microsystems, Germany)
12. Pulsed laser (PicoQuant, Germany)
13. Sapphire tunable laser (Mai Tai Broadband, Spectra-Physics, USA)
14. Glass beaker
15. Magnetic stirrer
16. Lab coat, eye protection

## Software

1. ImageJ (<http://imagej.nih.gov/ij/docs/index.html>)
2. MATLAB (MathWorks, Massachusetts, USA)

## Procedure

### A. Coupling of dye to aptamers

During this step a thiol-maleimide cross-linking reaction is performed to conjugate the fluorophore to aptamers. Alternatively, aptamers with a 3'-amino group can be used for further conjugation with NHS esters (*e.g.*, Atto647N NHS-ester). Some fluorescently labeled aptamers are also commercially available.

1. Add 10 nmoles of the thiolated aptamer with 10 mM Tris (2-carboxyethyl) phosphine solution (TCEP; see Recipe 1) in 100  $\mu$ l of 0.1 M TEAA. Heat the tube at 70 °C for 3 min and incubate the mixture at room temperature for 1 h.
2. Desalt this reaction by size exclusion chromatography on a Biospin 6 column according to the manufacturer's instructions.
3. Add to the reduced aptamer (from step A2) 4  $\mu$ l of 10  $\mu$ g/ $\mu$ l maleimide-functionalized Atto647N (previously dissolved in DMSO) and mix the contents well by pipetting or vortexing.
4. Incubate overnight at 4 °C.
5. Recover the fluorophore-labelled aptamer by ethanol precipitation: add 100  $\mu$ l of 300 mM NaCl and 450  $\mu$ l cold ethanol, mix carefully by inverting the closed sample several times and freeze the sample in

- dry ice for 20 min (or at -20 °C for several hours), centrifuge at 15,000  $\times g$  (rcf) at 4 °C for 30 min, discard the supernatant and wash the pellet in 50  $\mu l$  of 70% ethanol.
6. Resuspend in 50  $\mu l$  1x DPBS and desalt on a Biospin 6 column into 1x DPBS.
  7. Measure the absorbance ratio at 260 nm and 650 nm.
  8. Confirm the labeling efficiency and absence of free dye by reversed phase HPLC (*e.g.*, on a Nucleosil 100-5 C18 4 x 250 mm column using a gradient of 0-40% acetonitrile in TEAA buffer in 30 min with a flow rate of 1 ml/min at 30 °C) or by anion exchange HPLC (*e.g.*, Dionex DNAPac PA200 4 x 250 mm column using a gradient of 0-75% buffer B (see Recipe 12) in buffer A (see Recipe 11) in 40 min with a flow rate of 1 ml/min at 60 °C).
  9. Store the labeled aptamer sample at -20 °C until use.

#### B. Cell culture preparation prior to staining

Cell lines containing the receptor of interest (and cell lines lacking it, used as negative controls) should be seeded into 12-well plates containing coated coverslips with poly-L-lysine (PLL) one day before the aptamer staining. Depending on the cell line, choose adequate cell numbers (use the hemocytometer to count the cells) to reach approximately 70-80% confluence after 12-16 h incubation. The entire procedure described below must be performed under sterile conditions under a cell culture hood.

1. HeLa (Epha2a positive) cells are grown in plates with complete DMEM medium (see Recipe 2) and A-431 (EGFR positive) and SKBR3 (ErbB2R positive) cells are cultured in complete RPMI medium (see Recipe 3). All cell lines are maintained at 37 °C and 5% CO<sub>2</sub>.
2. To split cells, first wash cells with sterile 1x DPBS, add 2-3 ml of trypsin-EDTA to cover the surface of the plate and incubate the plate for 1-5 min at 37 °C or until cells are completely detached. Add 10 ml of complete DMEM medium or RPMI medium to inactivate trypsin. Gently pipette up and down the medium containing the inactivated trypsin to detach all cells from the plate and transfer them into a sterile 15 ml tube.
3. Centrifuge the cells at 1,000 rpm (~250  $\times g$ ) for 4 min at RT.
4. Aspirate the supernatant and resuspend the cell pellet in 10 ml of complete DMEM medium/RPMI medium. Dilute the resuspended cells to the desired concentration in fresh complete DMEM or RPMI medium and add 1 ml to every well of the 12-well plates containing PLL treated coverslips (for PLL stock solution preparation and dilution, see Recipe 4). Incubate the plates at 37 °C and 5% CO<sub>2</sub> until staining.

#### C. Preparation of functional aptamer: folding reaction

During this step, aptamers are exposed to a high temperature at an appropriate magnesium concentration which allows them to attain a proper folding prior to the staining procedure. For better results, the folding reaction should be freshly performed each time before staining. Before starting the folding reaction, prepare a stock solution diluting aptamers in 1x DPBS to a final concentration of 30  $\mu M$  and store it protected from light at 4 °C.

1. Prepare 10  $\mu\text{l}$  of 10  $\mu\text{M}$  functional aptamer by mixing 3.3  $\mu\text{l}$  of fluorescently labelled aptamer (30  $\mu\text{M}$  aptamer stock solution), 2  $\mu\text{l}$  of 5x PBS (see Recipe 5), 2  $\mu\text{l}$  of 5x MgCl<sub>2</sub> (see Recipe 6) and 2.7  $\mu\text{l}$  of ultrapure DNase- and RNase-free distilled water. Please note that this reaction should be carried out in PCR tubes that fit the thermal cycler.
2. Heat up the aptamer solution to 75 °C for 3 min and then cool down to 20 °C at a rate of 1 °C/min using a thermal cycler.

#### D. Aptamer live cells staining

1. Aspirate the medium from the cells prepared during Procedure B, rinse briefly once with complete DMEM or RPMI depending on the cell line and incubate for 10 min at 37 °C and 5% CO<sub>2</sub> (in the cell culture incubator) with 500  $\mu\text{l}$ /well of freshly prepared blocking solution containing sheared salmon sperm DNA and dextran sulfate (see Recipe 7).
2. In the meantime, prepare the metal plate used for staining/incubation at 37 °C. Fix with tape a piece of Parafilm® M (large enough to fit all coverslips to be stained) on the surface (see Video 1) and pre-heat the metal plate containing the Parafilm® M in the cell culture incubator.

**Video 1. Aptamers live staining part I.** This video shows the metal plate preparation for aptamer live staining. Please note that this video is for demonstration only and that this step should be performed inside a cell culture hood.



3. After blocking (step D1), carefully remove the coverslips from the 12-well plate using half-curved-forceps, remove the excess blocking solution by gently tapping the edges of the coverslips with a soft paper tissue and place the coverslips upside down on 60  $\mu\text{l}$  of staining solution (complete DMEM supplemented with 100  $\mu\text{g}/\text{ml}$  sheared salmon sperm DNA and 250 nM folded aptamer) spotted onto the Parafilm® M fixed to the metal plate (made in step D2) (see Video 2). Incubate the cells for 60 min at 37 °C and 5% CO<sub>2</sub>.

**Video 2. Aptamers live staining part II.** This video shows removal of coverslips containing cells from the 12-well plates using half-curved-forceps and incubation of cells (on coverslips) with staining solution. Please note that this video is for demonstration only and that this step should be performed inside the cell culture hood. To avoid contamination, gloves should be sprayed with 70% ethanol.



4. After incubation, carefully take the coverslips off the metal plate using half-curved-forceps, remove the excess staining solution by gently tapping the edges of the coverslips with a soft paper tissue, and then submerge it several times in large volumes (*e.g.*, 20-40 ml in a small beaker) of ice-cold 1x DPBS. Briefly remove the excess 1x DPBS from the coverslips by tapping them on a tissue paper and place each one (cell-side-up) into a well of a new 12-well plate filled with 1 ml/well ice-cold 4% PFA (see Recipe 8) for fixation (see Video 3).

**Video 3. Aptamers live staining part III.** This video shows the washing step after staining procedure. Please note that video is in open air for demonstration only and that 4% PFA should only be handled in the fume hood.



5. Fix the cells for 20 min on ice and subsequently at room temperature for another 25 min. During fixation, keep the plate protected from light to avoid fluorophore bleaching.

6. Aspirate the PFA solution and add 1 ml of quenching solution (see Recipe 9) to each well. Incubate for 15 min at room temperature protected from light.
7. Wash twice for 5 min with 1x DPBS (1 ml/well) and mount the coverslips with Mowiol® (see Recipe 10; e.g., 8-9 µl for an 18 mm coverslip) on microscopy glass slides.
8. Dry the mounted coverslips in an oven at 37 °C for 20-30 min or overnight at RT and store at 4 °C protected from light until imaging.

### Data analysis

**Imaging:** The images shown in this protocol (Figure 1) were acquired using a 100x 1.4 NA HCX PL APO oil objective. Excitation of Atto647N fluorophore was achieved with a 635 nm pulsed laser (PicoQuant, Germany), and the 750 nm depletion STED beam was obtained with a pulsed infrared titanium: sapphire tunable laser (Mai Tai Broadband, Spectra-Physics, USA). The pixel size was set to 20.2 nm, scanning speed to 1 kHz, line average to 96 times, pinhole to one Airy unit and signal was detected with an avalanche photodiode detector (APD).

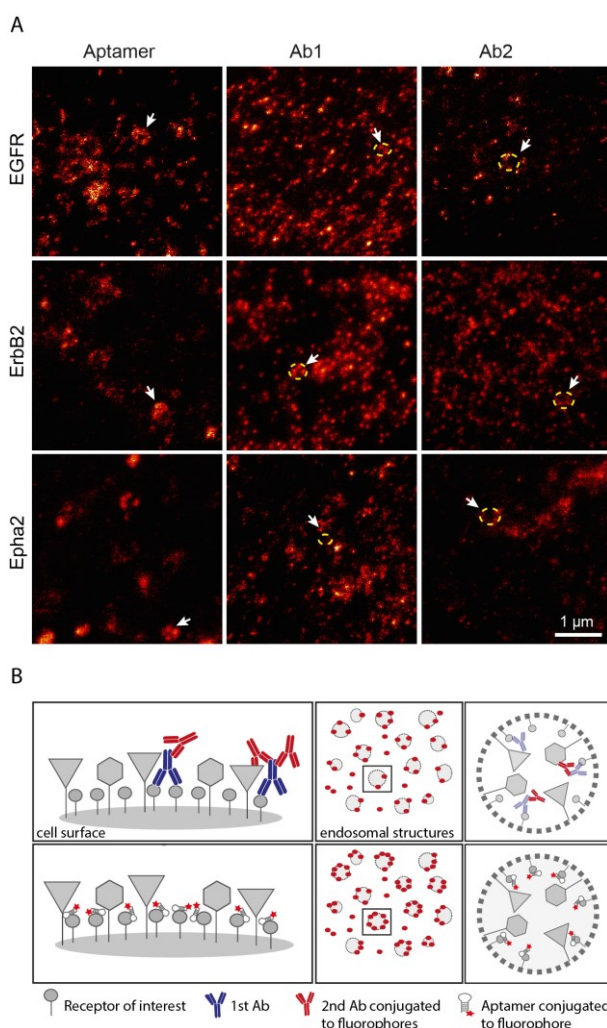


**Figure 1. Recognition of endosome-like structures in aptamer or antibody stained cells. A.** STED images comparing the cells stained with aptamers and antibodies against the same receptors (Ab1 and

Copyright © 2017 The Authors; exclusive licensee Bio-protocol LLC.

Ab2, under saturating conditions as described in (Gomes de Castro *et al.*, 2017). Arrowheads point to some examples of endosome-like structures. Staining using antibodies resulted in discontinuous labelling of the organelle contours (indicated by yellow dotted circles in the STED image). B. The scheme represents our current hypothesis, indicating that large affinity probes like antibodies (upper panel) might not detect all available epitopes and that small molecules like aptamers (lower panel) decorate the target structures better.

### Notes

1. To determine the saturating concentration or optimal staining concentration (best signal-to-noise ratio) for the aptamer of interest fixing the incubation time of staining (*e.g.*, 60 min) and testing different aptamers concentrations ranging from 10-500 nM (or more) in positive cell lines is recommended. After staining with different concentrations of the aptamers, fixation and mounting, cells can be imaged in any epifluorescence microscope and fluorescent intensities can be calculated using as an example ImageJ or MATLAB.
2. After defining the saturating conditions for the staining procedure, the next step is to test the binding specificity. This is achieved by evaluating the staining in the cells expressing the receptor and the cells that do not express it. Importantly, the staining conditions, the aptamer concentrations and the incubation times must be the same for both positive and negative cells. Once stained and fixed, cells can be imaged with an epifluorescence or confocal microscope. Negative cell lines should show virtually no specific fluorescent signal. For a proper control of the unspecific staining background, it is useful to test the immunolabeling with a random aptamer conjugated to the same fluorophore as the aptamer binding the specific target, in parallel. This control should not have any fluorescence signal. An additional control is the evaluation of the binding specificity by fluorescence flow cytometry analysis using the same controls.
3. Every receptor has its own internalization kinetics. In this work and protocol we intend to maximize the labeling by internalization and therefore choose longer incubation times.
4. If the aptamers contain BzdU (5-(N-benzylcarboxyamide)-2'-deoxyuridine) or any other hydrophobic groups, we recommend the addition of dextran sulfate to the blocking solution. An optimization of the dextran sulfate concentration in the pre-blocking solution strongly reduces the background caused by nonspecific binding due to electrostatic interaction of aptamers to the PLL-treated coverslip.
5. If unspecific binding of the aptamer persists, increase the concentration of sheared salmon sperm DNA and/or dextran sulphate in the staining solution. The polyanionic competitor/blocking agent dextran sulfate also substantially reduces the nonspecific binding caused by electrostatic attraction of polyanionic aptamers to positively charged sites in nuclei, such as histones.
6. For identification and quantification of endosome-like structures, colocalization studies are strongly recommended (Gomes de Castro *et al.*, 2017).

**Recipes**

1. 1 M Tris (2-carboxyethyl) phosphine hydrochloride stock solution (TCEP)  
For 100 ml:
  - a. Add 11.47 g TCEP to 35 ml cold ultrapure water
  - b. Bring the pH to 7.0 with 10 N NaOH and adjust the volume to 100 ml
  - c. Aliquot into 2.0 ml tubes and store at -20 °C
2. Complete DMEM medium
  - a. DMEM supplemented with 10% FBS, 4 mM L-glutamine and 100 U/ml each of penicillin and streptomycin
  - b. Sterilize by vacuum filtration
  - c. Store at 4 °C
3. Complete RPMI medium
  - a. RPMI supplemented with 10% FBS, 4 mM L-glutamine and 100 U/ml each of penicillin and streptomycin
  - b. Sterilize by vacuum filtration
  - c. Store at 4 °C
4. Poly-L-lysine (PLL) stock solution
  - a. Prepare 2 mg/ml stock solution in ultrapure water and sterilize through a syringe filter of 0.2 µm
  - b. Make aliquots and store at -20 °C
  - c. Prepare the plates containing PLL-treated coverslips under a sterile hood
  - d. Add 1 ml of 0.1 mg/ml PLL into every well containing a coverslip
  - e. Incubate for 1 h at RT
  - f. After incubation, wash twice with ultrapure water and leave the plates to air-dry inside the cell culture hood
  - g. Store the plates at 4 °C until use
5. 5x phosphate buffer saline (5x PBS)
  - a. Dilute the 10x concentrated PBS stock solution in ultrapure water. Filter the solutions inside a cell culture hood with a 0.2 µm syringe filter or autoclave. Store at RT
  - b. For 1 L 10x concentrated PBS stock solution:

14.4 g sodium phosphate  
2.4 g potassium phosphate  
2 g KCl  
80 g NaCl  
Dissolved in DNase-and RNase-free water  
Adjust the pH to 7.4  
Sterilize by filter sterilization or autoclaving  
Store at RT
6. 25 mM MgCl<sub>2</sub> solution (5x MgCl<sub>2</sub>)

- a. Dilute the 1 M MgCl<sub>2</sub> stock solution to 25 mM in DNase- and RNase-free distilled water. To avoid particles and contamination, filter the solutions inside a cell culture hood with a 0.2 µm syringe filter. Store at room temperature
- b. For 100 ml of 1 M MgCl<sub>2</sub> stock solution:  
Dissolve 20.3 g MgCl<sub>2</sub>·6H<sub>2</sub>O in 70 ml DNase-and RNase-free water and adjust the volume to 100 ml  
Store at RT
7. Blocking solution  
DMEM or RPMI complete medium supplemented with 100 µg/ml sheared salmon sperm DNA and 1 mM dextran sulfate
8. 4% paraformaldehyde (PFA)  
For 1 L PFA 4% preparation:
  - a. Add approximately 600 ml of 1x PBS to 40 g of PFA in a glass beaker and stir using a magnetic stirrer at ~50 °C
  - b. Adjust the pH to between 7 and 8
  - c. Adjust the volume to 1 L with 1x PBS, make aliquots and store at -20 °C

*Note: PFA is highly toxic: use gloves, lab coat, respiratory and eye protection while handling PFA.*
9. Quenching solution
  - a. 0.1 M glycine in 1x DPBS  
Store at RT until use
  - b. To prepare 100 ml of glycine 1 M stock solution:  
Dissolve 7.5 g glycine in ultrapure water  
Filter it through a 0.2 µm syringe filter and store at RT
10. Mowiol®
  - a. Mix 24 g glycerol, 9.6 g Mowiol® 4-88 reagent, 62.4 ml distilled water and 9.6 ml 1 M Tris buffer in a conical cylinder with a magnetic stirrer for 5-7 days
  - b. Optionally heat the mixture at 40-50 °C to dissolve Mowiol®
  - c. After precipitation divide the supernatant in aliquots (e.g., in 2.0 ml tubes) and store at 4 °C
11. (Optional) Buffer A  
25 mM Tris-HCl, pH 8  
6 M urea
12. (Optional) Buffer B  
0.5 M NaClO<sub>4</sub> in 25 mM Tris-HCl pH 8, 6 M urea

### **Acknowledgments**

This protocol described here in more detail has been published in (Gomes de Castro *et al.*, 2017). This work was supported by the Cluster of Excellence and DFG Research Center Nanoscale Microscopy and Molecular Physiology of the Brain (CNMPB).

**References**

1. Fornasiero, E. F. and Opazo, F. (2015). [Super-resolution imaging for cell biologists: concepts, applications, current challenges and developments](#). *Bioessays* 37(4): 436-451.
2. Gomes de Castro, M. A., Hobartner, C. and Opazo, F. (2017). [Aptamers provide superior stainings of cellular receptors studied under super-resolution microscopy](#). *PLoS One* 12(2): e0173050.
3. Mikhaylova, M., Cloin, B. M., Finan, K., van den Berg, R., Teeuw, J., Kijanka, M. M., Sokolowski, M., Katrukha, E. A., Maidorn, M., Opazo, F., Moutel, S., Vantard, M., Perez, F., van Bergen en Henegouwen, P. M., Hoogenraad, C. C., Ewers, H. and Kapitein, L. C. (2015). [Resolving bundled microtubules using anti-tubulin nanobodies](#). *Nat Commun* 6: 7933.
4. Opazo, F., Levy, M., Byrom, M., Schafer, C., Geisler, C., Groemer, T. W., Ellington, A. D. and Rizzoli, S. O. (2012). [Aptamers as potential tools for super-resolution microscopy](#). *Nat Methods* 9(10): 938-939.
5. Ries, J., Kaplan, C., Platonova, E., Eghlidi, H. and Ewers, H. (2012). [A simple, versatile method for GFP-based super-resolution microscopy via nanobodies](#). *Nat Methods* 9(6): 582-584.
6. Rothbauer, U., Zolghadr, K., Tillib, S., Nowak, D., Schermelleh, L., Gahl, A., Backmann, N., Conrath, K., Muyllemans, S., Cardoso, M. C. and Leonhardt, H. (2006). [Targeting and tracing antigens in live cells with fluorescent nanobodies](#). *Nat Methods* 3(11): 887-889.

## Dissection and Staining of Mouse Brain Ventricular Wall for the Analysis of Ependymal Cell Cilia Organization

Paul Labedan<sup>1</sup>, Cédric Matthews<sup>2</sup>, Laurent Kodjabachian<sup>2</sup>, Harold Cremer<sup>2</sup>, Fadel Tissir<sup>3</sup> and Camille Boutin<sup>2\*</sup>

<sup>1</sup>PLab, Marseille, France; <sup>2</sup>Aix Marseille Université, CNRS, Marseille, France; <sup>3</sup>Institute of Neuroscience, Developmental Neurobiology, Université catholique de Louvain, Brussels, Belgium

\*For correspondence: [camille.boutin@univ-amu.fr](mailto:camille.boutin@univ-amu.fr)

**[Abstract]** In the developing and mature central nervous system (CNS) the ventricular lumen is lined by the neuroepithelium and ependymal, respectively. These ventricular epithelia perform important functions related to the development, morphogenesis and physiology of the brain. In the mature CNS, ependyma constitutes a barrier between brain parenchyma and cerebro-spinal fluid (CSF). The most prominent feature of the apical surface of ependymal cells is the presence of multiple motile cilia that extend towards the ventricular lumen. The beating of cilia ensures the circulation of the CSF and its impairment leads to hydrocephalus. For an effective CSF flow, ciliary beating must be coordinated at the level of individual cells and at the tissue level. This coordination is achieved through the precise organization of cilia positioning within the plane of the ependyma. Two major features have been described regarding the planar organization of cilia in ependymal cells (Mirzadeh *et al.*, 2010) and both have a cellular and tissular aspect (Boutin *et al.*, 2014). The first one, rotational polarity, refers to the orientation of ciliary beating. At the cellular level, all cilia beat in the same direction (Figure 1B, black arrows). At the tissue level, each ependymal cell coordinates the direction of their beating with that of neighboring cells (Figure 1C, grey arrows). The second feature, translational polarity, is unique to ependymal cells and refers to the clustering of cilia in a tuft. At the cellular level, this tuft is displaced relative to the center of the ependymal cell (Figure 1B, red arrow). At the tissue level, the positioning of the ciliary tuft is coordinated between adjacent cells (Figure 1C). Alteration of any of these polarities at either level impairs CSF flow circulation (Mirzadeh *et al.*, 2010; Boutin *et al.*, 2014; Guirao *et al.*, 2010; Hirota *et al.*, 2010; Ohata *et al.*, 2014). Cilia axonemes arise from basal bodies (BB) which are cylindrical structures anchored perpendicular to the sub-apical surface of the cells (Figure 1D). BBs are polarized by the presence of appendices such as basal foot or striated rootlets. The basal foot protrudes in a direction correlated with the direction of cilia beating, while the striated rootlet protrudes in the opposite direction of cilia beating (Marshall, 2008). The ‘en face view’ observation of BBs’ organization allows the visualization of ependymal polarities (Mirzadeh *et al.*, 2010; Boutin *et al.*, 2014). Here, we describe an immunofluorescence (IF) protocol for observation of ciliated cells in mouse brain ventricular lateral wall whole mounts (LWWM). This protocol can be used for classical confocal microscopy analysis. In addition, it is well suited for super-resolution STimulated Emission Depletion (STED) microscopy if observation of structures that have features which are smaller than the optical diffraction limit is needed. Finally, we describe a combination of antibodies that allow the

concomitant observation, in a single sample, of ependymal polarities at the level of individual cilia, individual cells and at the tissue level.

### **Materials and Reagents**

1. Microscope slide
2. Coverslips
3. Mice at desired stage [between postnatal day 1 (P1) and 21 (P21)]
4. 1x PBS
5. Triton X-100
6. 4% Paraformaldehyde (PFA) (prepared by dilution of powder in 1x PBS)
7. Bovine Serum Albumin (BSA) (Sigma-Aldrich, catalog number: A-8022)
8. Hoechst 33258 solution (Sigma-Aldrich, catalog number: 94403)
9. Mowiol (Merck Millipore Corporation, Calbiochem®, catalog number: 475904)
10. Prolong Gold antifade reagent (Thermo Fisher Scientific, Molecular Probe™, catalog number: P36934)
11. ZO1 (Thermo Fisher Scientific, Invitrogen™, catalog number: 61-7300)
12.  $\gamma$ -tubulin [GTU-88] (Abcam, catalog number: ab11316)
13. FGFR1OP (FOP) (Abnova Corporation, catalog number: H00011116-M01)
14.  $\beta$ -catenin (BD, catalog number: 610153)
15. FoxJ1 (eBioscience, catalog number: 14-9965)
16. Acetylated- $\alpha$ -tubulin (Sigma-Aldrich, catalog number: T6793)
17. Secondary antibodies
  - a. Anti-Rabbit A647 (Invitrogen, catalog number: A21244)
  - b. Anti-Mouse IgG1 A568 (Invitrogen, catalog number: A21124)
  - c. Anti-Mouse IgG2b A488 (Invitrogen, catalog number: A21141)
  - d. Anti-Mouse IgG1 A488 (Invitrogen, catalog number: A21121)
  - e. Anti-Mouse IgG2b A568 (Invitrogen, catalog number: A21144)
18. Primary antibodies with the corresponding secondary antibodies (see Recipes)

### **Equipment**

1. Dissection tools including forceps (Zillow, Dumont, model: 55) and Ultra Fine Micro Knives (Fine Science Tools, catalog number: 10316-14)
2. Confocal microscope (OLYMPUS, model: Fluoview FV1000)
3. STED microscope (Leica Microsystems, model: SP8 3x STED) equipped with a 100x oil objective (HC-PL-APO; NA 1.40; STED white) and a 592 nm depletion laser

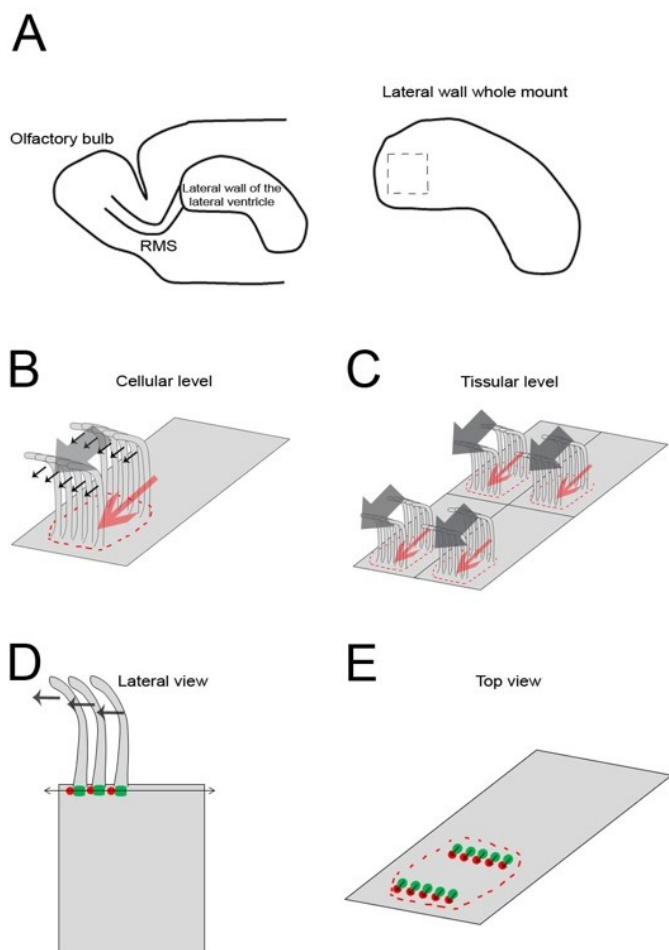
## **Software**

1. Biotool software (Boutin *et al.*, 2014)

## **Procedure**

The general procedure described here is suitable for staining ependymal cells from lateral wall whole mounts of P1 to P21 mice. However, the last sub-dissection step of the tissue has to be performed before the staining for mice older than P5 and after the staining for mice younger than P5 to ensure an optimal result.

1. After cervical dislocation of the mice, the brain is removed from the skull.
2. Dissection of the brain at RT in 1x PBS to reveal the ventricular lateral wall (Figure 2) [a protocol including a video is provided in Mirzadeh *et al.* (2010)].
3. Fixation of the whole mount by immersion in 500 µl fresh solution of 4% PFA-0.1% Triton X-100 12 min at room temperature (RT).
4. Wash 3 times 10 min in 1x PBS-0.1% Triton X-100 (1 ml) at RT with agitation.
5. Sub-dissection of the lateral wall by separating it from the underlying striatum [see Mirzadeh *et al.* (2010) for a precise description of this step]. Performing this sub-dissection at this step of the protocol improves the staining for tissues older than P5.
6. Incubation in blocking solution 1x PBS-3% BSA (1 ml) 1 h RT with agitation.
7. Incubation with primary antibody diluted in 1x PBS-3% BSA (250-500 µl) over-night RT with agitation.
8. Wash 3 times 1x PBS-0.1% Triton X-100 (1 ml) 10 min RT with agitation.
9. Incubate with secondary antibody (1:800) and Hoechst (1:1,000) diluted in 1x PBS (For confocal observation of samples) or with secondary antibody (1:800) diluted in 1x PBS only (for STED observation of samples) (800 µl) 1 h RT with agitation.
10. Wash 3 times 1x PBS-0.1% Triton X-100 (1 ml) 10 min RT with agitation.
11. For tissues younger than P5: sub-dissection of the LWWM by separating the lateral wall and the underlying striatum in 1x PBS [see Mirzadeh *et al.* (2010)].
12. Place the whole mount on the slide with ependymal face up.
13. Add 7-8 drops of Mowiol (for confocal observation of samples) or of Prolong mounting medium (for STED observation of samples) directly on the whole mount.
14. Place a coverslip on the sample.
15. Keep slides at room temperature, protected from the light, for at least 24 h before imaging.

**Representative data**

**Figure 1. Planar organization of ependymal cells in the lateral wall.** A. Schematic representation of the mouse forebrain depicting the localization of the lateral wall of the lateral ventricle. Dashed square highlights the region of interest considered for analysis of ependymal planar polarity. B-C. Schemes represent the planar organization of ependymal cells in the region of interest. B. At the cellular level, ependymal cilia are clustered in a tuft (dotted red line) which localize off center of the apical surface (red arrow). Ciliary beatings (small black arrows) are coordinated. The sum of individual ciliary beatings generates the tuft beating direction (Thick grey arrow). In individual cells, the direction of tuft positioning correlates with the direction of tuft beating. C. At the tissue level, beating direction (grey arrows) and positioning of the ciliary tuft (red arrows) are coordinated between neighboring ependymal cells. D-E. Schematic representation of the lateral (D) and ‘en face’ (E) view of individual ependymal cell organization. D. Multicilia axonemes arise from basal bodies (BBs) anchored perpendicularly to the apical surface of the cells (green). BBs display polarized appendices such as the basal foot (red dot) that indicates the effective beating direction of the cilium (small black arrow). E. Observation of cilia BBs from a top view reveals all ependymal polarity features.

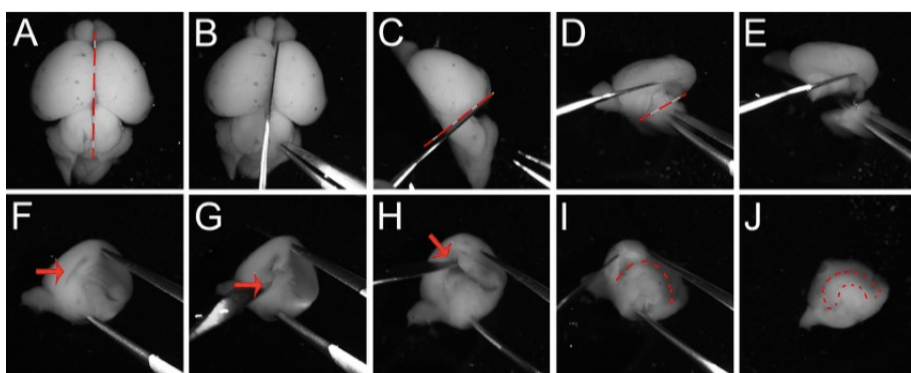


**Figure 2. Dissection steps for LWWM preparation.** LWWM preparation allows the “en face” observation of ependymal cells. A. Brain after removal from the skull. B. Cut the brain between the two hemispheres (dashed red line) using a microscalpel. C. Remove the cerebellum (dashed red line). D-F. Use a microscalpel to reveal the hippocampus (dashed red line). G-H. Insert the microscalpel in the ventricle (arrow) to remove the hippocampus and medial ventricular wall. I. Remove cortical wall following the dashed red line. J. Whole mount ready to be fixed, the lateral wall is outlined by the dashed red line.

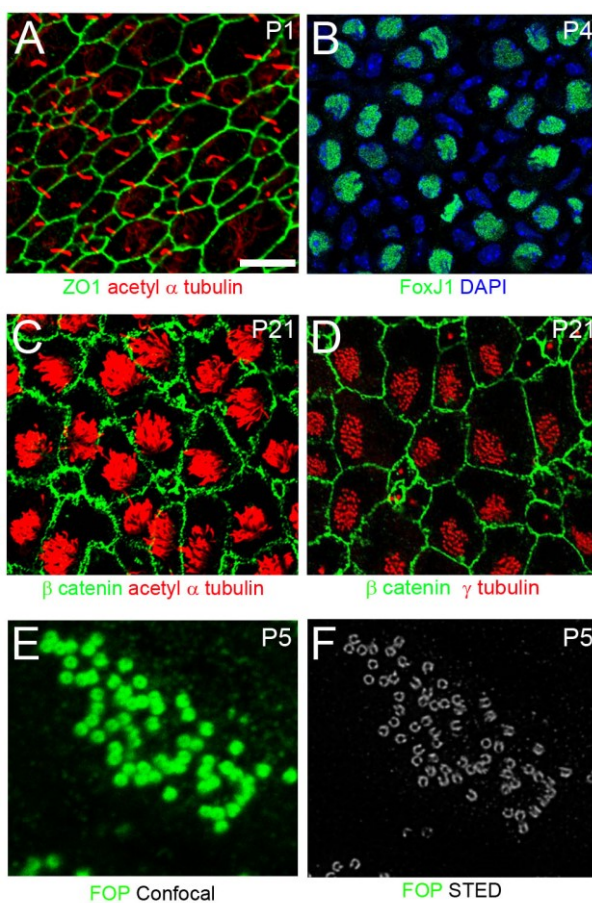


**Figure 3. Examples of staining on P1, P4, P5 and P21 LWWM Confocal (A-E) and STED (F) images.** LWWM stained for A. ZO1 (green) and Acetyl- $\alpha$ - tubulin (red) at P1. B. FoxJ1 (green)

and DAPI (blue) at P4. C.  $\beta$ -catenin (green) and Acetyl- $\alpha$ - tubulin (red) at P21. D.  $\beta$ -catenin (green) and  $\gamma$ -tubulin (red) at P21. E-F. FGFR1 Oncogene Partner (FOP) at P5. Scale bar: 10  $\mu$ m in A-B, 15  $\mu$ m in C-D and 2.5  $\mu$ m in E-F.

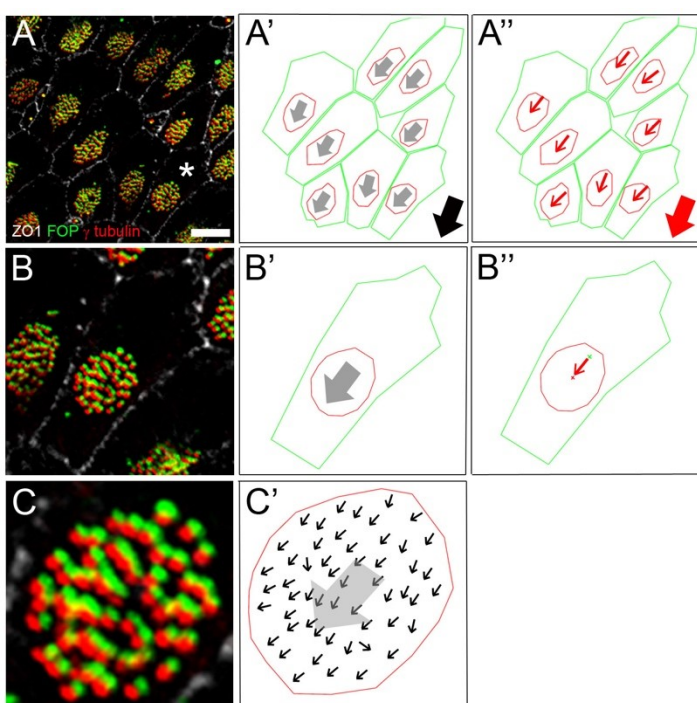


**Figure 4. Analysis of planar organization of ependymal cells in the lateral wall (A, B, C).** Triple immunostaining for ZO1 (white), FGFR1 Oncogene Partner (FOP, green) and  $\gamma$ -tubulin (red) on P21 LWWM allows the observation of translational and rotational polarities at the cellular and tissular level in a single sample. A. Large field picture displaying the tissue organization. B. Zoom on the cell marked with \* in (A). C. Zoom on the BBs patch from cell shown in (B). Analysis of ZO1/FOP/ $\gamma$ -tubulin triple staining using Biotooll software [described in Boutin *et al.* (2014)] allows the definition of polarity parameters at BB, cell and tissue level. C'. Definition of individual cilia polarity: each black vector represents the rotational polarity axis of individual BB defined as the direction from FOP (green) to  $\gamma$ -tubulin (red) positive dots. The biotool software calculates the mean BB orientation of the patch to define the cellular rotational polarity axis that corresponds to the beating direction of individual cell (grey arrow). B'-B''. Definition of polarity axis at the cellular level: Outline of cell (green) and BB patch (red). The grey vector in (B') represents the rotational polarity axis of the cell defined as shown in C'. The red arrow in (B'') represents the translational polarity axis of the cell defined as direction from the cell center (green cross) to the BB patch center (red cross). A'-A''. Analysis of polarity at the tissue level: The translational and rotational polarity axes are defined for each cell and compared to mean direction of the field (black and red thick arrows). Scale bar: 15  $\mu$ m in A, 2.5  $\mu$ m in B and 1  $\mu$ m in C.

**Notes**

1. Freshly made 4% PFA aliquots can be stored at -20 °C up to one year and defrosted just before fixation.
2. Short fixation time is mandatory for good staining. 12 min fixation is sufficient to fix large and small tissues while preserving the structure and giving the best results. We recommend not to exceed 20 min fixation for ependymal observation.

**Recipes**

1. Primary antibodies with the corresponding secondary antibodies.

**Table 1. List of primary and secondary antibodies**

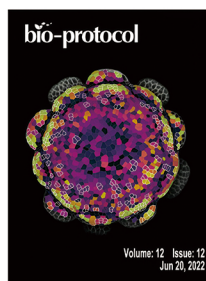
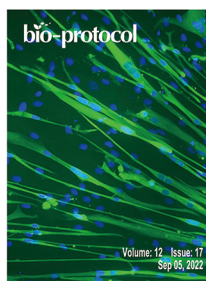
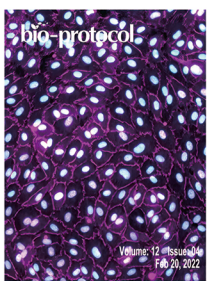
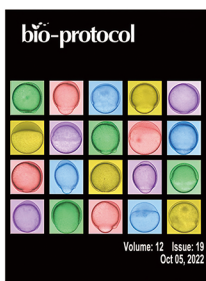
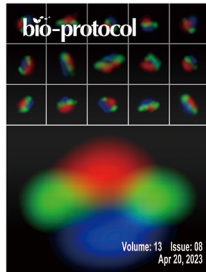
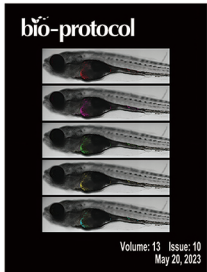
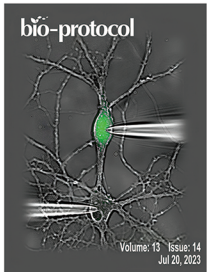
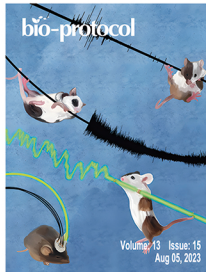
Antibody	Isotype	Reference	Dilution	Secondary antibody
ZO1	Rabbit	Invitrogen 61-7300	1:600	Anti-Rabbit A647
γ-tubulin [GTU-88]	Mouse IgG1	Abcam ab11316	1:400	Anti-Mouse IgG1 A568
FGFR1OP (FOP)	Mouse IgG2b	Abnova H00011116-M01	1:2,000	Anti-Mouse IgG2b A488
β-catenin	Mouse IgG1	BD Transduction Laboratories 610153	1:1,000	Anti-Mouse IgG1 A488
FoxJ1	Mouse IgG1	eBioscience 14-9965	1:2,000	Anti-Mouse IgG1 A488
Acetylated-α-tubulin	Mouse IgG2b	Sigma T6793	1:1,000	Anti-Mouse IgG2b A568

**Acknowledgments**

The method described in this article has been optimized for detection of ependymal cells organization and is based on a protocol described previously (Mirzadeh *et al.*, 2010). The original version of the protocol has been described in (Boutin *et al.*, 2014). The authors wish to thank the Spassky lab (ENS, Paris) for introduction to the LWWM dissection method. CB is a recipient of a postdoctoral fellowship from 'La Ligue Nationale Contre le Cancer'. HC acknowledges funding from the Agence Nationale de la Recherche (ANR-13-BSV4-0013-01-ATMIR). This work was supported by the French National Research Agency through the "Investments for the Future" program (France-BioImaging, ANR-10-INSB-04).

**References**

1. Boutin, C., Labedan, P., Dimidschstein, J., Richard, F., Cremer, H., Andre, P., Yang, Y., Montcouquiol, M., Goffinet, A. M. and Tissir, F. (2014). [A dual role for planar cell polarity genes in ciliated cells](#). *Proc Natl Acad Sci U S A* 111(30): E3129-3138.
2. Guirao, B., Meunier, A., Mortaud, S., Aguilar, A., Corsi, J. M., Strehl, L., Hirota, Y., Desoeuvre, A., Boutin, C., Han, Y. G., Mirzadeh, Z., Cremer, H., Montcouquiol, M., Sawamoto, K. and Spassky, N. (2010). [Coupling between hydrodynamic forces and planar cell polarity orients mammalian motile cilia](#). *Nature Cell Biology* 12(4): 341-U386.
3. Hirota, Y., Meunier, A., Huang, S., Shimozawa, T., Yamada, O., Kida, Y. S., Inoue, M., Ito, T., Kato, H., Sakaguchi, M., Sunabori, T., Nakaya, M. A., Nonaka, S., Ogura, T., Higuchi, H., Okano, H., Spassky, N. and Sawamoto, K. (2010). [Planar polarity of multiciliated ependymal cells involves the anterior migration of basal bodies regulated by non-muscle myosin II](#). *Development* 137(18): 3037-3046.
4. Marshall, W. F. (2008). [Basal bodies platforms for building cilia](#). *Curr Top Dev Biol* 85: 1-22.
5. Mirzadeh, Z., Doetsch, F., Sawamoto, K., Wichterle, H. and Alvarez-Buylla, A. (2010). [The subventricular zone en-face: wholmount staining and ependymal flow](#). *J Vis Exp*(39).
6. Mirzadeh, Z., Han, Y. G., Soriano-Navarro, M., Garcia-Verdugo, J. M. and Alvarez-Buylla, A. (2010). [Cilia organize ependymal planar polarity](#). *J Neurosci* 30(7): 2600-2610.
7. Ohata, S., Nakatani, J., Herranz-Perez, V., Cheng, J., Belinson, H., Inubushi, T., Snider, W. D., Garcia-Verdugo, J. M., Wynshaw-Boris, A. and Alvarez-Buylla, A. (2014). [Loss of Dishevelleds disrupts planar polarity in ependymal motile cilia and results in hydrocephalus](#). *Neuron* 83(3): 558-571.



## A peer-reviewed, open access protocol journal

>4,800 high quality, validated, step-by-step protocols

- Contributed by **20,000+** scientists
- >91% reproducibility (Bio-protocol user surveys)
- 1000+** videos of key procedural steps

Publish and share your protocols with us!



Bio-protocol Journal



Bio-protocol Preprint

**NEW!**

**Bio-protocol Preprint Repository**

A preprint repository  
for life sciences  
protocols

